LEVEL II

Final Technical Report

Improved Moisture Resistance
of Fiber-Reinforced Plastic

Grant No.

ARO DAAG 29-80C-0236

DTIC

JAN 4 1982

H

REPORT DOCUMENTATION PAGE	READ INSTRUCTIONS BEFORE COMPLETING FORM

1. REPORT NUMBER	2. GOVT ACCESSION NO.	3. RECIPIENT'S CATALOG NUMBER
14740.4-MS	AD-A109190	

4. TITLE (and Subtitle)	5. TYPE OF REPORT & PERIOD COVERED
Improved Moisture Resistance of Fiber-Reinforced Plastic	Final Report: 1 Jul 78 - 30 Sep 81
	6. PERFORMING ORG. REPORT NUMBER

7. AUTHOR(s)	8. CONTRACT OR GRANT NUMBER(s)
Jack L. Koenig	DAAG29 78 G 0148; DAAG29 80 C 0236

9. PERFORMING ORGANIZATION NAME AND ADDRESS	10. PROGRAM ELEMENT, PROJECT, TASK AREA & WORK UNIT NUMBERS
Case Western Reserve University Cleveland, OH 44106	

11. CONTROLLING OFFICE NAME AND ADDRESS	12. REPORT DATE
U. S. Army Research Office Post Office Box 12211 Research Triangle Park, NC 27709	Dec 81
	13. NUMBER OF PAGES
	181

14. MONITORING AGENCY NAME & ADDRESS(if different from Controlling Office)	15. SECURITY CLASS. (of this report)
	Unclassified
	15a. DECLASSIFICATION/DOWNGRADING SCHEDULE

16. DISTRIBUTION STATEMENT (of this Report)

Approved for public release; distribution unlimited.

17. DISTRIBUTION STATEMENT (of the abstract entered in Block 20, if different from Report)

NA

18. SUPPLEMENTARY NOTES

The view, opinions, and/or findings contained in this report are those of the author(s) and should not be construed as an official Department of the Army position, policy, or decision, unless so designated by other documentation.

19. KEY WORDS (Continue on reverse side if necessary and identify by block number)

plastics	interfaces	coupling agents
moisture resistance	epoxy matrix composites	silicon dioxide
fiber reinforced composites	glass fiber composites	surface chemistry
silanes	aminosilanes	chemical reactions

20. ABSTRACT (Continue on reverse side if necessary and identify by block number)

The text of seven papers is included: 1) Improved Moisture Resistance of Fiber-Reinforced Plastic (An Introduction); 2) The Structure of Aminofunctional Silane Coupling Agents: Part I: γ-Aminopropyltriethoxysilane and its Analogues; 3) Spectroscopic Characterization of the Matrix-Silane Coupling Agent Interface in Fiber-Reinforced Composites; 4) Interfacial Strength Studies of Fiber-Reinforced Composites; 5) Comparison of Primary and Secondary Aminosilane Coupling Agents in Anhydride-Cured Epoxy Fiberglass Composites; 6) Chemical Reactions Occurring at

DD FORM 1473 EDITION OF 1 NOV 65 IS OBSOLETE

sb

20.   ABSTRACT CONTINUED

the Interface of Epoxy Matrix and Aminosilane Coupling Agents in Fiber-Reinforced Composites; 7) Magic-Angle Cross Polarization Carbon-13 NMR Study of Aminosilane Coupling Agents on Silica Surfaces.

Final Technical Report

Improved Moisture Resistance of Fiber-Reinforced Plastic

Grant No.

ARO DAAG 29-80C-0236

submitted

by

Jack L. Koenig

Department of Macromolecular Science

Case Western Reserve University

Cleveland, Ohio 44106

TABLE OF CONTENTS

IMPROVED MOISTURE RESISTANCE OF FIBER-REINFORCED PLASTIC

- An Introduction

J.L. Koenig and Chwan-hwa Chiang

Department of Macromolecular Science
Case Western Reserve University
Cleveland, Ohio   44106

INTRODUCTION

Interfacial phenomena are important in all phases of composite technology. The properties of all components are affected by the nature of their surfaces which in turn significantly affect composite properties. Similarly, interfacial phenomena are important in composite fabrication, testing, and evaluation. Finally, interfacial behavior can strongly affect the response of the composite to the thermal, mechanical, and environmental conditions arising from service application [1-4].

From a materials point of view, the details of the nature of composite interfaces can be described to nearly any extent desired. The problem, however, is to relate these details to the behavior of the composites. The macroscopic average properties of a composite are not sufficient for evaluating the materials aspect of composite interfaces. Thus, the micromechanics of composites behavior may provide the only suitable method of analysis for evaluating interfacial effects. Although different interfacial phenomena will occur in different composite systems, and even though the internal mechanics may differ, there are a number of features of both the nature of interface and the micromechanics of composites which are common to all systems.

Applications of coupling agents for surface modification of filler and reinforcements in plastics have generally been directed toward improved mechanical strength and chemical resistance of composites [5-7]. The bonding created by an adhesion promoter occurs by virtue of its having functional groups which can react with the substrate and the organic polymer phase. The most common case, silanes on glass,

entire mechanical-thermal history of the composite as well as the chemical and structural characteristics of the bulk constituents [18]. The mechanical and water resistance properties of polymer resins are dependent upon the morphological structure of the resin, although three-dimensional crosslinked polymer systems have been generally treated as completely amorphous disordered structures on the molecular level. The presence of small cavities in the resin, for instance, is an important determinant influencing the rate of water penetration [19]. Dynamic mechanical and swelling properties of epoxy resins [20] have led to the suggestion that in fact two separate phases may exist in the disordered material. Microscopic examination of several glass-reinforced crosslinked epoxy resins have revealed that globular structures in the resin are affected to various degrees by water. Boiling water also lowered the T_g of the materials, and the observed decline in flexural strength was attributed to cracking and changes in the supramolecular structure [21].

Although there are some complications, most researchers agree, water primarily degrades the fiberglass-matrix interface via hydrolysis of the silane coupling agent in addition to attack on the matrix and filler [22]. However, a basic structural model of interface in composite at the molecular level has not been well established. In order to improve the moisture resistance of composite, the basic aspects of these related subjects will be discussed. Especially we will concentrate on the molecular structure, the hydrothermal stability, and the mechanical properties of the interface between the anhydride-cured epoxy resin and the amino-silane treated fiberglass.

THE NATURE AND TYPES OF INTERFACES IN COMPOSITES

An interface can be described by specifying the type of discontinuity observed, along with a description of the extent at the interface. This description will usually involve the changes occurring at a resin-fiber interface, such as state of aggregation, composition, crystal structure, orientation, and chemical structure. A given interface may involve several of these features. A rigorous classification would be quite difficult. If chemical interactions occur between the silane coupling agent and polymer matrix, then additional features of the interface must be considered. What initially was an interface on a macroscopic scale may become an interfacial zone characterized by multiple interfaces and additional phases (Figure 1). A complete description of the interfacial zone might require a number of parameters in composites, i.e., geometry and dimensions, microstructure and morphology, mechanical, physical, chemical, and thermal properties of different phases or localized areas in the interfacial zone. The selection of the components of a composite is usually based initially on the mechanical and physical properties of the individual constituents. The types and nature of the interfacial interactions that can occur will vary considerably with the nature of the composite

has been presented as forming siloxane bonds from the reactant to the glass surface and covalent bonds from the coupling agent to the matrix phase. This phenomenon then provides not only strong interfacial primary bonding but also a condition not easily disturbed by environmental conditions [9-10]. The interface in a fiber-matrix composite becomes a surface which is common to both fiber and matrix with the coupling agent acting as an interfacial region. It has physical and mechanical properties which are neither those of the fiber nor the polymer matrix.

For the past years several theories have been proposed to interpret the mechanism of reinforcement in composites. The chemical bonding theory is the most widely accepted of these theories and suggests that the coupling agent forms covalent bonds to both the glass surface and the resin [11]. Other theories have been advanced in which the interactions at the glass-coupling agent interface are believed to be hydrogen bonding phenomena occurring between silanols in the coupling agent and glass surface [12]. Still others contend that Van der Waals forces at the interface are sufficiently strong to account for the mechanical strengths of laminates [13].

Kumins and Roteman suggested that the boundary region, of which the coupling agent is a part, between a high modulus reinforcement and a lower modulus resin can transfer stresses most uniformly if it has a modulus intermediate between that of the resin and the reinforcement [14]. It is difficult to reconcile this concept with the need for stress relaxation at an interface because of differential thermal shrinkage between polymer and filler. Hooper proposed that the silane treatment contributed a mode of mechanical relaxation through a deformable layer of silicone resin [15]. However, the layer of silane in a typical glass finish is too thin to provide stress relaxation through mechanical flexibility. A preferential adsorption theory proposed by Erickson et al. [16] is a modification of the deformable layer theory. This theory was based on the assumption that different finishes on glass fibers have, to different degrees, the power to deactivate, destroy, or adsorb out of the uncured liquid resin mixture, certain constituents necessary to complete resin curing. Such a layer would need ductility and strength to provide relaxation and effective transfer of stress between the fibers in load-bearing situations. Plueddemann suggested a reversible hydrolyzable bond theory which is a combination of the chemical bonding theory, the restricted layer theory, and the deformable layer theory [17]. This theory proposes a reversible breaking and remaking of stressed bonds between coupling agent and glass in the presence of water thus allowing relaxation of stresses without loss of adhesion.

Many other functions can possibly be served by coupling agents at a matrix-glass interface. The coupling agent may protect the interface against stress corrosion by water. The nature of the interfaces existing in a composite at any instant is dependent upon the

system. In fact, organic polymer matrices are expected to show a marked chemical reactivity with the silane-treated fiber [23].

It is generally held that the matrix and fibers must be bonded together if the desired properties of composites are to be realized. The term "bonding" can be convienent to distinguish three kinds of bonding interactions: mechanical, physical, and chemical. Mechanical bonding refers to the type of interlocking that occurs as a consequence of the geometrical shape of the bodies, or as a result of purely rheological interactions. Physical bonding refers to interactions resulting from physical forces such as gravity, and magnetic fields. Chemical bonding covers all those interactions at the molecular level which result from electronic interactions between atoms or chemical reactions between functional groups. From a practical point of view, the relative importance of mechanical and chemical bonding is uncertain at present, but they are stronger than physical bonding in the composites [24].

Chemical bonds are usually designated according to the type of chemical mechanisms involved, and chemical mechanisms of bonding are customarily grouped into primary and secondary bonds. The primary bonds include the ionic, covalent, and metallic bonds, whereas the secondary bonds include the hydrogen bonds and Van der Waals bonds. The terms primary and secondary emphasize the relative magnitude of the forces involved, but not necessarily their relative importance [2].

As with any composite, the properties depend on the proportions of two components, on their properties, on the degree and nature of the interfacial adhesion, and often on the phase size. If adhesion is poor, strength and modulus will be reduced, and each constituent will exhibit its own T_g . If adhesion is good, the modulus will fall between upper and lower bounds. An exception is the use of block or graft copolymers, which exhibit good interfacial adhesion due to the covalent linkages between the phases [25].

It is clear that chemical bonding can potentially develop across the interface between any two solids if they are in intimate contact. The theoretical strength of such an interface provides a convienent frame of reference for considering the strength of solid-solid interfaces. In general, there are two approaches to the calculation of bond strength: 1: the atomic or molecular approach based upon classical or quantum mechanics, and 2: the thermodynamic approach [26,27]. The theoretical strength of interfacial bonding can be obtained by these two methods.

It is important to understand the type of interfacial regions that exist in the two different components and their surface conditions. The silane modified glass surface generates several different types of interfaces. Chemically, it can be a chemically bonded or non-bonded interface. Physically, it can be a compatible or non-

compatible interface, and mechanically, it can be a smooth or rough interface. These interfacial bondings are fundamentally for predicating the load transfer through the interfaces in composites.

THE GLASS SURFACES

There are two fundamental properties which determine the untreated silica or silicate glass appropriate to an end use. These are the surface areas and the extent of hydration. Amorphous silica consists of silicon and oxygen tetrahydrally bonded into an imperfect three-dimensional structure. The most commonly used glass fiber is E-glass which contains 55% SiO_2 as the main component with the remainder being oxides of other metals such as Al, Ca, Mg, Fe, etc. After contact with water, the surface oxides are hydrated and form hydroxide groups which are considered to be adsorption sites for coupling agent molecules [28]. It is evident that surface silanols are a major factor in determining various structures with different environments. Koenig and Shih have demonstrated that the structural difference of the surface silanol can be detected utilizing Raman spectroscopy [29]. There are several peaks appearing in the 1050-950 cm^{-1} region due to the SiO_2 stretching mode of the surface silanols. Glass microspheres display two lines at 980 cm^{-1} for a wet sample and at 1005 cm^{-1} for a dry sample. These two frequencies are related to the silanols which are hydrogen bonded to the adsorbed water molecules. There is an additional peak at 992 cm^{-1} for the glass microspheres. This peak is responsible for the silanols which are hydrogen bonded to adjacent silanols. The typical silanol groups on the silica surface are shown in Figure 2. The roughness of the glass surfaces are also very important in determining the extent of surface modification.

THE STRUCTURE OF SILANES IN AQUEOUS SOLUTION

All commercial silane coupling agents are of the structure X_3Si-R where X are hydrolyzable groups on silicaon, and R is an organofunctional group with organic chain which is available for reaction with a given resin. The composition of silane coupling agents in dilute aqueous solution depends on the nature of the organofunctional group on the silicaon and the PH value of the solution. Neutral organofunctional silane coupling agents, usually prepared in dilute acetic solution, hydrolyze rapidly to silane triols, and then condense slowly to oligomeric siloxanes. The monomer and small oligomers are soluble in water and large oligomers precipitate from solution. Aqueous solutions of the silanes have only limited stability and must be used within a few hours [30].

Amino-organofunctional silane coupling agents are the only silanes that hydrolyze almost immediately in water. But solution of aminosilane coupling agents in toluene or other nonpolar organic

solvents give precipitates upon contact with moist atmosphere. Since
it is well known that cyclic 6-membered chelate rings have extraordi-
nary stability, it is found that an internal cyclic chelate ring struc-
ture is formed in solution of aminosilanes [31,32]. The chelate ring
structure is destroyed when the proper ionizing chemical is added to
the solution, such as acid or alkaline chemicals. In the acid solu-
tion, there is a chemical transfer of a proton to the amino group and
the amino group becomes an amonium ion in aqueous solution. The sila-
nol group will not react with the ammonium ion and the silane molecule
stays as the linear form in the solutions. In the alkaline (KOH) solu-
tion, all the silanol groups lose hydrogen and become SiO_2 groups, and
the silane molecules do not condense with each other. The molecular
structures of the monomeric γ-aminopropyltriethoxysilane (APS) in the
acid, neutral, and alkaline aqueous solutions are shown in Figure 3.
More work must be done in order to understand the detailed structural
composition of silane in solutions as well as the solids. The proper-
ties of silane solution and the nature of the silane molecule could
affect the structure and the reactivity of the silane deposited on the
surfaces.

THE NATURE OF SILANES ON GLASS SURFACES

The silane molecules are usually deposited on glass surfaces as a
monolayer film and the amount deposited is dependent on the concentra-
tion of the solution (Figure 4). Schrader reported that the coupling
agent when deposited on the glass surfaces usually from heterogeneous
layers consisting of physisorbed and chemisorbed fractions [33]. The
outer fraction, about 95% of the total adsorbed silane, can be extrac-
ted by water at room temperature. The second or inner fraction can be
extracted by boiling water, but the third or surface fraction is firm-
ly bound to the substrate and survives extraction in boiling water for
up to 100 min. These results have also been confirmed by Fourier
transform infrared spectroscopy [34]. It was found that γ-MAPS forms
essentially three different structures in the interphase, analogous to
APS interphase. The outermost layers consist of small oligomers which
are simply physisorbed so that they can be washed away by organic sol-
vents. Nearer the glass surface, there is a second region which con-
sists of oligomers similar to the outer layers except for a few bonds
connecting the oligomers. In the region near the glass surface, the
interconnecting crosslinks become extensive and a regular three-dimen-
sional network is found. Thus, a gradient in the structure of the
coupling agent interphase exists and the type of gradient determines
the hydrolytic stability of the interphase.

THE ROLE OF THE EPOXY RESIN IN COMPOSITES

The versatility of epoxy resins has resulted in their use in many
industrial, commercial, military, and consumer applications. Reinfor-

ced plastics, produced via laminating and molding methods, have found applications in the chemical, electrical, and electronics industries. The various forms and types of epoxy resin, in their thermoplastic or uncured state, are converted or hardened into useful thermosets by reaction with a variety of hardeners [35]. Depending upon the resin and hardener comprising the system, the amount of hardener used can vary from as low as 1 part hardner per 100 parts of resin to greater than 100 phr. Epoxy resins are hardened into thermoset compounds by any of three general reactions: 1. self-polymerization forming direct linkages between the epoxy groups, 2. linkage of epoxy groups with aromatic or aliphatic hydroxyls, and 3. crosslinking with the hardener through various radicals [36].

Resistance to chemical attack is determined by exposure of the cured systems to the materials of interest, e.g., acid, alkaline, solvents, etc. A weight change as well as the alternation of mechanical and electrical properties serve to characterize the performance of epoxy systems in corrosive environments [36]. It is found that long term exposure of the epoxy matrix to water causes the hydrolysis and leaching of unreacted anhydride molecules. Hydrolysis of the ester linkages in the unstressed resin is significant only in a highly alkaline medijm. However, the application of high tensile stress to the matrix dramatically accelerates hydrolytic attack in films exposed to neutral PH or alkaline media. The mechanochemical degradation is modelled by an exponential dependence of the hydrolysis rate on the applied stress [37].

THE NATURE OF THE SILANE-RESIN INTERFACE

Although silane coupling agents were first introduced to improve the water resistance of reinforced plastics, it was soon observed that they also imparted significant improvement to the initial properties of laminates. The degree of improvement obtained even under optimum conditions varied with the resin, the glass content, and the severity of the test. There is no correlation between the polarity of the silane, or wettability of silane-treated glass, and the effectiveness of the silane coupling agent [38]. Better wetting of silane-treated glass will allow more complete displacement of air from the glass surface and reduce the number of voids in the composite.

The coupling agent-matrix interface is more stable to attack of water. Thus, it may be important to maximize the extent of the interfacial bonding at the interface. Such bonding is necessary to obtain high performance of FRP [39]. Bjorksten and Yaeger proposed a chemical reaction between the vinylsilane and the polyester resin through the vinyl group [11]. The vinyl group of 3-methacryloxpropyltrimethoxysilane copolymerizes with styrene or acrylate [40]. However, the evidence was not strong that the vinyl group of silane on the surfaces copolymerized to the vinyl group of the polyester resin. The coupling

agent interphase can homopolymerize through the organic groups or co-polymerize with the matrix resin [41].

Direct evidence for chemical bonding at the interface between an anhydride-cured epoxy resin and the aminosilane treated fiber has been obtained by using Fourier transform infrared spectroscopy [42]. It was found that the nadic methyl anhydride can react with γ-aminopropyl-triethoxysilane (APS) and N-methylaminopropyltrimethoxysilane (MAPS). In comparing the relative reactivities of these two coupling agents with the epoxy resin, the secondary aminosilane has a higher reactiv-ity than the primary aminosilane. The primary aminosilane forms a cyclic imide with the nadic methyl anhydride at the interface of the composite [43]. The formation of this imide group inhibits the further copolymerization of the matrix and the silane layers, so interfacial bonding does not occur. The molecular structure of the interface in MAPS treated fiberglass reinforced composites is different from that of the APS-treated fiber composites. The silane-resin interface con-stitutes copolymers of the epoxy resin and the aminosilane coupling agents. The penetrating ability of the uncured resin and the nature of the siloxane interphase on the fiber surfaces determines the struc-ture of the resin-silane interphase [44]. In addition, the silane-induced esterification incresaes the curing density of the epoxy mat-rix about 5-10% relative to the bulk resin. Thus, there is a gradient of matrix composition and structure from the fiber surface to the bulk resin. This interface region could protect against the moisture attack at the interface in composites.

THE ROLE OF INTERFACIAL BONDING IN HYDROTHERMAL STABILITY

Exposure of a composite to cyclic temperature and humidity varia-tions induces cyclic stress within a composite [22]. The degradation is accompanied by debonding of the resin from the fiber reinforcement due to the difference in the thermal expansion coefficients between the matrix and the fiber. Silane coupling agents are applied to the fiber reinforced composites to stabilize the interface by chemical bonding of the matrix to the glass. In order to account for the enhanced effect of the silane coupling agent at the interface of the composites several methods have been developed to measure fiber-matrix inter-facial strength [45-50]. All methods typically suffer from a lack of reproducibility and produce data with coefficients of variation great-er than 10 percent. One of these methods is to measure the force required to pullout a fiber embedded in a matrix. This method, in addition to its relative simplicity of sample preparation and measure-ment, is expected to give realistic information when one considers the pullout of the fibers from the fracture surfaces of composites. A general relationship between the fiber strength and the interfacial strength has been established theoretically as a function of the em-bedded length of fiber by Grenzczuk [51]. Lawrence has developed a theory on the effect of partial debonding on the maximum debonding

stress, including the effect of friction [52]. However, most of these experiments have dealt with steel filaments (not a real fiberglass) and epoxy, polyethylene, and polypropylene resin [53].

In order to measure the interfacial strength of the fiber rein-forced composites, an improved pull-out test has been developed in our laboratory. The joint shear strengths between 25 mil diameter fiber-glass filaments and epoxy resins are tested in a transparent media to display the fracture. It was found that the adhesion is dependent on the curing conditions of epoxy resins. Three major types of failures of the specimens have been found when the fibers pulled-out of the cured epoxy resins. These failures include fiber failure, matrix failure, and the interface failure. For the pre-cured sample, the matrix deformation can be observed and the result shows only the elas-tic behavior of the incompletely cured eopxy matrix. For post-cured samples, the fiber broke inside the matrix because of the large resi-dual pressure in the matrix. Thus, only the pulled-out fiber sample can provide the value of the maximum shear stress at the interface in composites. These tests make it clear that there are many variables influencing the rate of bond degradation and these include the nature of silane, amount of silane, temperature of water, PH of the water, resin formulation, surface constitution, and processing condition of composites.

It is certain that the water migration is sensitive to the resin structure [54]. The water molecules can reach and weaken the resin-fiber interface by diffusion through the resin or along the interface itself. Because the resin-silane interfacial bonds are more stable to the attack of water, the major degradation should appear at the coup-ling agent interphase and the glass-silane interface. Therefore, the reaction of the siloxanes with the water controls the interfacial strength of the composites. As long as the interface is rigid or has flow, bond forming and scission in the presence of water is revers-ible [1]. An increase in the amount of water in the interface region causes a shift of the equilibrium to be less favorable for bond for-mation and decreases the interfacial strength of the interface. The acid and alkaline chemicals generated from the surface would influence the rate of hydrolysis and the state of equilibrium and so would res-ult in poor mechanical performance of composites.

The long term mechanical performance of glass reinforced compos-ites depends on their stability in various environmental atmospheres. Glass reinforced plastics adsorb moisture after extended periods of exposure to high humidity and this moisture often degrades their mech-anical and structural integrity [55]. There is a strong indication that degradation mainly occurs by a weakening of the fiber-resin interface, with a subsequent loss in the shear strength of the composites.

CONCLUSIONS

The great improvement in properties imparted to the fiberglass reinforced composite by traces of appropriate reactive silanes at the interface suggests that an understanding of the molecular structure of the interface might be the key to understanding the mechanical behavior of composites. The effect of water at the interface of composites is quite complex, depending upon the nature of the polymer system and that of the fibers. Thermosetting resins like epoxy absorb water with swelling and reduction in modulus. Molecular water diffuses readily through the resin phase and attacks the interface of composites. Liquid water can leach soluble materials from the interface and the matrix phase. Silane coupling agents may partially prevent water from attacking the fiber-resin interface. So the strength retention of the silane-treated fiber composite is better than that of non-silane treated fiber composites.

REFERENCES

1. E.P. Pluddemann, Interface in Polymer Matrix Composites, Acedemic Press, Vol. 6, 1974, Chapters 1 and 6.
2. D.L. Harroad and R.T. Bagley, Sci. of Adv. Materl. and Proc. Eng., Vol. 10, E1 (1966).
3. R.T. Schwartzand, H.S. Schwartz, Fundamental Aspects of Fiber Reinforced Plastics Composites, Interscience Publishers, 1968, p. 163.
4. D.T. Clark and W.J. Feust, Polymer Surfaces, John Wiley & Sons, 1977, p. 47.
5. R.L. McCullough, Concepts of Fiber-Reinforced Composites, Marcel Dekker, 1971, p. 62.
6. P.E. Cassidy, J.M. Johnson, and G.C. Rolls, Ind. Eng. Chem. Proc. Re- Develop., 11, 170 (1972).
7. S. Oswitch and R.F. Golownia, Reinforced Plastics, 252 (1970).
8. T.B. Husbands, C.F. Derrington, and L. Pepper, Gorv. Rept., AD-730744 (1971).
9. W.A. Jemian, R.C. Wilcox, and A.C.T. Hau, Grov. Rept., AD-A011289/6st (1974).
10. C.E. Browning, Proc. 28th Ann. Tech. Conf., Reinforced Plastics Div., SPI, 15-A (1973).
11. J. Bjorksten and L.L. Yaeger, Mod. Plast., 29, 124 (1952).
12. J.G. Vail, Soluble Silicates, Vol. 1, Reinhold, 171 (1952).
13. W.A. Zisman, Proc. 19th Ann. Tech. Conf., Reinforced Plastics Div., SPI, 21-B (1964).
14. C.A. Kumins and J. Roteman, J. Polym. Sci., 1, 527 (1963).
15. R.C. Hooper, Proc. 11th Ann. Tech. Conf., Reinforced Plastics Div., SPI, 8-A (1956).
16. P.W. Erickson, Proc. 27th Ann. Tech. Conf., Reinforced Plastics Div., SPI, 13-A (1970).
17. E.P. Plueddemann, J. Adhesion 2, 184 (1970).

18. K.J. Brookfield, Reinforced Plastics, 136 (1972).
19. J.L. Parham, Permeability of Epoxy Systems, Grov. Rept., AD-726930 (1971).
20. A.S. Kenyon and L.E. Nielson, J. Macromol. Sci., A3, 275 (1969).
21. K.E. Hoffer, M. Stander, and L.C. Bennett, Proc. 32nd Ann. Tech. Con., Reinforced Plastics Div., SPI, 11-I (1977).
22. C.E. Browning, "The Mechanisms of Elevated Temperature Property Losses in High Performance Structural Epoxy Resin", Ph.D. Thesis, University of Dayton (1976).
23. E.P. Plueddemann, Filler and Reinforcements of Plastics, 1, 86 (1978).
24. H.W. Yip and J.B. Shortall, J. Adhesion, 8, 155 (1976).
25. J.A. Manson and H. Sperling, "Polymer Blends and Composites", N.Y., 1978, p. 62.
26. P.J.W. Debye, Adhesion and Cohesion, Elsevier Publ., 1962.
27. D.D. Eley, Adhesion, Oxford Univ., 1961,
28. M.P. Wagner, Rubber Chem. and Tech., 49, 703 (1977).
29. J.L. Koenig and P.T.K. Shih, Materials Sci. and Eng., 20, 127 (1975).
30. E.P. Plueddemann, Additives for Plastics, 1, 123 (1978).
31. C-h. Chiang, H. Ishida, and J.L. Koenig, J. Colloid & Interface Sci., 74, 396 (1980).
32. C-h. Chiang, Nan-I Liu and J.L. Koenig, J. Colloid & Interface Sci., (accepted).
33. M.E. Schrader, I. Lerner, J.L. D'Oria, and L. Deutsch, Proc. 22nd Ann. Tech. Conf., Reinforced Plastics Div., SPI, 13-A (1961).
34. H. Ishida and J.L. Koenig, J. Polym. Sci., Physics, 18, 193 (1980).
35. H. Lee and K. Neville Handbook of Epoxy Resins, McGraw Hill, New York, 1967.
36. M.K. Antoon and J.L. Koenig, J. Polym. Sci., Chem. Ed., 18, 480 (1980).
37. M.K. Antoon, "FT-IR Investigation of the Structure and Moisture Stability of the Epoxy Matrix in Glass-Reinforced Composites", Ph.D. Thesis, Case Western Reserve University, 1980.
38. W.D. Bascom and J.B. Romans, Ind. Eng. Chem. Prod. R & D, 7, 172 (1968).
39. E.P. Plueddemann and G.L. Stark, Modern Plastics, August, 1976 (1977).
40. S. Sterman and J.G. Marsden, Proc. 18th Ann. Tech. Conf., Reinforced Plastics Div., SPI, 1-D (1963).
41. H. Ishida and J.L. Koenig, J. Polym. Sci., Physics, 17 615 (1979).
42. C-h. Chiang and J.L. Koenig, Polymer Composites, 2, 88 (1980).
43. C-h. ChiangProc. 36th Ann Tech. Conf., SPI, Reinforced Plastics Div., 2-D (1981).
44. C-h. Chiang and J.L. Koenig, "Spectroscopic Characterization of the Matrix-Silane Coupling Agents Interface in Fiber Reinforced Composites", (Unpublished Paper).
45. K. Kendall, J. Materials Sci., 10, 1011 (1975).
46. H.A. Clark and E.P. Plueddemann, Modern Plastics, 133 (1963).

47. J.F. Mandall, J.H. Chen, and F.J. McGarry, International J. of
    Adhesion and Adhesives, 40 (1980).
48. A. Takaku and R.G.C. Arridge, Appl Phys., 6, 2038 (1973).
49. L.J. Broutman, Interfaces in Composites, ASTM, 27 (1968).
50. W.A. Fraser, F.H. Achker, and A.T. DiBenedetto, Proc. 30th SPI
    Annual Tech. Conf., Reinforced Plastics Div., SPI, 22-A (1975).
51. L.B. Greszczuk, Interfaces in Composites, ASTM, 49 (1969).
52. L. Lawrence, J. Materials Sci., 7, 1 (1972).
53. R.R. Mayers and J.S. Long, Treatise on Coatings, Marcel Dekker,
    Vol. 1, Part 3 (1961).
54. B.S. Mekta, A.T. DiBenedetto, and J.L. Kardos, Proc. 31st Ann.
    Tech. Conf., Reinforced Plastics. Div., SPI., 21-A (1976).
55. D.A. Scola, Proc. 31st Ann. Tech. Conf., Reinforced Plastics Div.,
    SPI, 14-A (1976).

FIBERGLASS REINFORCED PLASTICS
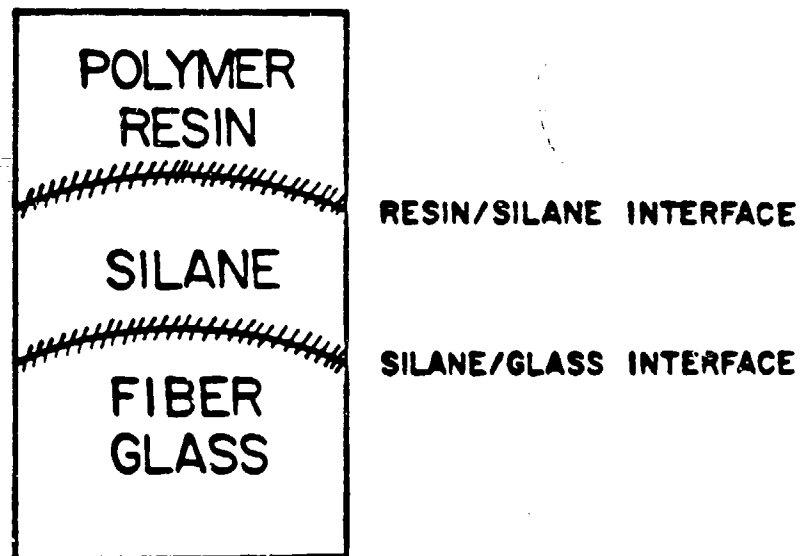
Fig. 1.   Schematic of interfaces in composites.

SURFACE OF SILICA

ISOLATED HYDROXYL   HYDROGEN-BONDED HYDROXYL
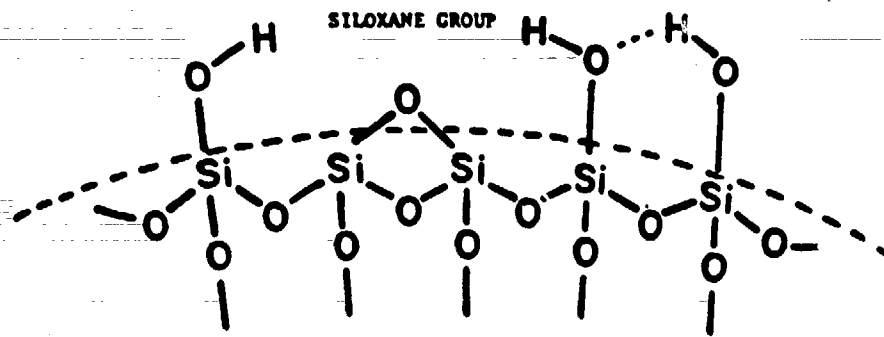
Fig. 2. Typical groups which can occur on the pure silica surfaces.

MOLECULAR STRUCTURE OF γ-AMINOPROPYLSILANTRIOL

1. In Acid Solution:

$$HO \atop HO \atop HO \diagdown Si-CH_2-CH_2-CH_2-NH_3^+$$
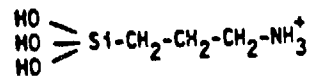
2. In Neutral Solution:
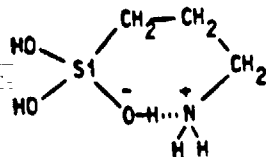
3. In Alkaline Solution:

$$O^- \atop O^- \atop O^- \diagdown Si-CH_2-CH_2-CH_2-NH_2$$
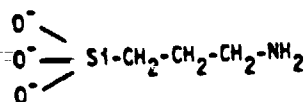
Fig. 3. The proposed molecular structure of γ-aminopropylsilantriols in acid, neutral, and alkaline aqueous solutions.

DEPOSITION OF SILANE

$$(CH_3O)_3Si-R \xrightarrow{\ H_2O\ }$$

$$HO-\underset{\underset{OH}{|}}{\overset{\overset{R}{|}}{Si}}-OH$$

$$+$$

$$\overset{OH \quad OH}{\underline{\textit{GLASS}}}$$
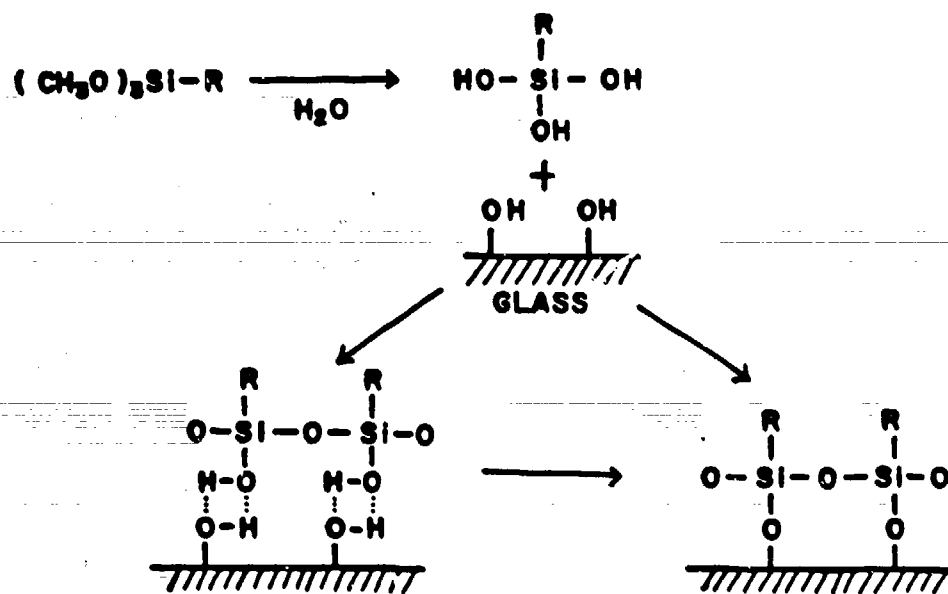
Fig. 4. The silane coupling agents hydrolyzed in aqueous solution
and adsorbed on the silica surfaces.

The Structure of Aminofunctional Silane Coupling Agents: Part I

γ - aminopropyltriethoxysilane and its analogues.

by

Hatsuo Ishida, Chwan-hwa Chiang and Jack L. Koenig

Department of Macromolecular Science

Case Institute of Technology

Case Western Reserve University

Cleveland, Ohio   44106

THE STRUCTURE OF AMINOFUNCTIONAL SILANE COUPLING AGENTS: PART I

γ-AMINOPROPYLTRIETHOXYSILANE AND ITS ANALOGUES

by

Hatsuo Ishida, Chwan-hwa Chiang and Jack L. Koenig
Department of Macromolecular Science
Case Western Reserve University
Cleveland, Ohio 44106

Abstract

Gamma-aminopropyltriethoxysilane (γ-APS) and its analogues are studied as aqueous solutions as well as solids by Fourier transform infrared spectroscopy (FT-IR) and laser Raman spectroscopy. Emphasis was placed on a determination of the nature of the interaction between the amine groups and the residual silanol groups in partially cured solids. Comparison with γ-aminopropyltrisilanolate and partially cured solids obtained from γ-amino-propylmethyldiethoxysilane and γ-aminopropyldimethylethoxysilane lead us to conclude that the residual silanol groups are strongly hydrogen bonded to the amine groups as $SiOH...NH_2$ rather than $SiO^-...^+NH_3$. Hydrolysis of γ-APS at concentrations ranging 2 - 80% by weight showed that the solutions below 40% by weight have few unhydrolyzed alkoxy groups. The amine groups are mutually hydrogen bonded in unhydrolyzed silane. However, in an aqueous solution and highly cured solids, the amine groups are either free or are interacting predominantly with water molecules.

INTRODUCTION

The usefulness of aminosilanes has been demonstrated in a number of areas of applications, as silane coupling agents for fiber-glass reinforced plastics. To date, however, the molecular structures of the hydrolyzates of aminosilanes are not known. Aminosilanes show a complicated molecular nature and they are often sensitive to the conditions of sample preparation.

Unlike many other organotrialkoxysilanes, aminosilanes exhibit a remarkable stability in aqueous solutions even at high concentrations. In order to explain this stability, Plueddemann (1) first postulated either five or six membered rings in which either the nitrogen atom interacts with the silicon atom or one of the silanols.

(I)   (II)
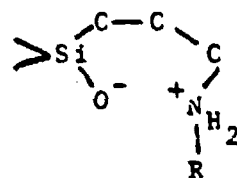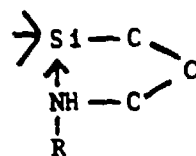
Extensive effort has been made to elucidate the macroscopic nature of aminosilanes on substrates (2-7). Bascom (8) using infrared attenuated total reflection spectroscopy (ATR) and Shih and Koenig (9) using laser Raman spectroscopy pioneered the study of the molecular structure of aminosilanes. The aminosilanes deposited on germanium plates from both aqueous and cyclohexane solutions showed multilayers of polymerized silane (8).

Boerio and others (10) utilized infrared reflection-absorption spectroscopy to study an aminosilane deposited on electropolished metal surfaces. They assigned the observed infrared band at 1510 cm^{-1} to the NH_3^+ as a consequence of the six membered ring structure (I) and the band at 1575 cm^{-1} to the five membered ring structure (II) which leads to a penta-coordinated silicon atom. Unfortunately, due to the unavailability of proper model compounds, no unambiguous evidence for the penta-coordinated silicon was reported.

Anderson et al. (11) used x-ray photoelectron spectroscopy for chemical analysis (ESCA) and observed the N ls ESCA band of an aminosilane on a silicon wafer as a doublet. They attributed the higher energy peak to the protonated amine, $-NH_3^+$. Addition of hexafluoroisopropanol reduced the NH_3^+ species and, as a result, increased the population of the SiOH groups of the hydrolyzate of the aminosilane. Moses et al. (12) also used ESCA to study the aminosilanes on electrode surfaces. They realized the multiplicity of the structures of aminosilanes depended upon the environments and proposed the following two structures.
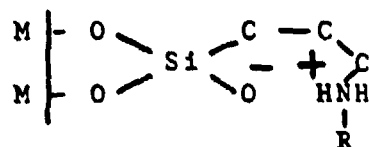
(III)   (IV)
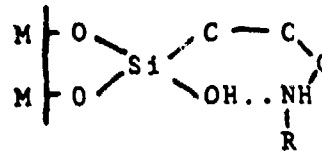
The N ls ESCA band at 401.9 and 400.3 eV are assigned to the protonated and free base, respectively. The population of free base increases at higher pH values of the environment. Our previous work (13) showed that the aminopropyl chain can be either a ring

structure or extended chain shown below depending on the degree
of curing.

$$O \diagdown Si \diagup C - C \diagdown$$
$$O \diagup \qquad O^{-}...H...^{+}N \diagup$$
$$\qquad\qquad H_2$$

$$\begin{array}{c} -O \\ -O \\ -O \end{array} \diagup Si\ (CH_2)_3\ NH_2$$

(V) (VI)

Ion scattering spectroscopy (ISS.) and secondary ion mass
spectroscopy (SIMS) have been applied by DiBenedetto and Scola
(14) in order to study the structure of an aminosilane on
S-glass fibers. The depth profile of the structure of a multilayer
of aminosilane on the fibers cured at 100°C for 45 min. was studied
employing the sputtering technique by ^{3}He ion beam. They reported
that the aminosilane at the air/silane interface consisted of a
high molecular weight polysiloxane layer and the middle of the
silane layer consisted of oligomeric polysiloxanes. The region
near the silane/glass interface had a high molecular weight
polysiloxane layer. The effect of humidity at elevated temperature
was reported to enhance polymerization of the oligomeric layer of
the aminosilane.

Preliminary results of inelastic electron tunneling spectro-
copy (15) by Diaz et al. and Auger electron spectroscopy (16)
by Cain and Sacher on aminosilanes deposited on aluminum oxide
and silicon wafers, respectively, have been reported. γ-amino-
propyltriethoxysilane formed a more dense polymerized layer when
deposited from the silane hydrolyzed by water only when deposited
from the 50% : 50% mixture in volume of water and methanol.

The results described above reveal the complicated nature of
aminosilanes. Apparently, further investigation is needed to

elucidate the molecular structures of aminosilanes and understand the mechanism of their effectiveness as adhesion promotors. Since the structures of the silane layers on the glass surfaces are strongly influenced by the structure of a silane in an aqueous solution (17), it is essential to investigate the structure of aminosilanes in aqueous solutions. To date, the molecular structure of aminosilanes in aqueous solutions and the polymers without substrate have not been studied. Fourier transform infrared spectroscopy (FT-IR) is extremely useful for studying aqueous solutions of silanes (13, 18, 19). The weak interference by water is also advantageous in laser Raman spectroscopy (18 - 20) and the information from infrared and Raman spectra are complementary. Therefore, we will utilize the combination of FT-IR and laser Raman spectroscopy in order to study the structures of amine and silanol groups in greater detail.

EXPERIMENTAL

A Fourier transform infrared spectrophotometer (Digilab FTS-14®) and a laser Raman spectrometer (Spectra Physics Ar^+ ion laser; model 165 and Spex holographic grating double monochromator) are the same as our previous papers (18, 19). Spectral resolution of 2 cm^{-1} and 4 cm^{-1} are the common set ups for infrared and Raman spectra, respectively. All infrared spectra in this paper are shown in the absorbance mode. The difference between the maximum and the minimum absorbances of the spectrum is designated as ΔA.

γ-aminopropyltrimethoxysilane, γ-aminopropyltriethoxysilane, γ-aminopropyl-
methyldiethoxysilane and γ-aminopropyldimethylethoxysilane were purchased from
Petrarch Systems and only freshly purchased samples which had been stored under
nitrogen atmosphere were used. Vinyltrimethoxysilane was kindly provided by Dr.
E.P.Plueddemann, Dow Corning Co., The silanes were hydrolyzed with deionized
distilled water and the spectral examination was undertaken usually between 20
and 45 min. after the hydrolysis unless kinetic experiments were to be performed.
The polyaminopropylsiloxane film was prepared by depositing the aqueous solution
of 20% by weight aminopropyltriethoxysilane onto a AgBr plate and dried at room
temperature for 30 min. γ-aminopropyltrisilanolate and vinyltrisilanolate were
prepared by adding the starting silanes slowly with rigorous agitation into the
KOH solution at a mole ratio of 1:6 (silane:KOH) yielding $H_2N(CH_2)_3 Si O_3$ and
$CH_2=CH Si O^{-3}$, respectively. The concentration of the silanes was 20% by weight.

RESULTS

The Raman spectrum of γ-aminopropyltrimethoxysilane (figure 1) shows two
strong lines at 645 and 614 cm^{-1} due to the symmetric SiOC stretching mode of the
trialkoxy group. This splitting is commonly observed when the organic chain has
more than three carbons due to vibrational interactions along the C-C-C-Si-O
skeleton. The magnitude of separation of the two frequencies is strongly influenced
by the nature of the attached alkoxy groups (21). The symmetric SiO stretching
mode is usually one of the strongest Raman lines in organotrialkoxysilanes as well
as organosilanetriols. A strong line at 645 cm^{-1} is unique to the structure $RSi(OX)_3$
where R represents organofunctionality and X is the species such as CH_3 or H. The
dimer does not show this mode nor any explicit characteristic lines, thus, Raman
spectroscopy, using the strong lines in the range 750-620 cm^{-1}, can verify the
existance of organosilane monomers in solutions.

The Raman spectrum of hydrolyzed γ-aminopropyltriethoxysilane as a 20% by
weight aqueous solution is shown in figure 2. Spectrum A does not show this strong
symmetric SiO stretching mode of the $Si(OH)_3$ group in the range 750-650 cm^{-1} nor the

characteristic bands due to the SiO bending modes of the $Si(OH)_3$ group in the range 450-350 cm^{-1} indicating absence of silanetriol monomer. The very strong line at 1021 cm^{-1} is due to the ethanol produced as a byproduct of the hydrolysis of the ethoxy groups. Figure 2 also includes the spectrum (B) of γ-aminopropyl-triethoxysilane in concentrated KOH solution. Spectrum A resembles the spectrum of a highly crosslinked polyaminopropylsiloxane (figure 3) as a powder except for the lines due to water and ethanol. The band at 525 cm^{-1} in figure 3 is due to the symmetric SiOSi stretching mode and its relative intensity to the CH_2 bending mode of the propyl chain at 1455 cm^{-1} is similar to the polyaminopropylsiloxane in the solid state indicating that the aminosilane in the solution at this level of concentration exists predominantly as condensed oligomers.

In general, when the concentration of silane solutions is low, the size of silane oligomers is small. It is thus useful to study the effect of silane concentration on the spectral changes. The difference spectra of hydrolyzed γ-aminopropyltriethoxysilane at concentrations 2, 5. 10, 20, 40, 60, and 80% by weight hydrolyzed for 0.5 hour are shown in figure 4 where the contributions of ethanol as a byproduct of hydrolysis and water are excluded. Slight frequency shifts of the ethanol bands, for example around 1020 cm^{-1}, are due to the different environments of ethanol in the silane solution compared to ethanol in water. More detailed spectral features can be seen in figure 5 which shows the spectrum of 20% solution of the silane by weight. An expanded spectrum of the solution of 2% by weight is also shown in figure 6 in order to examine the spectral features of the silane at low concentrations.

From figure 4 one observes that the band around 1115 cm^{-1} due to the SiOSi antisymmetric stretching mode increases in intensity with respect to the intensities of other bands as the concentration increases.

However, in spite of the wide range of concentrations, i.e. from 2 to 80% by weight, the relative intensities of the band around 920 cm^{-1} which is due to the SiO stretching mode of the SiOH groups and the band around 1115 cm^{-1} mentioned above do not show large differences. As a result, one can assume similarity in the oligomers of aminosilane in water throughout the concentration range studied here in contrast to the observation of the aqueous solution of 10% by weight vinyltrimethoxysilane as predominantly monomers (1, 18). This difference probably arises from the self-catalyzed condensation of the aminosilane even at low concentrations.

A band around 960 cm^{-1}, obvious at concentrations above 40% by weight, is associated with the unhydrolyzed ethoxy groups. Another ethoxy band at 1390 cm^{-1} is also present in these spectra indicating that the aminosilane contains a small amount of unhydrolyzed ethoxy groups at concentrations above 40% by weight when hydrolyzed for 0.5 h. No evidence of unhydrolyzed species was detected at low concentrations. The band at 1006 cm^{-1} in figure 5 is probably due to the propyl group attached to the silicon atom because ethyltrimethoxysilane shows a band at 1010 cm^{-1}, n-propyltrimethoxysilane at 1005 cm^{-1} and n-butyltrimethoxysilane at 1000 cm^{-1} (21). Neither the methoxy group nor the methyl group give rise to a band in this frequency range. Hence, it is attributed to the propyl groups which still exist after the hydrolysis of the aminosilane. According to Murata et.al. (22), an infrared band at 1001 cm^{-1} of butylsilane can be assigned to the C-C

stretching mode. In the spectra of polyaminopropylsiloxane (fibure 7) this mode is obscured by the very strong SiOSi antisymmetric stretching mode around $1200 - 1050$ cm^{-1}.

A band around 920 cm^{-1} occurs in the general range of the SiO stretching modes of SiOH groups (18, 19). The highest frequency observed from a study of 10 organosilanetriols is at 930 cm^{-1} (21) and this frequency decreases to around 890 cm^{-1} when the silanetriol condenses to a silanediol or silanol. However, strong hydrogen bonding may increase this frequency.

Organotrisilanolates, $RSiO_3^{-3}$, were prepared using vinyltrimethoxysilane as a model system because detailed band assignments have been reported. Figure 8 compares the Raman spectra of 20% by weight vinyltrimethoxysilane in water (spectrum A) and in KOH solution (spectrum B) at a mole ratio of 1:6 (silane : KOH). Thus, the silanes are predominantly $CH_2=CHSi(OH)_3$ and $CH_2=CHSiO_3^{-3}$, respectively. The three SiO stretching modes at 933, 848 and 678 cm^{-1} for the $Si(OH)_3$ group are shifted to 956, 907 and 664 cm^{-1} for the SiO_3^{-3} group. The stretching mode at 664 cm^{-1} due to the SiO_3^{-3} group considerably weakens while the $Si(OH)_3$ mode at 678 cm^{-1} shows one of the strongest lines in the spectrum. The vibrational modes of the $Si(OH)_2$ or SiOH groups of the vinyl functional silane appear very close to the average value of the two SiO antisymmetric stretching modes of the $Si(OH)_3$ group. Namely, the SiO stretching mode of the polyvinylsiloxanol appears at 890 cm^{-1} and an average of 888 cm^{-1} is calculated using the 927 and 848 cm^{-1} lines (927 + 848 / 2 = 888) observed for the $Si(OH)_3$ group. By analogy, it is reasonable to expect the modes due to the groups $CH_2=CHSiO_2^{-2}$ or $CH_2=CHSiO^-$ around 936 cm^{-1} (965 + 907 / 2 = 936).

A 20% by weight aminopropyltriethoxysilane in KOH solution
at a mole ratio of 1 : 6 (silane : KOH) was also prepared and
the Raman spectrum of the solution is shown in figure 2 as
spectrum B, where the Raman spectrum of 20% by weight γ-amino
propyltriethoxysilane in water (spectrum A) is also shown for
purposes of comparison. As previously cited, no obvious SiO
symmetric stretching mode of the silanetriol in the region
720 - 650 cm^{-1} is seen in the spectrum of the aminosilane in
water. A resemblance is seen between the spectra of vinyl and
amine functional silanes in KOH solutions suggesting that the
aminosilane in KOH solution is predominantly aminopropyltri-
silanolate, $H_2N(CH_2)_3SiO_3^{-3}$.

The FT-IR difference spectrum of the $H_2N(CH_2)_3SiO_3^{-3}$
obtained from the solution used for the Raman experiment is shown
in figure 9. The difference spectrum again confirms that the
condensation of the aminosilane is minimal since there is no
noticeable band around 1115 cm^{-1} due to the SiOSi groups. A very
strong broad band at 972 cm^{-1} with a shoulder at 909 cm^{-1} has been
observed. These two bands can be assigned to the antisymmetric
SiO$^-$ stretching modes and the line at 705 cm^{-1} in the Raman
spectrum (figure 2) to the symmetric SiO$^-$ stretching mode of the
SiO_3^{-3} groups. Using an analogy previously described for the vinyl
functional silane, the SiO$^-$ stretching mode of the $H_2N(CH_2)_3SiO_2^{-2}$

or $H_2N(CH_2)_3SiO^-$ is expected to be in the vicinity of 941 cm^{-1} which is slightly too high for the mode observed in the amino- silane in water (920 cm^{-1}), again implying that the band around 920 cm^{-1} is due to the strongly hydrogen bonded SiOH group instead of SiO^- groups.

In order to further study the possible interaction between the NH_2 and SiOH groups, a model compound, γ-aminopropyldimethy- lethoxysilane, was used. This silane yields only one silanol group after hydrolysis so that the condensation product consists only of a dimer. Hence, it is much simpler to follow the structural changes.

The Raman spectra of γ-aminopropyldimethylethoxysilane and its 20% by weight aqueous solution are shown in figure 10 where the strongest mode at 622 cm^{-1} due to the symmetric SiC_3 stretching mode shifts to 632 cm^{-1} upon hydrolysis. The spectrum was taken within 45 min. after the hydrolysis. After 1 h, the homogeneous solution showed a phase separation and the oily top layer consisted mainly of the dimer, $H_2N(CH_2)_3Si(CH_3)_2-O-(CH_3)_2Si(CH_2)_3NH_2$, with a small amount of monomer. The oily layer was heated at 80°C for 30 min. to ensure the complete condensation of residual monomers. The Raman spectrum of the dimer (figure 11) clearly shows the evidence of dimerization characterized by the strong broad line at 533 cm^{-1} due to the symmetric SiOSi stretching mode, which is analogous to the same mode at 523 cm^{-1} of $(CH_3)_3SiOSi(CH_3)_3$ (23). The absence of this strong line in the spectrum of the aqueous

solution in figure 10 indicates that most silane molecules
exist as monomers.

The FT-IR difference spectrum of the 20% by weight of γ-amino-
propyldimethylethoxysilane aqueous solution along with the spectra
of the original silane solution and ethanol/water mixture are
illustrated in figure 12. An interesting fact is that a strong
band appears at 874 cm^{-1} which is a normal SiO stretching frequency
of the SiOH groups. A comparison with the FT-IR spectrum of the
dimer (figure 13) reveals that the band at 874 cm^{-1} is unique
to the hydrolyzed monomer. The amine band of the hydrolyzed
monomer at 1598 cm^{-1} is essentially unchanged in frequency upon
dimerization. However, a frequency decrease from 1607 to 1597 cm^{-1}
is seen as one compares the unhydrolyzed monomer and the condensed
dimer. This frequency change is not due to the hydrogen bonding
with water or silanols because no hydroxyl groups are available
in these samples. Probably the unhydrolyzed aminosilane exists
as hydrogen bonded amines which are then hydrated and separated
from each other in aqueous solutions. The unhydrolyzed amines
show a doublet indicating the hydrogen bonding of the type, NH····N,
where one amine is a donor and the other is an acceptor.

Another model aminosilane is γ-aminopropylmethyldiethoxysilane,
$H_2N(CH_2)_3Si(CH_3)(OC_2H_5)$. This silane yields linear polysiloxane
chains with varying lengths upon hydrolysis and subsequent conden-
sation. Therefore, only the amine groups at the both ends of the

chain can intramolecularly hydrogen bond with silanols. This silane is difficult to dissolve in water and requires an alcohol/water mixture to hydrolyze. Incompletely cured oligomers (Figure 14 : spectrum A) show two bands at 960 and 914 cm^{-1}.

DISCUSSION

The major question of this paper concerns the structures of the amine and silanol groups in solution and the incompletely cured solid. There are spectral differences between the incompletely condensed aminosilanes as an aqueous solution and a solid even though the degree of condensation is similar. The amine group in solution usually shows a single band around 1599 cm^{-1} regardless of the degree of condensation. However, when the solvents evaporate and either a viscous liquid or solid form, this weak amine band gains intensity and shifts down to around 1570 cm^{-1}. A new strong band appears at 1484 cm^{-1}. A symmetry analysis predicts two bands from the NH_3^+ group and, therefore, it is thought t arise from an interaction of the type, $SiO^- \cdots \cdots ^+NH_3$. This ructure would lead to the observation of the SiO^- stretching mode. All primary amine salts show these two strong modes (24) though the frequencies depend on the counter ions. In addition to the two modes mentioned above, amine salts show further characteris-tic features. A very broad intense band appears in the range 3200 - 2800 cm^{-1} and its low frequency side often shows fine structure. Moreover, a weak to medium but characteristic band arises around 2300 - 2000 cm^{-1} due to the combination band of the

NH_3^+ bending and torsional modes. All these modes are not observed in the solution spectra. Spectral features of the amine bands favor the existence of the NH_3^+ group though not necessarily conclusively.

As mentioned above, the formation of amine salt requires the observation of SiO^- groups. An incompletely cured poly-aminopropylsiloxane (figure 7) shows two bands around 960 cm^{-1} and 930 cm^{-1} which may be assigned to the SiO^- and $SiOH$ groups, respectively. The 960 cm^{-1} band overlaps with the previously discussed band at 960 cm^{-1} of the unhydrolyzed silanes. However, the sample shown in figure 7 is prepared from a well hydrolyzed, low concentration solution. However, a series of hydrolyzed and incompletely cured γ-aminopropyltriethoxysilane, γ-aminopropylmethyl-dimethoxysialane and γ-aminopropyldimethylmethoxysilane, show the two modes at 960 and 930 cm^{-1}, 960 and 914 cm^{-1}, and 960 and 874 cm^{-1}, respectively. It is reported that the SiO stretching mode decreases in frequency when the oxygen atoms are replaced by carbon atoms (25). The modes at higher frequency are, however, insensitive to the replacement of oxygen atoms to carbon atoms. If these are assigned to the SiO^- stretching modes, a similar tendency is expected since the effect of electronegativity of the carbon atoms on the silicon atom is the same for the SiO^- and $SiOH$ groups. On the contrary, no frequency shift is observed, which leads us to postulate that the band at 960 cm^{-1} is a vibrational mode of a group unaffected or far from the silicon atom. No amine bands are

known in this range. Moreover, a medium intensity Raman line around 964 cm^{-1} is seen in the spectra of completely cured polyaminopropylsiloxane and the dimer of the hydrolyzate of γ-aminopropyldimethylmethoxysilane. Hence, the C-C group next to the amine group is probably responsible for this mode. Accordingly, only one band is assignable either to SiO^- or SiOH vibration.

The band at 920 cm^{-1} of the polyaminopropylsiloxane in water is lower than the expected SiO^- stretching mode by 21 cm^{-1} as described earlier. In addition, the incompletely cured poly-aminopropylsiloxane condenses and forms SiOSi bonds even in dry air and shows a decrease of the intensity of the band at 930 cm^{-1} indicating that the 930 cm^{-1} is due to the SiOH groups. Further-more, the difference spectrum shows a broad band at 3300 cm^{-1} which decreases, corresponding to the decrease in the 930 cm^{-1} band, and almost no intensity change at the 1635 cm^{-1} band which is probably due to the adsorbed water. The weakening of the bands at 3300 and 930 cm^{-1} are, therefore, due to the OH stretching mode and SiO stretching mode of the residual SiOH groups (26). Weakening of hydrogen bonding of the $SiO^-\cdots H\cdots^+NH_2$ also leads to similar effects. However, it should be noted that a weakening of the hydrogen bonding results in a frequency increase of the OH stretch-ing mode. The resultant spectral feature of the difference spectrum is, therefore, a derivative appearance instead of the observed monotonous intensity decrease.

CONCLUSIONS

We have studied the FT-IR and Raman spectra of γ-aminopropyltriethoxysilane (γ-APS) and its analogues before and after hydrolysis and condensation reactions. The band at 930 cm^{-1} of the incompletely cured γ-APS is assigned to the residual SiOH groups. There is no evidence of the existence of SiO^- groups under the conditions examined. One may picture $SiO^- \cdots NH_3^+$ as an extreme case of $SiO \cdots H \cdots {}^+NH_2$. However, the perturbations of the SiO stretching mode are not strong enough to compare with such ionic groups as $RSi(O^-K^+)_3$. In light of the mild conditions required for complete elimination of SiOH groups, the structure $SiO^- \cdots H \cdots {}^+NH$ is favored instead of $SiO^- \cdots NH_3^+$.

REFERENCES

1. E. P. Plueddemann ed., "Interfaces in Polymer Matrix Composites, in a series "Composite Materials; Vol G", ed. by L.J. Brautman and R. H. Krock, Academic Press, New York (1974).

2. S. Sterman, and H. B. Bradley, SPE Trans., 1, 224 (1961).

3. O. K. Johanson, F. O. Stark, and R. Baney, AFML-TRI-65-303, Part I (1965), G. E. Vogel, O. K. Johanson, F. O. Stark, and R. M. Fleishmann, Proc. 22nd Ann. Tech. Conf., Reinforced Plast. Div., SPI, Section 13-B (1967). O.K.Johanson, F. O. Stark, G.E. Vogel, and R. M. Fleishmann, J. Comp. Mater., 1, 278 (1967).

4. D.J. Tutas, R. Stromberg, and E. Passaglia, SPE Trans.,4, 256 (1964).

5. L. H. Lee, Proc. 23rd Ann. Tech. Conf., Reinforced Plast. Div., SPI, Section 9-D (1968). L. H. Lee, J. Colloid Interface Sci., 27, 751 (1968).

6. M. E. Schrader, I. Lerner, and F. J. D'Oria, Mod. Plast., 45, 195 (1967).

7. M. E. Schrader, J. Adhesion, 2, 202 (1970).

8. W. D. Bascom, Macromolecules, 5, 792 (1972).

9. P.T.K. Shih, and J. L. Koenig, Mat. Sci. Eng., 20, 145 (1975).

10. F. J. Boerio, L. H. Shoenlein, and J. E. Greivenkamp, J. Appl. Polym. Sci., 22, 203 (1978). E. G. Brame, Jr., ed., "Applications of Polymer Spectroscopy", Academic Press, New York (1978), Ch. 11 by F. J. Boerio.

11. H. R. Anderson, Jr., F. M. Fowkes, and F. H. Hielscher, J. Polym. Sci.-Phys., 14, 879 (1976).

12. P. R. Moses, L. M. Wier, J. C. Lennox, H. O. Finklea, J. R. Lenhard, and R. W. Murrary, Analytical Chem., 50, 576 (1978).

13. C. H. Chiang, H. Ishida, and J. L. Koenig, J. Colloid Interface Sci., 74, 396 (1980).

14. A. T. DiBenedetto, and D. A. Scola, J. Colloid Interface Sci., 99, 6780 (1978).

15. A. F. Diaz, U. Hetzler, and E. Kay, J. Am. Chem. Soc., 99, 6780 (1977).

16. J. F. Cain, and E. Sacher, J. Colloid Interface Sci., 67, 538 (1978).

17. H. Ishida, and J. L. Koenig, J. Polym. Sci.-Phys., 17, 1807 (1979).

18. H. Ishida, and J. L. Koenig, Appl. Spectry., 32, 462 (1978).

19. H. Ishida, and J. L. Koenig, Polymer, submitted.

20. P. T. K. Shih, and J. L. Koenig, Mat. Sci. Eng., 20, 137 (1975).

21. H. Ishida, and J. L. Koenig, unpublished results.

22. H. Murata, H. Matsuura, K. Ohno, and T. Sato, J. Mol. Struct., 52, 1 (1979).

23. A. L. Smith, "Analysis of Silicones", Wiley-Interscience, New York (1974) p. 262.

24. N. B. Colthup, L. H. Daly, and S. E. Wiberley", Introduction to Infrared and Raman Spectroscopy", Academic Press, New York (1975).

25. P.T.K.Shih and J. L. Koenig, Mat. Sci. Eng., 20, 145 (1975).

26. H. Ishida and J. L. Koenig, to be published.

FIGURE CAPTIONS

Figure 1. The Raman spectrum of unhydrolyzed γ-aminopropyltrimeth-
    oxysilane.

Figure 2. The Raman spectra of the hydrolyzate of γ-aminopropl-
    trimethoxysilane. A; 20% by weight in H_2O. B; 20% by weight
    in KOH solution. The mole ratio of the silane and KOH is 1:6.

Figure 3. Completely cured polyaminopropylsiloxane treated at
    110°C for 1 h under vacuum.

Figure 4. The FT-IR difference spectra of hydrolyzed γ-aminopropy-
    ltriethoxysilane in H_2O at various concentrations. The absor-
    bance contributions of the ethanol and water are subtracted.

Figure 5. The FT-IR difference spectrum of hydrolyzed γ-aminopropyl-
    triethoxysilane in H_2O at 20% by weight.

Figure 6. The FT-IR difference spectrum of hydrolyzed γ-aminopropyl-
    triethoxysilane in H_2O at 2% by weight.

Figure 7. The FT-IR spectra of polyaminopropylsiloxane. A;
    incompletely cured. B; completely cured at 110°C for 1 h
    under vacuum.

Figure 8. The Raman spectra of the hydrolyzate of vinyltrimetho-
    xysilane. A; 20% by weight in H_2O. B; 20% by weight in KOH
    solution. The mole ratio of the silane and KOH is 1:6.

Figure 9. The FT-IR difference spectrum of γ-aminopropyltrisilanolate
    in KOH solution. The concentration of the original silane is
    20% by weight and the mole ratio of the silane and KOH is 1:6.
    The absorbance contributions of the ethanol and KOH solution
    are subtracted.

Figure 10. The Raman spectra of γ-aminopropyldimethylethoxysilane
    (A) and its hydrolyzate in H_2O at a concentration of 20% by
    weight (B).

Figure 11. The Raman spectrum of the condensed dimer of the
    hydrolyzate of γ-aminopropyldimethylethoxysilane.

Figure 12. The FT-IR spectra of the hydrolyzed γ-aminopropyldi-
    methylethoxysilane A; 20% by weight aqueous solution of the
    silane. B; 20% by weight aqueous solution of ethanol. C;
    the difference spectrum showing predominantly γ-aminopropyl-
    dimethylsilanol.

Figure 13. The FT-IR spectrum of the condensed dimer of the hydrolyzate of γ-aminopropyldimethylethoxysilane.

Figure 14. The FT-IR spectra of the hydrolyzate of γ-aminopropyl-methyldiethoxysilane. A; incompletely cured silane. B; completely cured silane at 110°C for 1 h under vacuum.
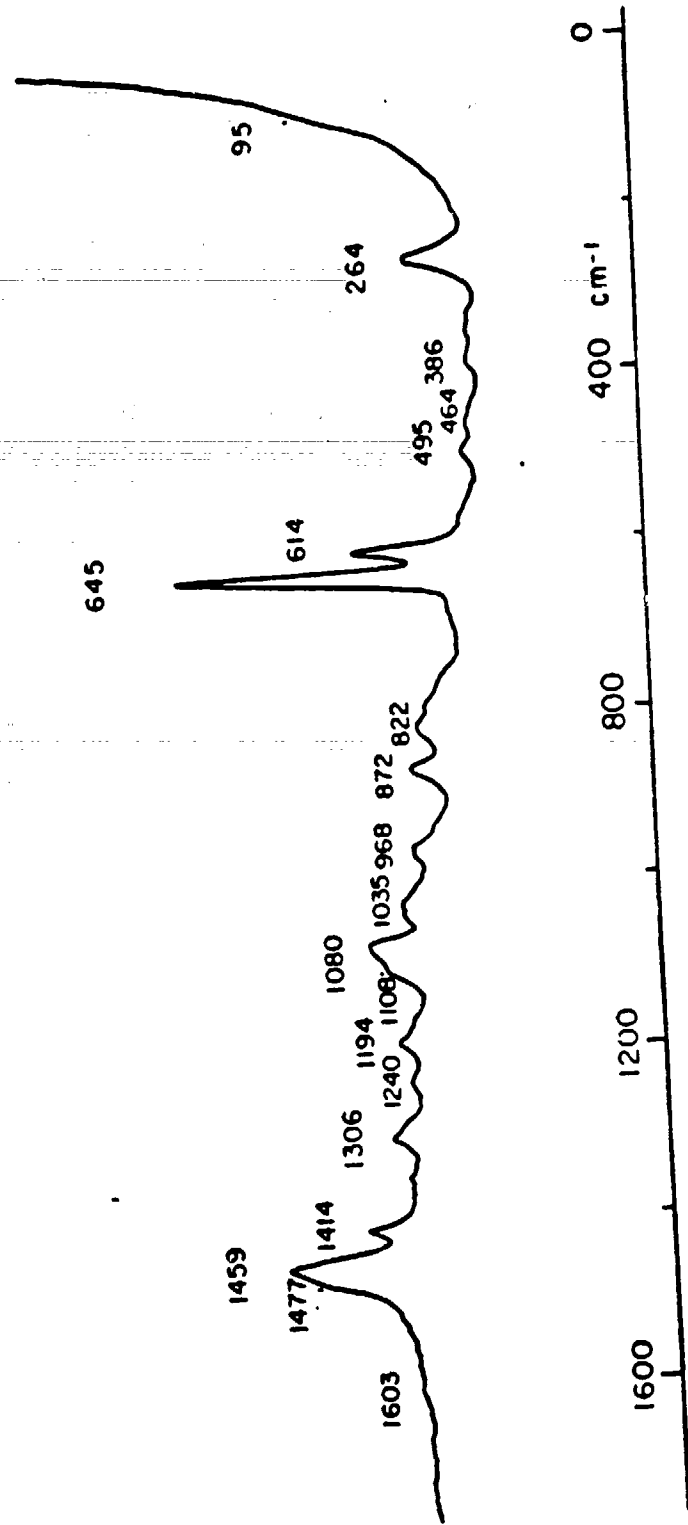
Figure 1
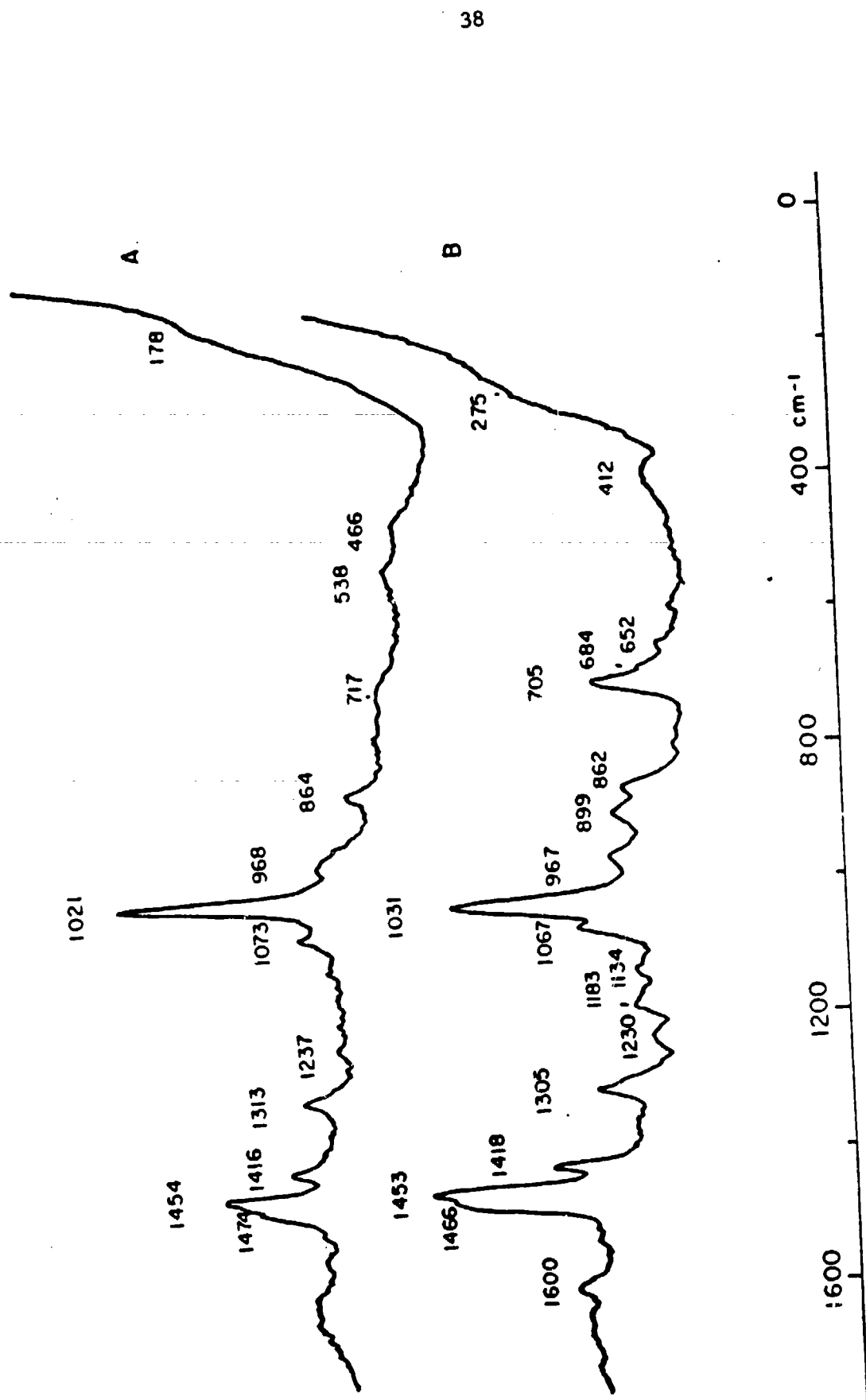
Figure 2

Figure 3

40
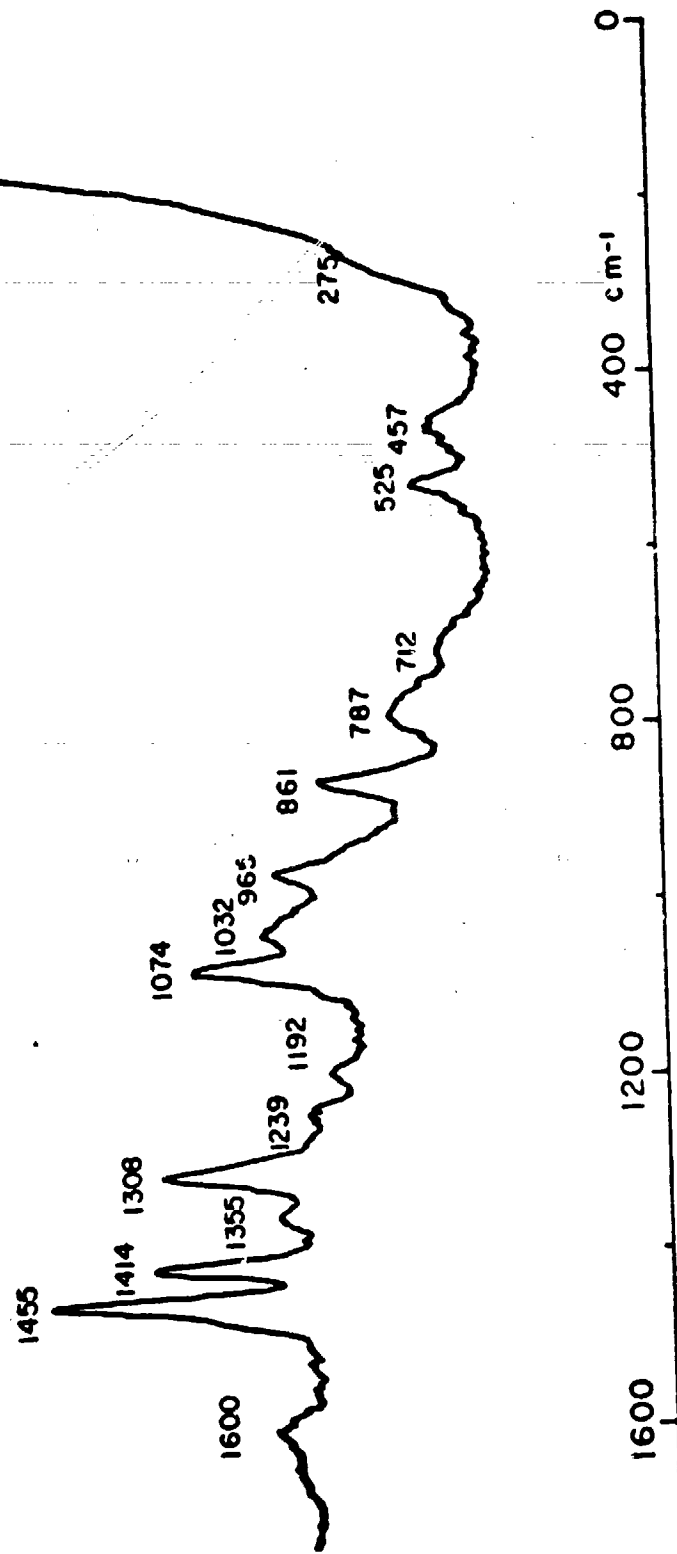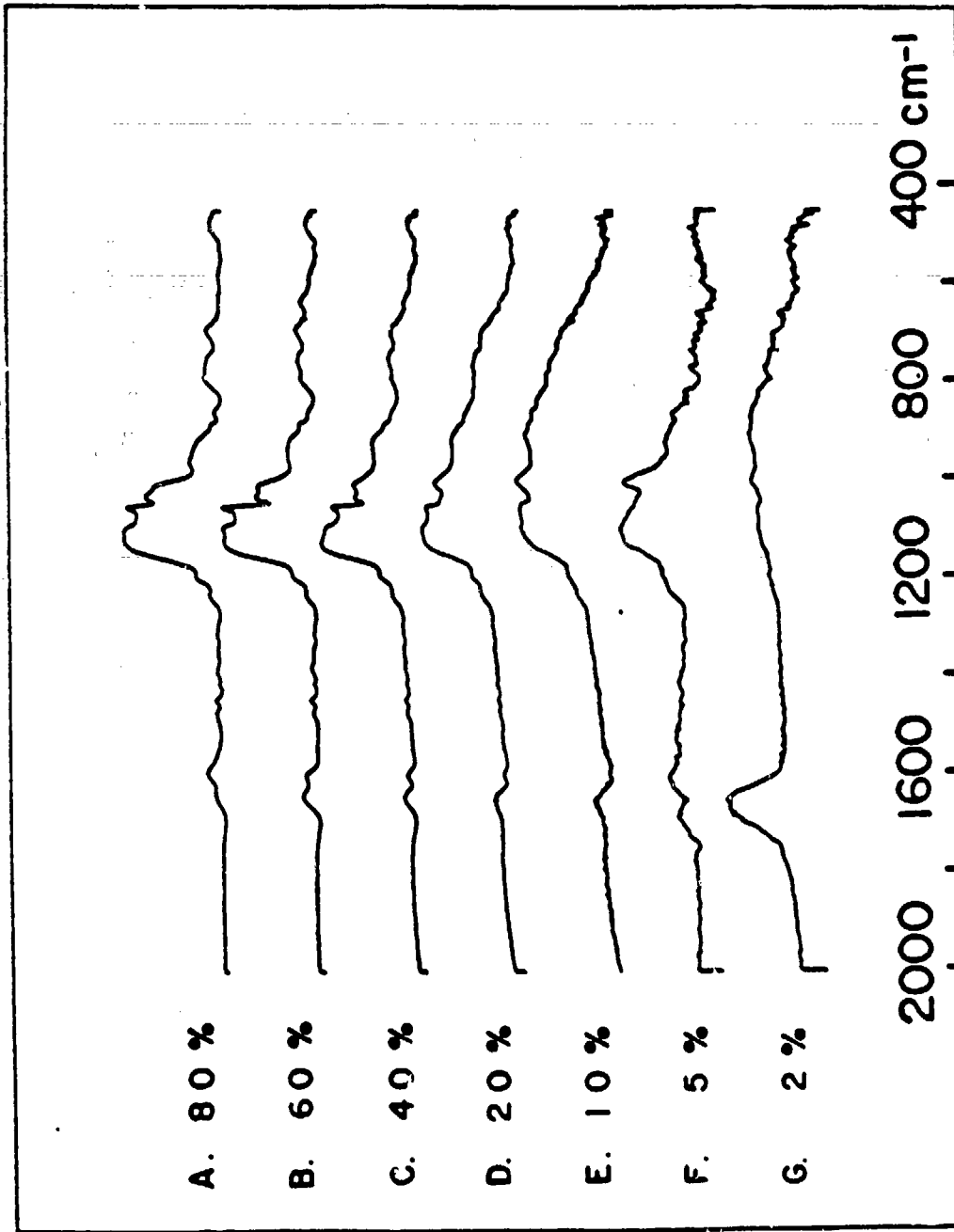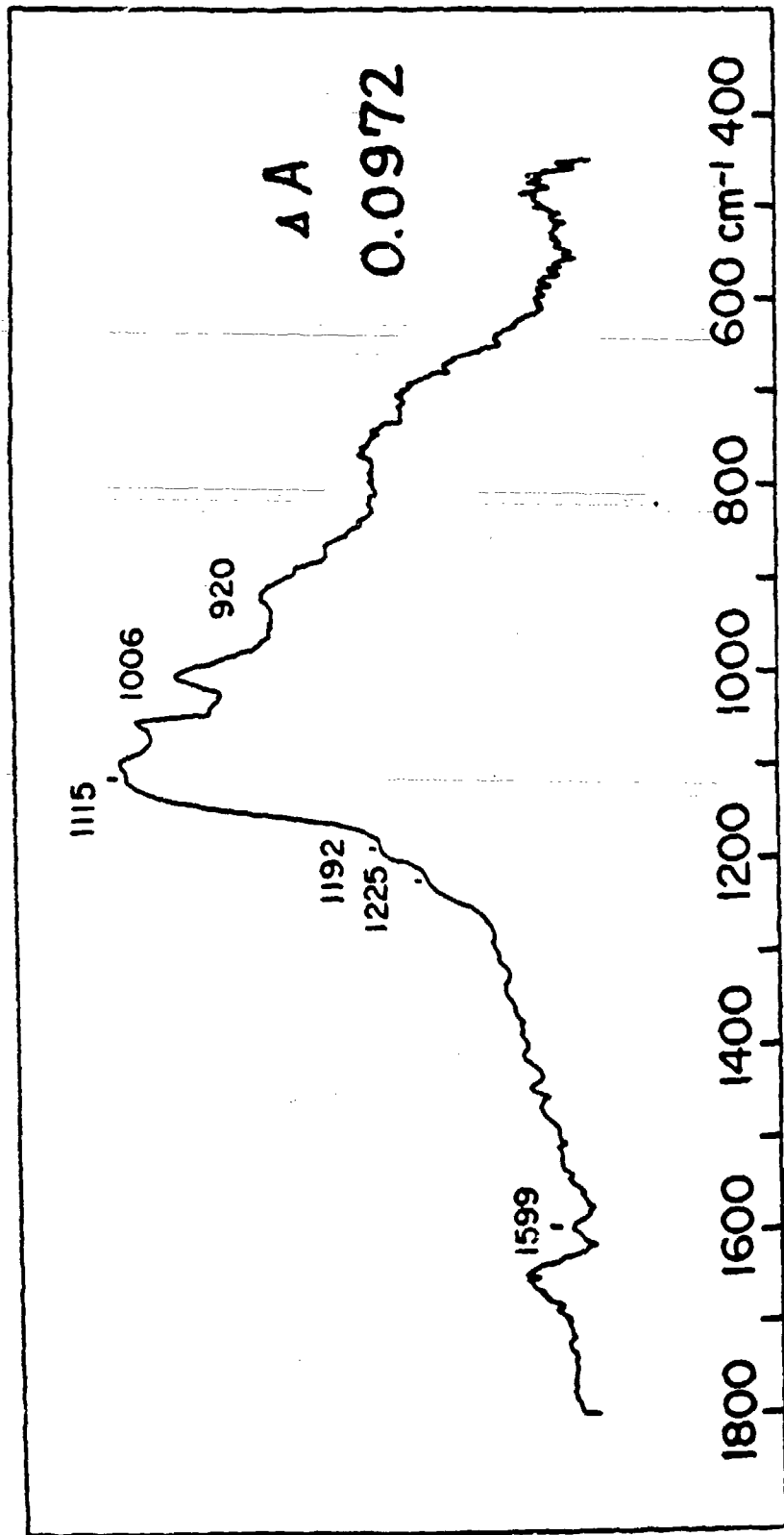
Figure 4.

Figure 5

Figure 6

Figure 7

Figure 8

$H_2N(CH_2)_3Si(O^-K^+)_3$

972

909

780

718

480

1183

1598

45

Figure 9

Figure 10

$$H_2N(CH_2)_3Si-O-Si-(CH_2)_3NH_2$$

with substituents CH_3, CH_3 on the first Si and CH_3, CH_3 on the second Si.

Figure 11

Figure 12

$$CH_3 \quad CH_3$$
$$H_2N(CH_2)_3\text{-}Si\text{-}O\text{-}Si\text{-}(CH_2)_3NH_2$$
$$CH_3 \quad CH_3$$
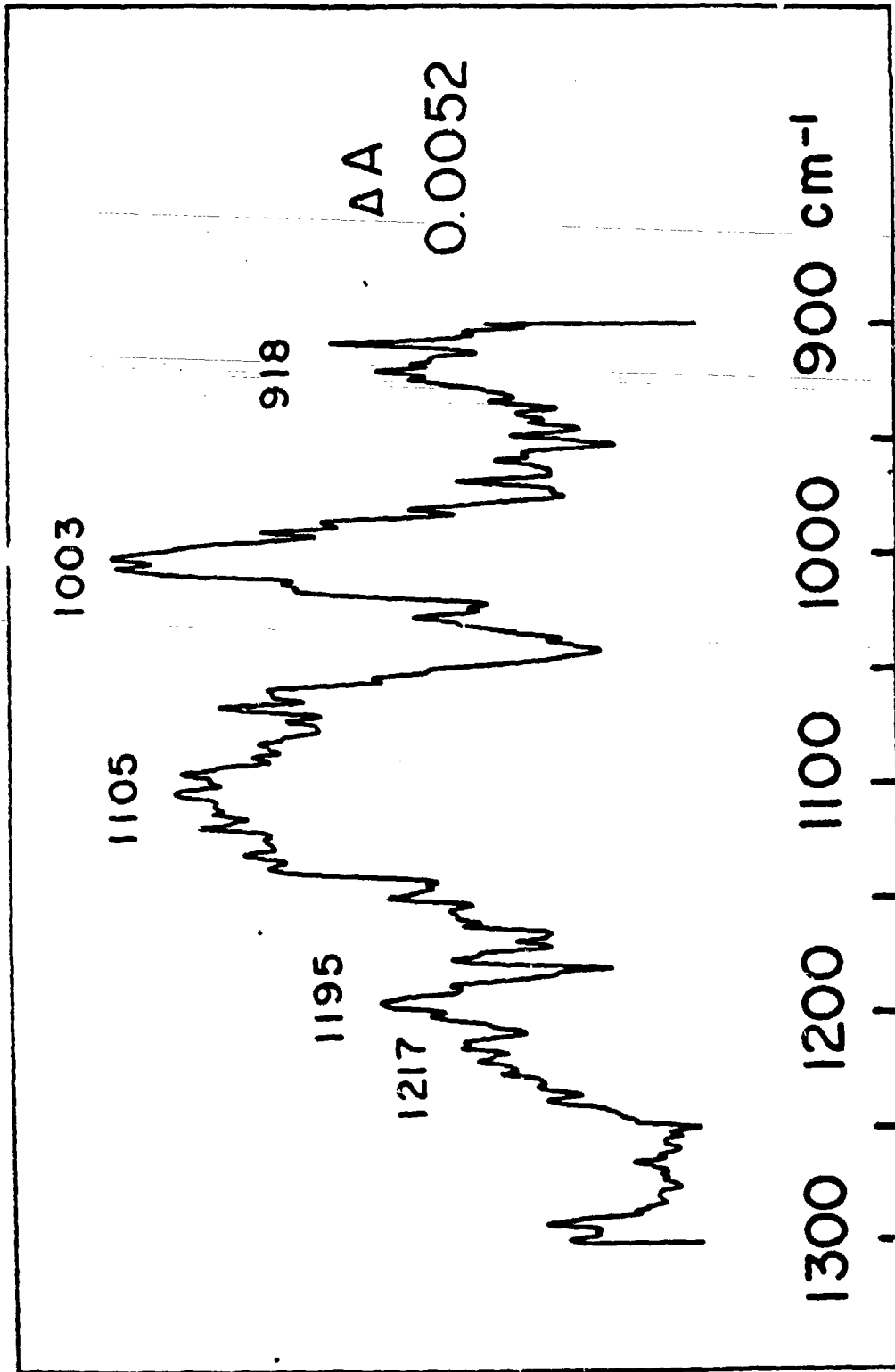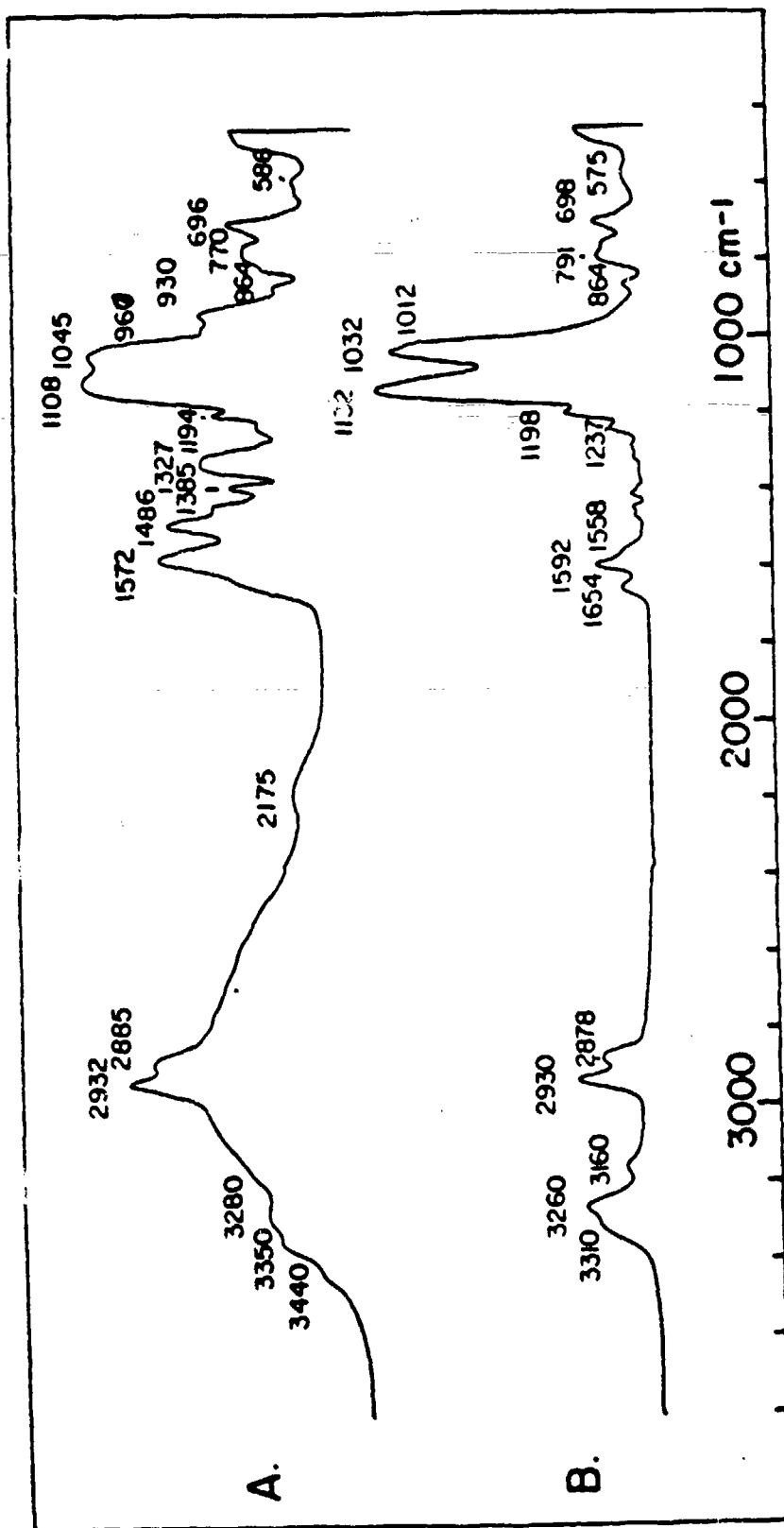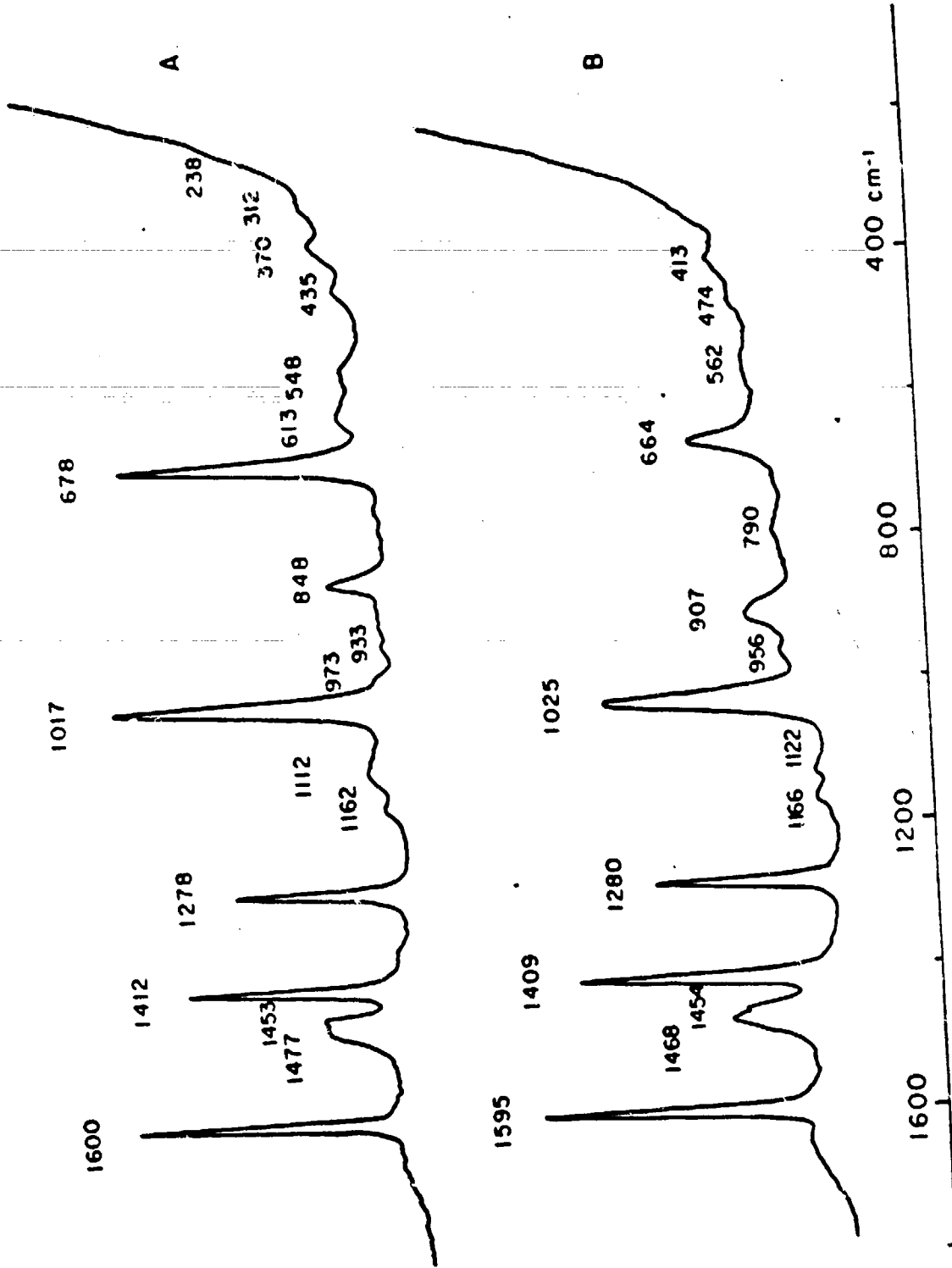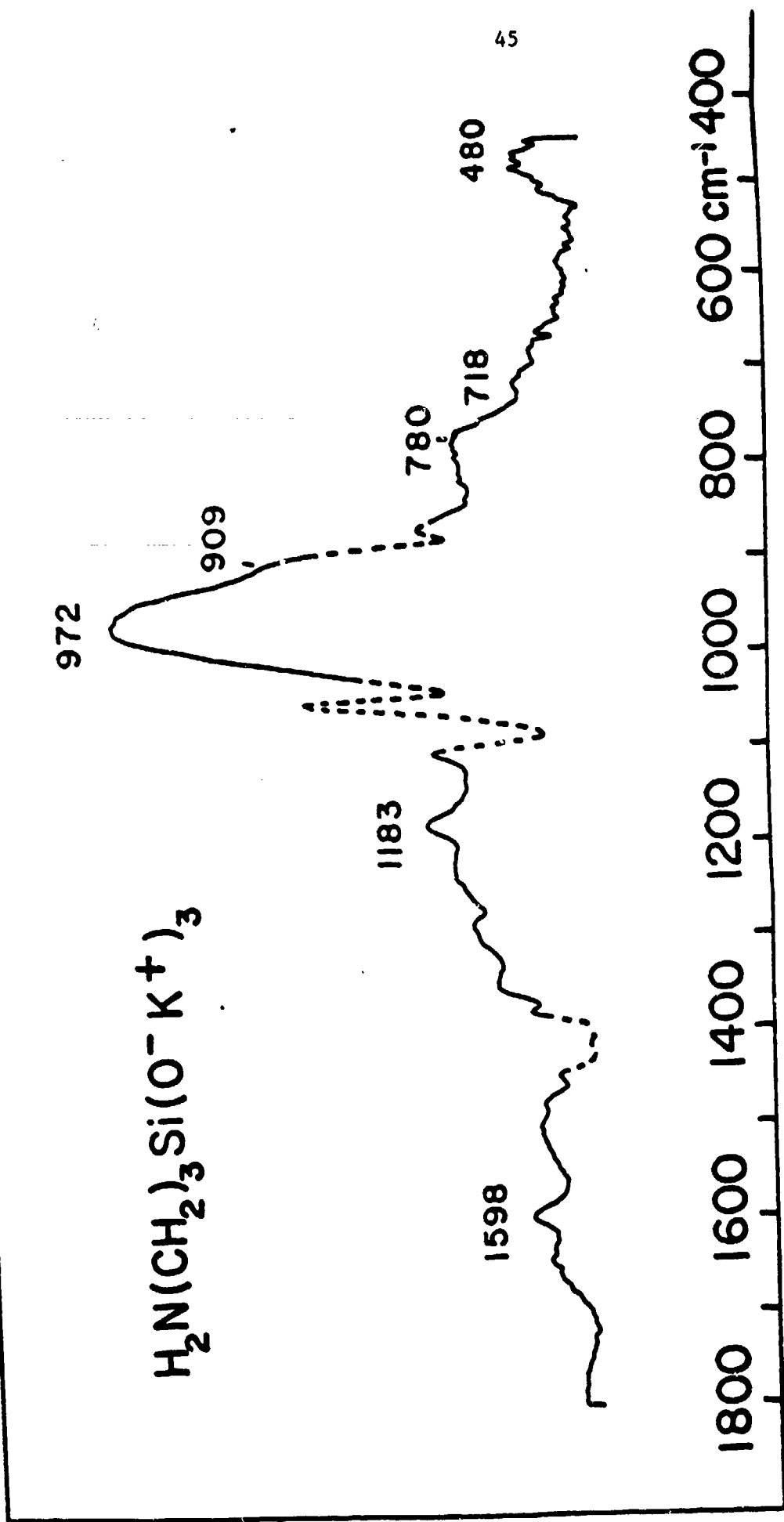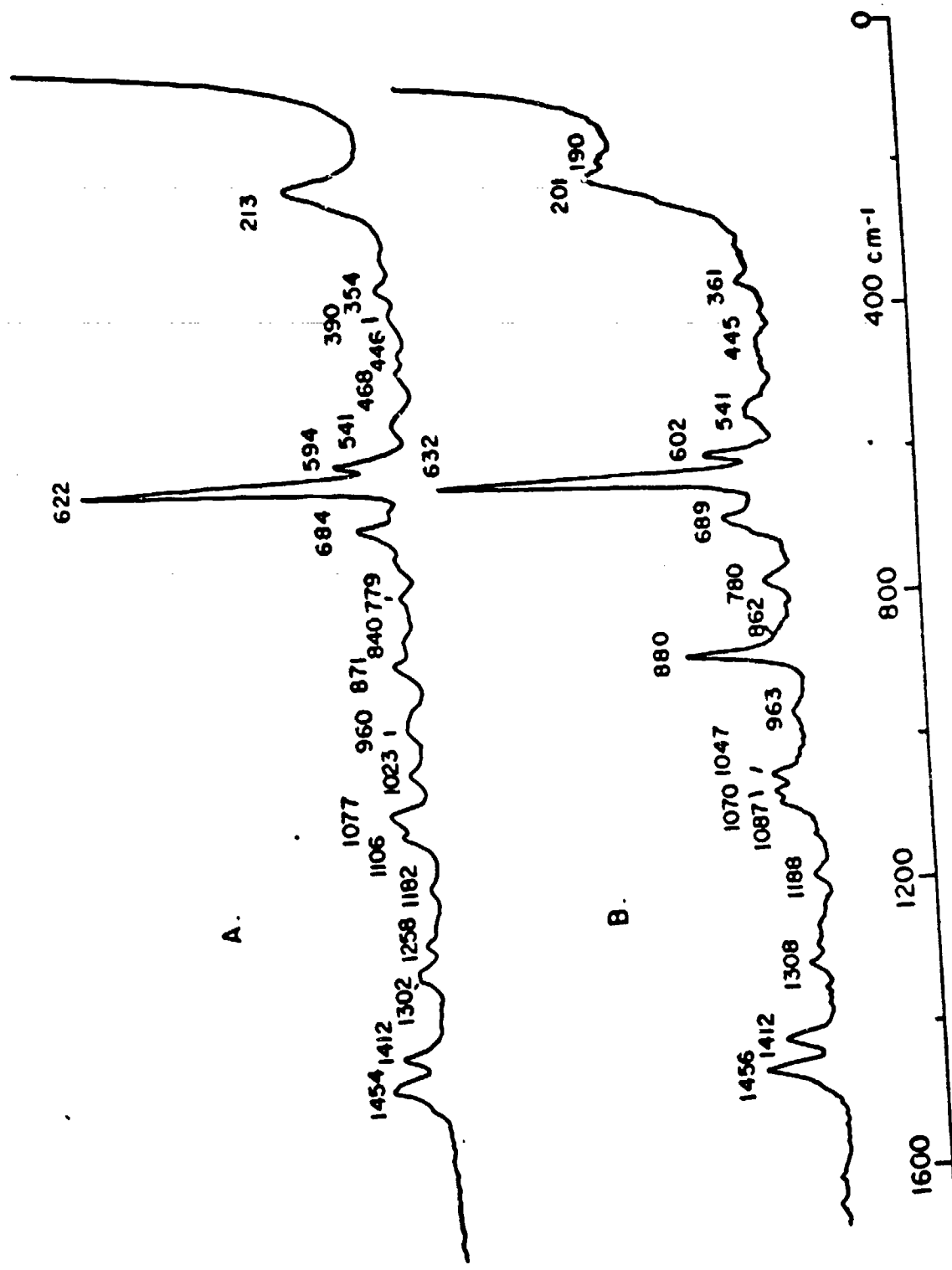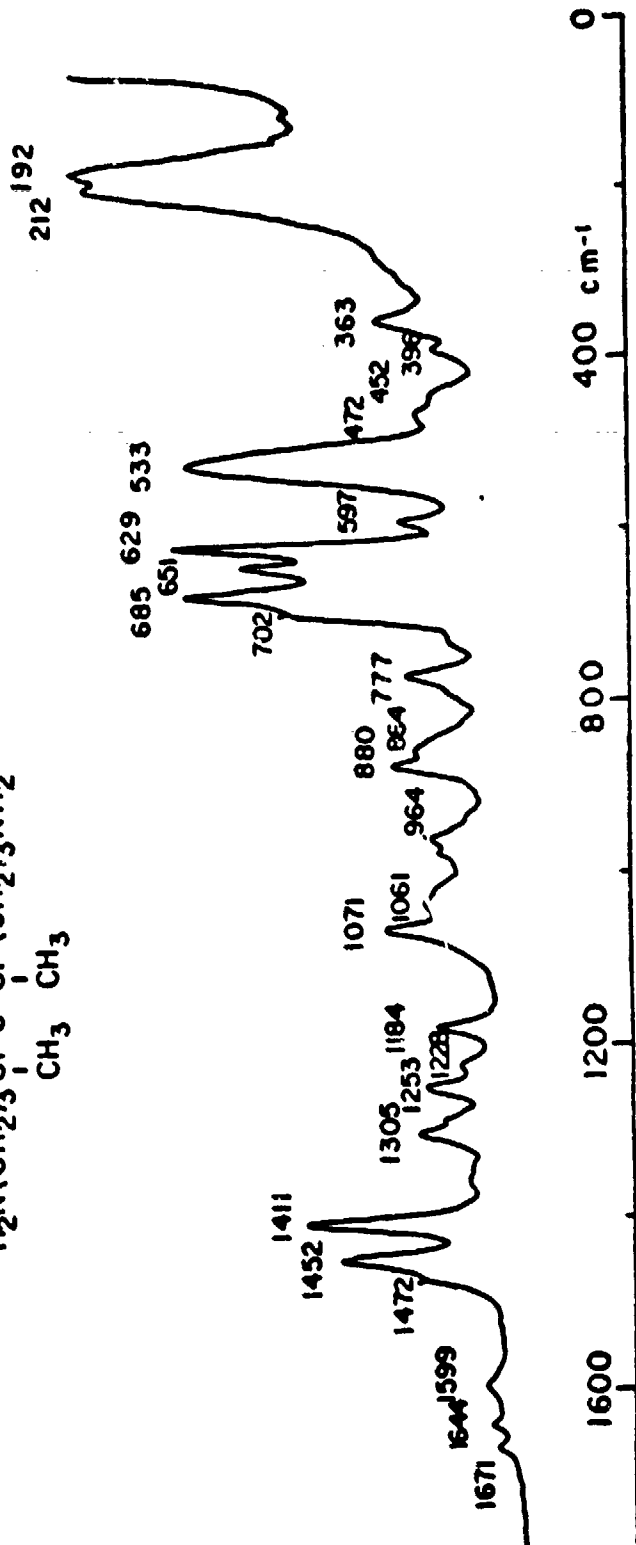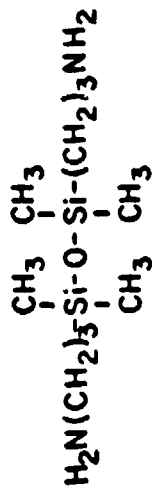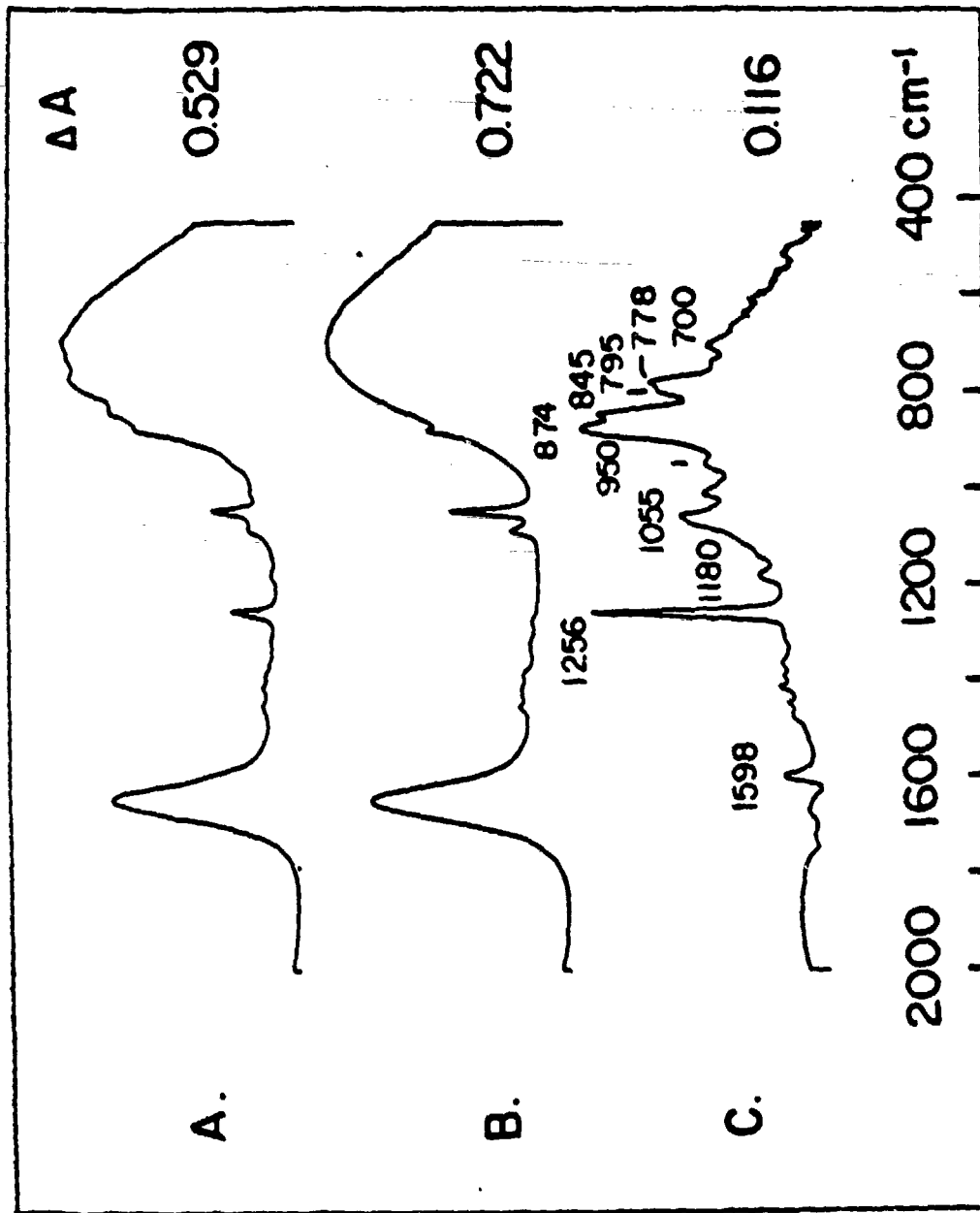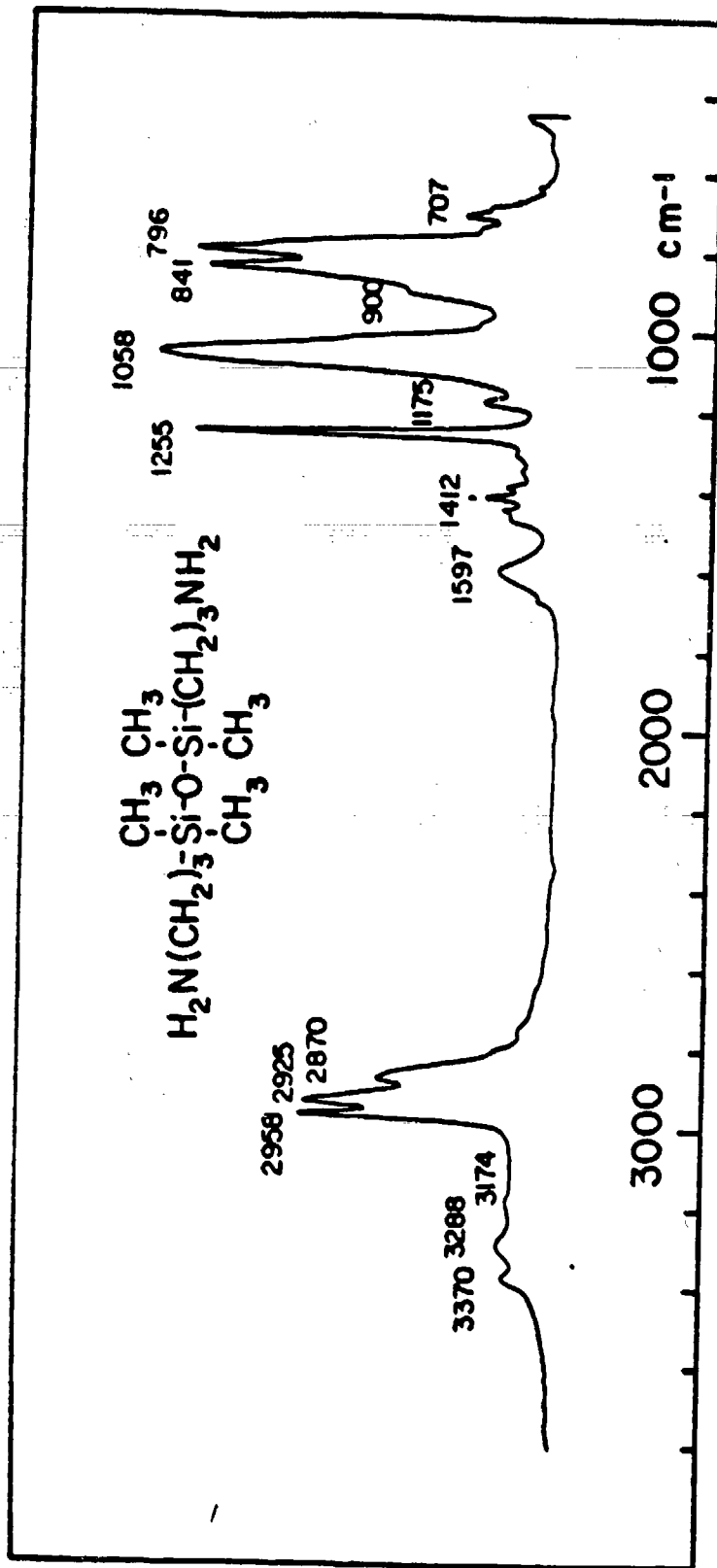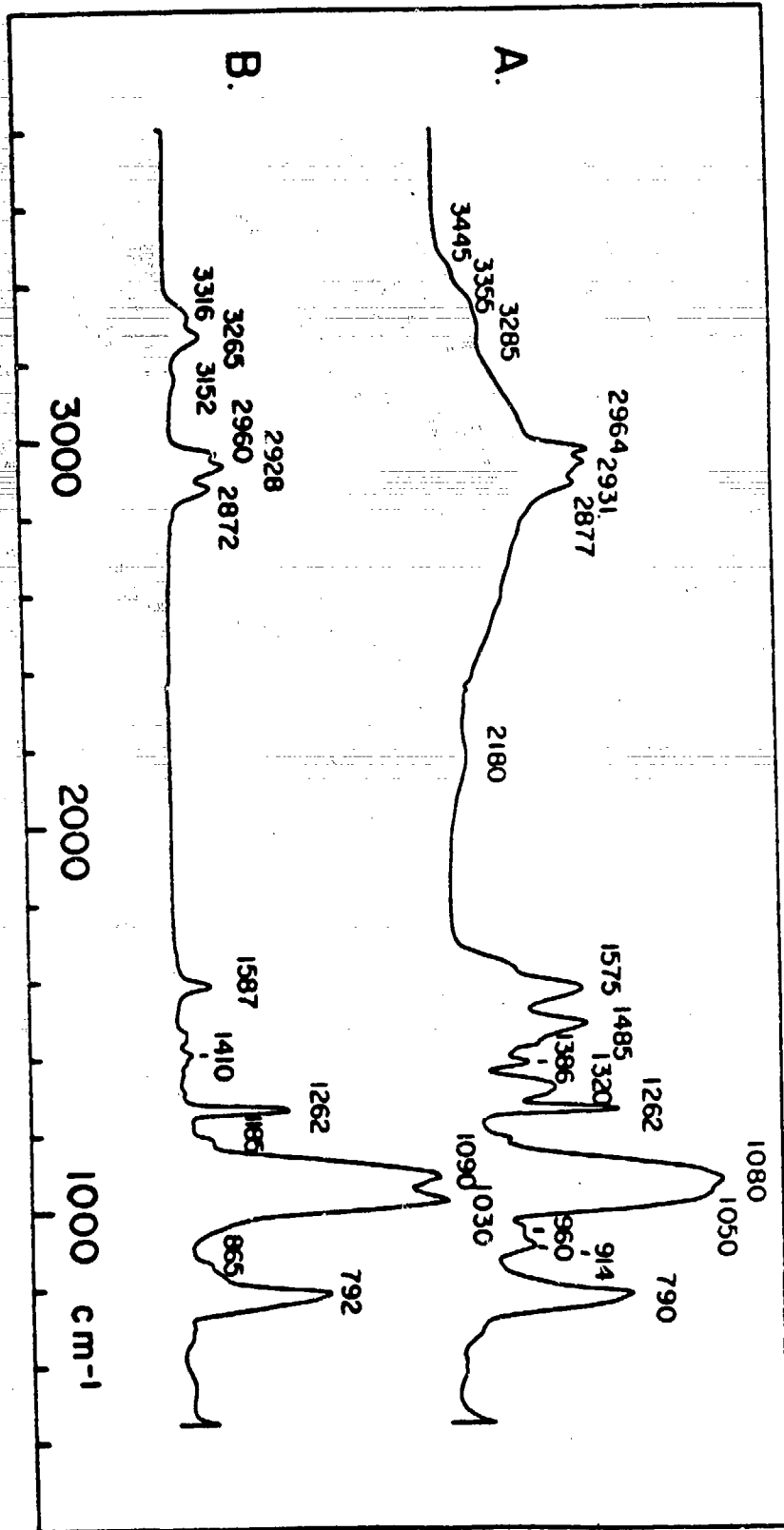
Figure 13

Figure 14

SPECTROSCOPIC CHARACTERIZATION OF THE MATRIX-SILANE COUPLING

AGENT INTERFACE IN FIBER REINFORCED COMPOSITES

by

* Chwan-hwa Chiang and Jack L. Koenig

Department of Macromolecular Science

Case Western Reserve University

Cleveland, Ohio   44106

* Present Address: Research Center, Sherwin-Williams Co.
                     10909 S. Cottage Grove, Chicago, IL 60628

SPECTROSCOPIC CHARACTERIZATION OF THE MATRIX-SILANE COUPLING AGENT INTERFACE IN FIBER REINFORCED COMPOSITES

by

Chwan-hwa Chiang and Jack L. Koenig

Department of Macromolecular Science

Case Western Reserve University

Cleveland, Ohio 44106

ABSTRACT

The copolymerizations of anhydride-cured epoxy resin on fiberglass sur-
faces treated with a N-methylaminopropyltrimethoxysilane (MAPS) coupling agent
has been investigated using Fourier-transform Infrared Spectroscopy. The
structure of the interface of the silane and the resin in fiber-reinforced
composites is composed of copolymers of the epoxy resin with the organofunc-
tionality of the deposited silanes. The number of interfacial bonds formed
depends on the amount of silane coupling agent deposited on the fiberglass and
the reaction conditions. The silane induces additional esterification and
increases the curing density of the epoxy matrix near the fiber surface,
about 5-10% relative to the bulk resin. Thus, there is a gradient in the com-
position of the matrix from the fiber surface to the bulk. This gradient in
structure would appear to influence the ultimate composite properties.

INTRODUCTION

It is generally accepted that the function of the low modulus polymeric matrix in fiber reinforced composites is to distribute stress to the high modulus fibers which carry essentially the entire loads. Since stress is transferred in shear through the interface, good adhesion between the matrix and fiber is required. The chemical treatment of the surface of glass has long been part of the processing technology to improve the adhesion in fiber reinforced composites. Applications of silane coupling agents usually yields higher mechanical properties and improved chemical resistance of composites (1-4).

Due to the existence of multiple interfaces in fiberglass reinforced composites, good adhesion must be obtained at all interfaces. Good interfacial adhesion can be obtained if covalent linkages are formed between the two phases (5). Under suitable process conditions the fiber glass and the coupling agent are connected through chemical bonds. The silane coupling agents exist as multilayered films on the glass surfaces with the molecules joined by Si-O-Si bonds (6,7). The molecular organization of the coupling agent deposited on surfaces depends on the nature of silanes and the processing conditions (8,10). On the other hand, little research work has been presented concerning the coupling agent-matrix interface in composites. Plueddemann has reported on a number of unsaturated silanes used in glass polyester resin composites (11). The amount of vinyl functional groups decreased as a result of interfacial bonds formed between the matrix and coupling agent phases (11). In our previous work (12,13), we have studied the chemical reactions occuring at the interface of aminosilane coupling agents and anhydride-cured epoxy matrices in fiber reinforced composites. However, detailed studies

of the amount of interfacial bonding between the epoxy matrix and coupling

agent on the fiber have not been reported. Therefore, more quantitative work

is required in order to characterize the structure of the interface.

By varying the amount of the silane on the fiber surface one can obtain

information about the extent of the resin-silane reactions and the structure

of the resin-silane interface. Variations of fiber fraction also influence

the surface-to-volume ratios of the matrix phase and provide information of

the effect of surface induced chemical reactions on the state of cure of the

matrix in contact with the coupling agent. The purpose of this paper is to

present our determinations of the molecular structure at the coupling agent-

resin interface in fiber reinforced composites. A model of the interface

region at the molecular level is proposed and this may be useful in under-

standing the mechanical behavior of composite materials.

EXPERIMENTAL

A. Materials:

The N-methylaminopropyltrimethoxysilane (MAPS) was purchased from

Petrarch Systems Inc. E-Glass fiber (Craneglas grade 50-01) was heat-cleaned

at 500°C in air for one day before being used (1). The cleaned glass fiber

was treated with 0.5% to 2.0% by weight of MAPS in PH=5 aqueous solutions and

dried in air for one day. Subsequently, the fibers were evacuated at 50°C

for an additional ten hours and stored in a desiccator.

The matrix system under investigation was EPON 828 (Shell Co.), a diglycer-

ide of bisphenol A-based epoxy resin, crosslinked by nadic methyl anhydride (NMA)

(Fischer Scientific). The crosslinking reaction, accelerated by small amounts

of benzyldimethylamine (BDMA) (Eastman Kodak), results in the formation of a

crosslinked 3-dimensional polyester matrix. The ratio of epoxy resin, anhy-

dride, and accelerator for making the composites is 100:100:1 by weight.

The silane-treated fiber was mixed with uncured epoxy resin at room tempera-

ture and then cured at 150°C for 3 hours between two iron plates with a fixed

spacing.

B.   INSTRUMENTATION

A Fourier transform infrared spectrometer (DigiLab FTS-14) was utilized.

The absorbance spectra of E-glass reinforced composites were obtained from

30 mgs of KBr pellets containing approximately 2 mgs of finely-ground mater-

ials removed from the composites with a metal file. The spectra are recorded

in double precision at a resolution at 4 cm^{-1} with a total of 200 scans for

signal averaging. The frequency scale is calibrated internally with a refer-

ence helium-neon laser to an accuracy of 0.01 cm^{-1}. Spectra were stored in

the absorbance mode on magnetic tape pending further analysis. The digital

subtraction method and integrated absorbance measurements are run on the dedi-

cated minicomputer serving the spectrometer as described previously (14).

RESULTS

First, we studied the effect of silane treatment of the glass on the

curing of the anhydride-cured epoxy resin (EPON 828, Shell Co.). Initially, the

polymerization process was followed in the presence of different amounts of

E-glass fiber. The infrared absorbance spectra of these composites with fiber

weight percent of 12, 17, 22, 28, and 35% have been investigated. The spectrum of the pure epoxy matrix was also obtained, which was made under the same conditions but with no fiber. The copolymerization of the anhydride cured epoxy resin was followed by means of absorbance bands appearing at 1183, 1250, and 1744 cm^{-1} that are due to the vibrational modes of ester groups in the matrix (15).

Five control composites were made using the same procedures and the same content of untreated fiber. The spectra of the silane-treated glass and non-treated glass composites that had 28% by weight glass fiber are shown in Figures 1-A and 1-B, respectively. The difference spectrum is shown in Figure 1-C. The band appearing at 1511 cm^{-1} which is due to the C-C stretching in the benzene ring from the backbone of epoxy resin was chosen as an internal standard to calibrate the amount of organic matrix in the composites (12). The absorbance of glass fiber was removed from the total absorbance of the composite by an IR subtraction method (15). The negative absorbances below the baseline indicate the consumption of epoxy (914 cm^{-1}), anhydride (1780 cm^{-1}), and amine (3290 cm^{-1}) with curing of the composites. The positive bands appearing at 1744 cm^{-1} (ester), 1640 cm^{-1} (amide), 1183 cm^{-1} (ester), and 1098 cm^{-1} (ester) are due to the reaction products arising from differences between these two composites. The difference spectra indicate that the aminosilane treated fiber surface causes an increase in the curing of the matrix. These chemical reactions affect the crosslink density and change the properties of the resin in the vicinity of the glass surface.

The absorbance band at 1860 cm^{-1} is attributed to a carbonyl stretching mode of the anhydride. The conscentration of unreacted anhydride in cured composites is measured by the absorbance of this band. The amounts of unreacted

NMA in MAPS-treated and heat-cleaned fiber composites are shown in Figure 2. It was found that the amount of uncured NMA only slightly changed when the amount of fiber glass changed from zero to 35% by weight. From this we conclude that the heat-cleaned fiber surface does not significantly affect the curing of the matrix. On the contrary, for the MAPS-treated fiberglass, it was found that the concentration of NMA decreases when the fiber content in composites increases.

If NMA reacts with MAPS, an amide band should be observed. The absorbance band appearing at 1640 cm^{-1} in the difference spectrum is due to the amide group (12). The intensities of the amide absorbance versus the fiber contents for these composites are shown in Figure 3. The results suggest that the increased formation of the amide group is proportional to the amount of MAPS in the composites. The addition reaction of NMA and MAPS generates a hydroxyl group which can initiate the copolymerization of NMA and the epoxy resin. The product of this reaction, a MAPS-induced copolymerization, is an ester compound which we have correlated with the degree of curing of the resin phase in composites. It was found that the increase in the concentration of the ester product is a function of the amount of treated fiber content in these composites (Figure 4). We conclude that the total degree of curing of the matrix increases with the amount of silane molecules on the fiber surfaces. Thus, a gradient may exist in the extent of cure of the matrix from the surface of the fiber to the bulk. This result suggests the presence of a matrix interphase going from a state of high cure at the matrix-coupling agent interface to the average state of cure of the bulk resin.

In order to obtain more information about the structure of the matrix interphase, experiments were performed by modifying the amount of MAPS coupling

agent on the glass fiber. The fibers were treated with concentrations of 0.5, 1.0, 1.5, 2.0% MAPS in aqueous solutions. The fiber reinforced composites were made by adding epoxy resin to these MAPS-treated E-glass fiber (28% by weight) and curing at 150°C for 3 hours. Due to the weak absorbances of the amide and the amine bands and the small amount of coupling agent on the glass surface, an infrared subtraction method was employed to measure the absorbance changes of these bands. It was found that the absorbance of the anhydride band appearing at 1780 cm^{-1} decreases when the amount of MAPS increases on the fiber surfaces. The intensities of the band at 1744 cm^{-1}, assigned to the carbonyl group of ester, only increases slightly when the concentration of MAPS increases. The absorptions of amide and amine bands increase as the concentration of MAPS increases on the glass surfaces. Therefore, as expected, the amount of interfacial chemical reaction depends on the amount of silane on the fiber. A comparison of the concentration of the ester groups in the resin phase for silane-treated and non-treated fiber reinforced composites is shown in Figure 5. The results indicate that the MAPS treated surface causes an increase in the amount of curing by about 5-10% compared to the non-treated surfaces. This result is consistent with the MAPS acting as an initiator for the epoxy polymer.

Infrared subtraction and integrated absorbance methods were employed to measure the amount of reacted aminosilane coupling agent in the composites. From the decrease of the integrated intensities of the N-H band at 3290 cm^{-1}, the total amounts of reacted silane molecules in these composites were calculated and are shown in Figure 6. The results indicate that the amount of reacted silane increases when the amount of total deposited silane increases on the glass surfaces.

DISCUSSION

Application of silane coupling agents for surface modification of the substrate usually improves the adhesion (16). An important contribution to adhesion is thought to be provided by the coupling agent via a chemical bonding mechanism. This chemical bonding theory requires the establishment of covalent bands between the silane and both the glass surface and organic matrix. A number of investigators have studied the reactions between silane and glass and concluded that silanes can anchor themselves to the glass surface via Si-O-Si bonds (1). In addition to the hydrolyzable groups, the silane contain an organic non-hydrolyzable group which can potentially react with the matrix resin (17). In the case of an epoxy resin, this functional group may be an amine or epoxy group. We have found that a secondary aminosilane (MAPS) reacts with the epoxy resin (15). The copolymerization of the resin and the silane generates amide and tertiary amine groups and consumes the secondary amine groups of the silane in the composites. Based on our experimental results a structural model of the fiberglass reinforced composites on the molecular level is suggested in Figure 7. The basis of this model is based on the following considerations.

It has long been known that when the silanes are applied to glass fibers from aqueous solution, a smooth continuous film is not obtained but agglomerated particles are also deposited on the surfaces depending upon the method of sample preparation. This phenomenon was studied by electron microscopy and the structure is termed a sea-island structure (18). Schrader reported that coupling agents deposited on glass surfaces usually form heterogeneous layers consisting of physisorbed and chemisorbed fractions. The outer fraction, about 95% of the total absorbed material, can be extracted by water at room temperature. The second or inner fraction can be extracted by boiling water, but the third or surface fraction is firmly bound to the substrate and survives extraction

in boiling water for up to 100 min (19). The distribution and organization of silane molecules on the fiber surfaces and the amount of the coupling agent reduced by hydrolytic degradation have been studied by FT-IR spectroscopy. It was confirmed that extraction of treated E-glass fibers with toluene failed to remove any coupling agent, but extraction with boiling water quickly removed most of the adsorbed silanes (10). Apparently thick films are formed by the deposition of hydrolyzed silane during the treatment of the fibers. The silane molecules near the surface form continuous, uniform, nearly close-packed, oriented, and highly crosslinked layers (1). The outermost layers are composed of hydrolyzed linear silane oligomers, which are weakly bound to the fiber surfaces and constitute a more open layered structure. This is the model of the coupling agent interphase which we will use to interpret our results.

For MAPS-treated glass fibers, the amount of silane deposited on the surface is proportional to the concentration of the silane aqueous solution (20). The organic functional groups of the silane are chemically inert under the conditions required for the mixing operation with the resin. The low viscosity liquid of unreacted resin will penetrate the open siloxane layers especially the outer portion of the siloxanes which are not highly crosslinked. During the resin curing stage, the silane copolymerizes with the resin matrix to become a copolymer and further initiate curing of the resin. Apparently, the number of secondary amine groups of silanes decreases in the cured composites. The total amount of reacted silane increases when the thickness of the silane layer increases.

As one approaches the glass surface, the extent of crosslinking of the silane increases, thus the penetration of the resin into the network is more

difficult. Since over 50% of the silanes have reacted with the epoxy resin, this suggests that the low molecular weight epoxy resin must penetrate the silane layer. Consequently, there is a concentration gradient from the bulk resin into the silane interphase. Thus, the reactions of the resin and silane build chemical anchors through an interpenetrating polymer network. But there is a gradient in the silane-resin concentration from the highly cross-linked silane layers on the glass surface with no copolymer with the resin to a maximum at approximately 50 layers after which the amount of copolymer decreases in favor of the bulk resin. The increased 5-10% ester absorbance is due to the increased ester concentration. This is the result of surface-induced initiation due to the amine catalyst of the coupling agent. The thickness for such zones has been suggested to range from 35-100 $\overset{o}{A}$, 200-500 $\overset{o}{A}$, and up to 1 micron (21-23). From our infrared measurements we cannot determine the dimensions of this region.

The interpenetrating copolymer network formed in the silane-resin inter-phase (24), has a modulus intermediate between that of the resin and the coupling agent interphase network. On the other hand, the higher cured matrix interphase also has a higher modulus than that of bulk resin. Perhaps, this is the circumstance leading to optimum stress transfer between a higher modulus filler and a lower modulus resin. Also, the diffusion rate of water in the higher cross-linked resin region and the copolymer interphase is slower than that in the bulk resin. Thus, the silane treatment protects against moisture attack at the interface region in composites.

CONCLUSIONS

The nature of the silane-treated fiber surface, not only in its initial state, but also as it exists during the various processing and composite fabrication operations, plays an important role in establishing the fiber-matrix interface in the fabricated composite. The silane-resin interphase is formed by the epoxy resin copolymerizing with the coupling agent. This interphase chemically bonds the epoxy matrix to the coupling agent and extensive copolymerization is required for a strong resin-glass bond strength.

The resin phase has a gradient in the degree of cure induced by the coupling agent acting as an initiator. The properties of this resin interphase are different from the properties of the bulk resin. Whether the influence of this resin interphase and resin-silane interface bears any relevance to significant modifications of the mechanical properties of composites is unclear. Knowing the extent and structural distribution of those interfaces should be useful in predicting the chemical resistance of fiber reinforced composites.

Acknowledgment

REFERENCES

1. H. Ishida and J.L. Koenig, Polym. Eng. & Sci., 18, 128 (1978).

2. H. Ishida and J.L. Koenig, J. Colloid & Interface Sci., 64, 555 (1978).

3. H.A. Clark and E.P. Plueddemann, Mod. Plast., 40, 133 (1971).

4. D.K. Johanson, F.O. Stark, and R. Baney, AFMF-TRI, 65-303, Part 1 (1965).

5. H. Ishida and J.L. Koenig, J. Polym Sci., Physics, 17, 615 (1979).

6. H. Ishida and J.L. Koenig,, J. Colloid & Interface Sci., 64, 565 (1978).

7. F.N. DeLollis and O. Montaya, J. Appl. Polym. Sci., 11, 983 (1967).

8. A.T. DiBenedetto and D.A. Scola, J. Colloid & Interface Sci., 64, 480 (1978).

9. F.J. Kahn, Appl. Phys. Lett., 22, 386 (1973)

10. H. Ishida and J.L. Koenig, J. Polym. Sci., Physics, 18, 1931 (1980).

11. E.P. Plueddemann, Proc. 20th Ann. Tech. Conf., Reinforced Plastics Div., SPI, Section 2-D (1965).

12. C.H. Chiang and J.L. Koenig, Polymer Composites, 1(2), 88 (1980).

13. C.H. Chiang and J.L. Koenig, Proc. 35th Ann. Tech. Conf., Reinf. Plastics Div., SPI, Section 23-D (1980).

14. C.H. Chiang, H. Ishida, and J.L. Koenig., J. Colloid & Interface Sci., 74, 396 (1980).

15. C.H. Chiang and J.L. Koenig, Proc. 36th Ann. Tech. Conf., Reinforced Plastics Div., 2-D (1981).

16. E.P. Plueddemann, Interfaces in Polymer Matrix Composites, Academic Press, N.Y., 1974, Chapter 6.

17. J.J. Biderman, The Science of Adhesive Joints, Academic Press, N.Y., 1961, p.26.

18. S. Sterman and H.B. Bradley, Proc. 16th Ann. Tech. Conf., Reinforced Plastics Div., 8-D (1960).

19. M.E. Schrader, Proc. 25th Ann. Tech. Conf., Reinforced Plastics Div.,
     13-E (1970).

20. C.H. Chiang, Ph.D. Thesis, Case Western Reserve University, Chap. 2,
     (1981).

21. P.W. Erickson, A. Volpe, and E.P. Popper, Proc. 19th Ann. Tech. Conf.
     Reinforced Plastics Div., 21-A (1966).

22. D.H. Droste and A.T. DiBenedetto, J. Appl. Polym. Sci., 13, 2149 (1969).

23. T.T. Wang and H. Schonhorn, J. Appl. Phys., 40, 5131 (1969).

24. E.P. Plueddemann, Additives for Plastics, 1, 123 (1978).

Figure 1   65

A. COMPOSITE

1780
1740
1511
1609
1248
1183
1044
915 830

B. CONTROL SAMPLE

1183

C. DIFFERENCE SPECTRUM

1740
1640
1780
916
B.L.

2000   1600   1200   800

WAVENUMBERS

Figure 2

67

Figure 3

FIBER CONTENT WT %

I1640 / I1609

68

Figure 4

SURFACE – INDUCED ESTERIFICATION
IN FIBER COMPOSITES

Figure 5

SURFACE-INDUCED COPOLYMERIZATION
IN FIBER REINFORCED COMPOSITES
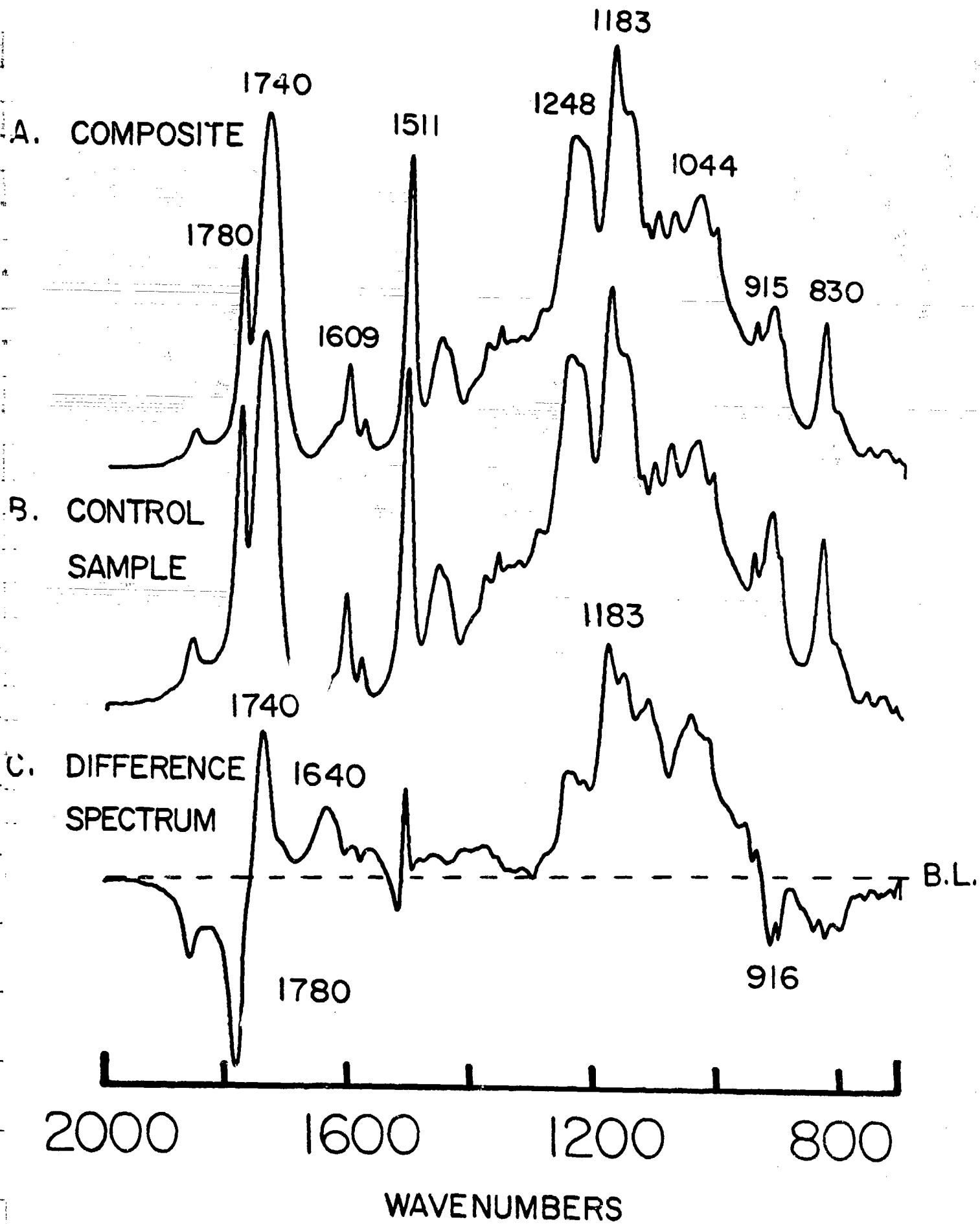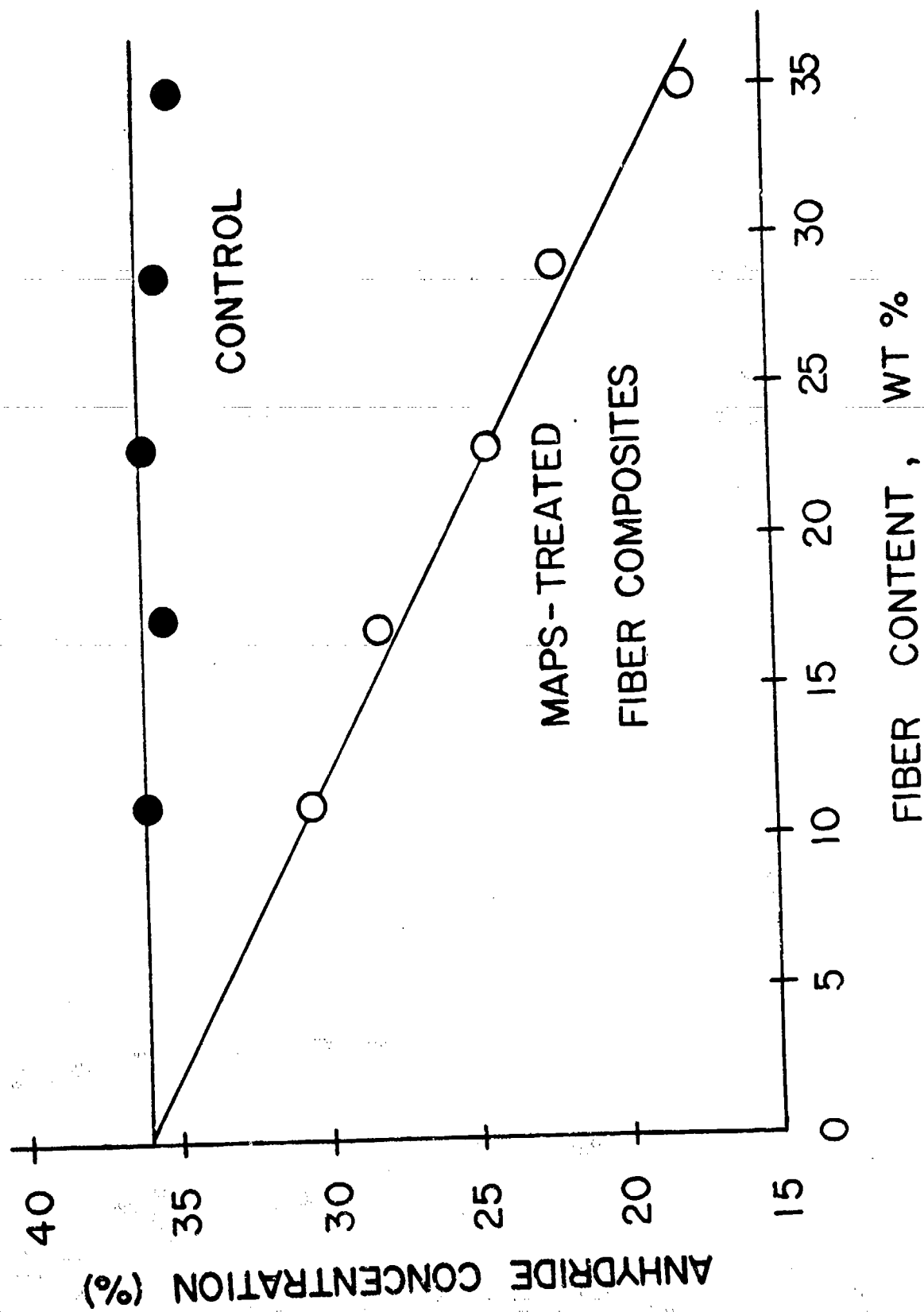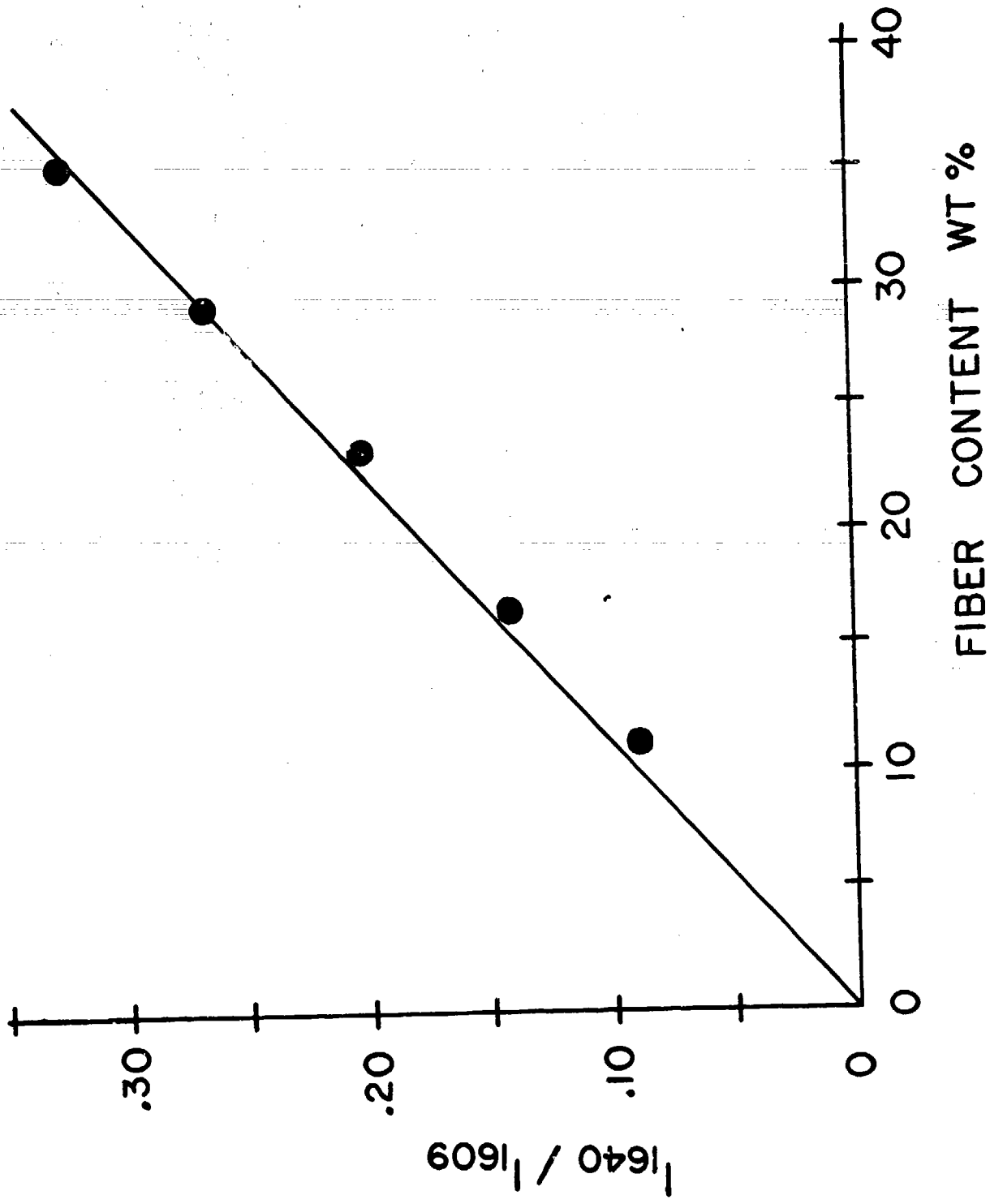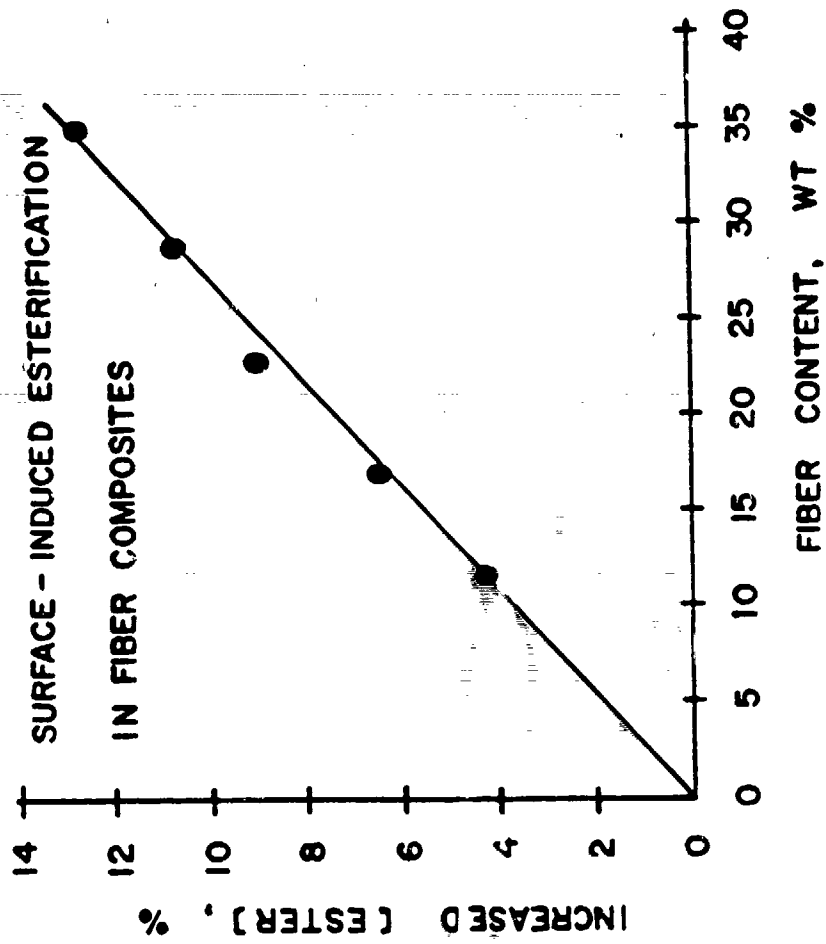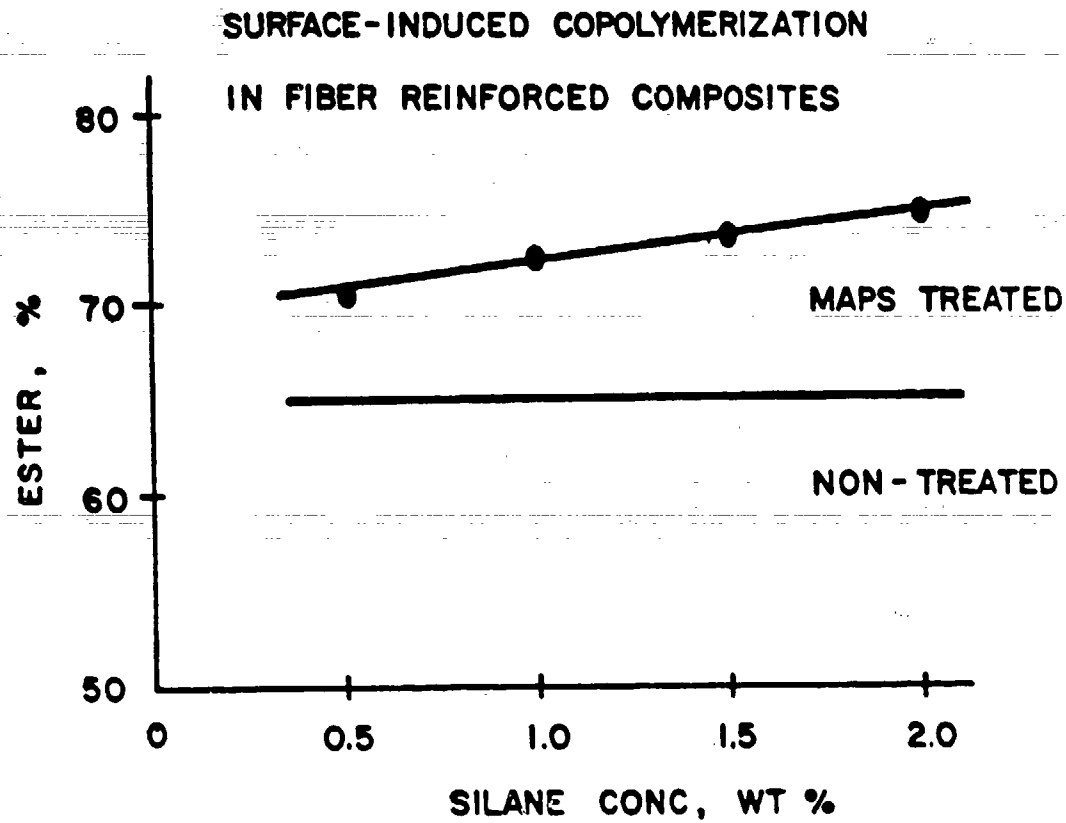
MAPS ON FIBER SURFACE

X : TOTAL UNREACTED SILANES

O : REACTED SILANES
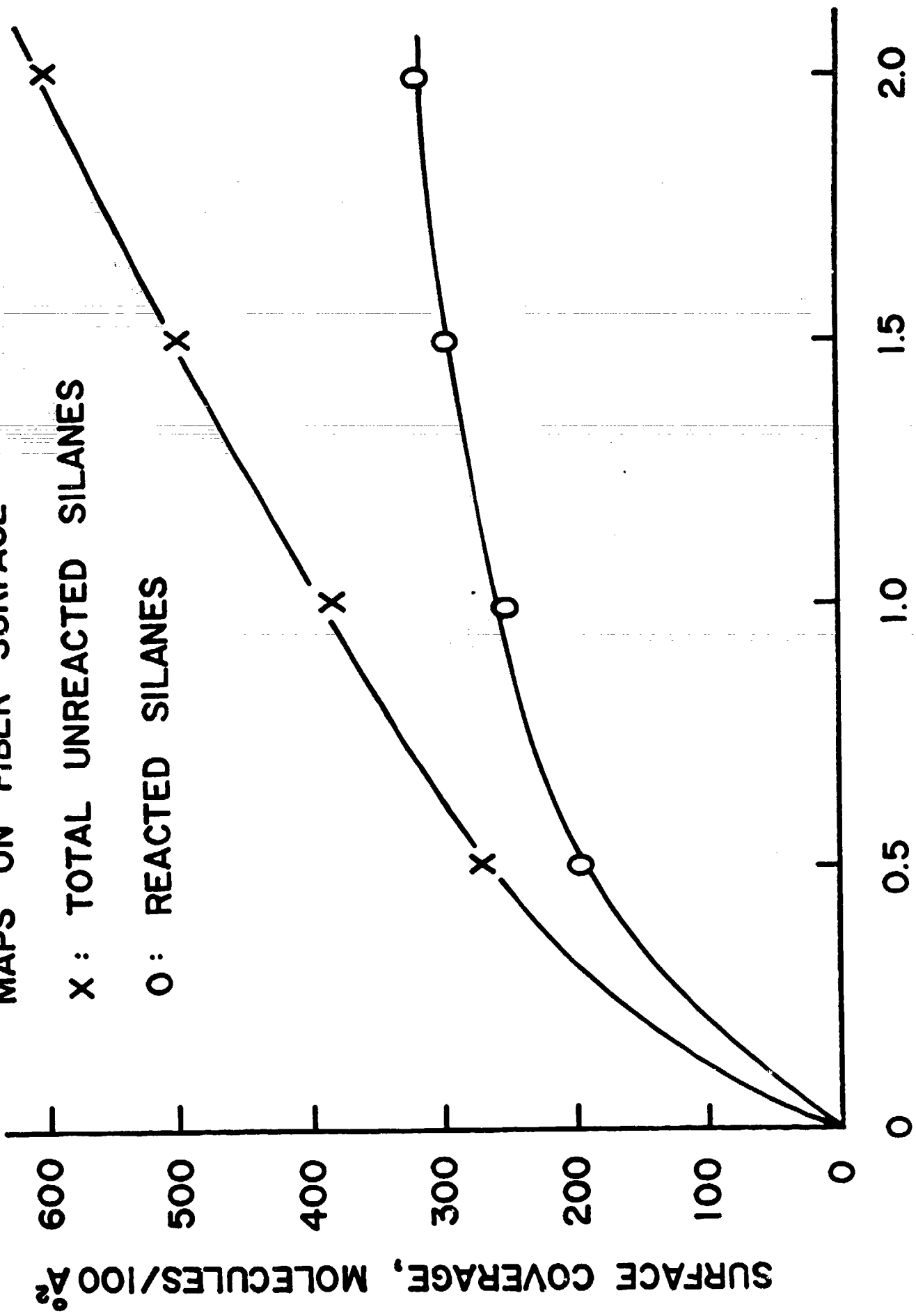
SURFACE COVERAGE, MOLECULES/100 Å^2

SILANE CONCENTRATION, WT %

71

MOLECULAR STRUCTURE OF COMPOSITE
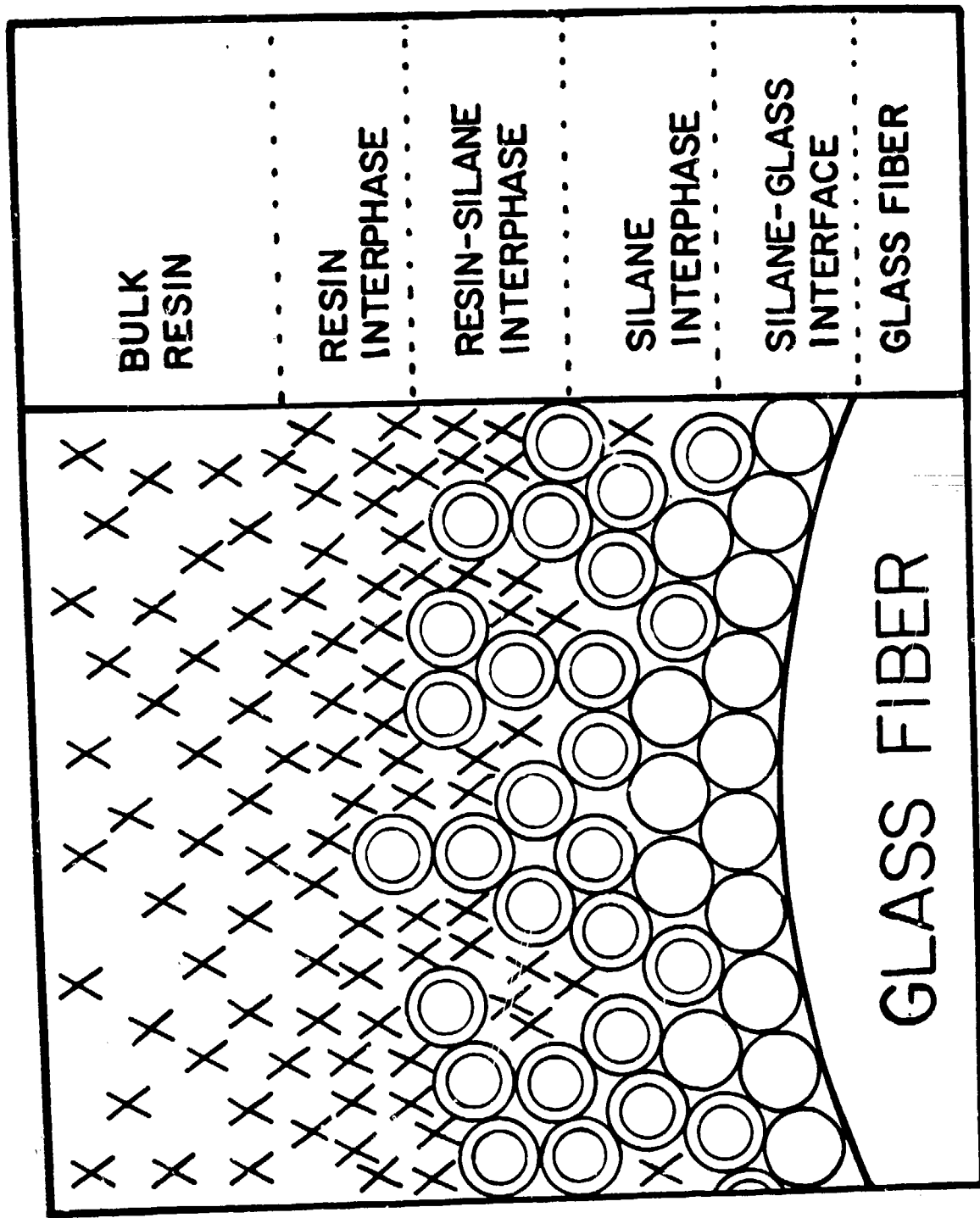
Figure 7

BULK
RESIN

RESIN
INTERPHASE

RESIN-SILANE
INTERPHASE

SILANE
INTERPHASE

SILANE-GLASS
INTERFACE

GLASS FIBER

GLASS FIBER

INTERFACIAL STRENGTH STUDIES OF

FIBER-REINFORCED COMPOSITES

by

H. Emadipour, P. Chiang and J.L. Koenig

Department of Macromolecular Science

Case Western Reserve University

Cleveland, Ohio 44106

INTERFACIAL STRENGTH STUDIES OF FIBER-REINFORCED COMPOSITES

by

H. Emadipour, P. Chiang and J.L. Koenig
Department of Macromolecular Science
Case Western Reserve University
Cleveland, Ohio 44106

Abstract

The effect of amino silane coupling agents on the mechanical strength and hydrothermal stability of the interfacial bonds of E-glass fiber-epoxy resin composites has been investigated, using a single fiber pullout test. A mechanical test system utilizing a model glass-fiber composite has been developed in order to measure quantitatively the actual interfacial strength of the composite.

Varying concentrations of different bifunctional amino silanes are used for treating the glass fiber. The treated fiber, partially embedded in an epoxy matrix, is sheared in the direction of the fiber by means of a pullout force, giving the shear debonding stress of the interface. To investigate the hydrothermal effect, the composite is immersed in 95°C water for varying periods of time, and the interfacial strength is determined.

The use of a bifunctional silane coupling agent enhances the mechanical strength and hydrothermal resistance of the interface. It is found that N-2-aminoethyl-3-aminopropyltrimethoxy-silane (AAPS) imparts the most favorable results in comparison with 3-aminopropyltriethoxysilane (APS), and N-methylaminopropyltriethoxysilane (MAPS).

INTRODUCTION

Throughout the evolution of fiber-reinforced polymers a great deal of theoretical and experimental studies have been devoted to improving the mechical properties and hydrothermal stability of interfaces in composites.

In this study the effect of amino silane coupling agents on interfacial bond strength of E. glass fiber-epoxy resin composite, and the hydrothermal stability of silane treated interfaces have been investigated. Glass fiber is used to improve the fracture toughness of composites. To do so, the interface must transmit stress and deflect crack growth. However, epoxy resin does not uniformly wet the glass, and there is no appreciable bonding between the two. Furthermore, since the coefficient of thermal expansion of epoxy is about ten times as great as that of glass, large stresses are set up at the interface when the composite cools, initiating cracks and causing a major loss in physical strength. (1,6).

Interfacial stability of untreated composites, especially its resistance to heat and moisture, is not satisfactory. In order to improve the mechanical properties and hydrothermal stability of the interface, several types of fiber treatment, notably utilizing silane coupling agent, have been reported. (1-7, 9, 17-22).

Silane coupling agents are generally characterized by the presence of organo-functional and silicon functional groups,

2

$$R - \underset{\underset{X}{|}}{\overset{\overset{X}{|}}{S_i}} - X$$
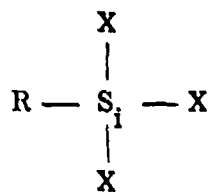
R: $CH_2 = CH -$, $NH_2(CH_2)_3 -$, etc.

X: $-OCH_3$, $-OC_2H_5$, cl , etc.

where X represents a readily hydrolyzable group and R represents a reactive organic functional group. This bifunctionality of the silane permits the coupling of the silane with organic resins and hydroxyl-containing substrates (2).

Silane coupling agents react chemically by bonding covalently to both the glass surface and epoxy resin matrix (3-5, 7-9). Hence, the bifunctional silane molecules through coreactivity with both the glass and the resin form three-dimensional networks at glass-silane-resin interfaces leading to improvement in interfacial strength and enhancement of hydrothermal resistance of the inter-faces.

The purpose of this study is to develop a mechanical test system utilizing a model glass-fiber composite in order to measure quantitatively the actual interfacial strength of the E-glass fiber-epoxy resin composite. The method involves a mechanical test by which a single glass fiber, partially embedded in an epoxy resin matrix, is sheared in the direction of the fiber by means of a pullout force, giving the shear debonding stress of the interface. Using this model and technique, the effect of different parameters on the interfacial strength of the composite can be determined. This model system can give quantitative measurements of the in-situ interfacial strength of the composite.

2.0 <u>EXPERIMENTAL</u>

Fiber pullout techniques have been used by several investigators, (6, 8, 10-15), utilizing mainly metallic fibers, to evaluate the interfacial mechanical properties of composites.

In this study E-glass monofilament, one of the most widely used rein-forcements in composites, was used. Due to the delicate nature of the fiber and the model, careful sample preparation is required to minimize the experi-mental variables and prepare reproducible specimens.

2.1 Specimen Preparation and Testing

E-glass fiber (Dow Corning) of circular cross section of 0.025±0.001 inches in diameter was used. The fiber contained 61.2% SiO_2 as the main component, 17% Al_2O_3 and 12.9% Na_2O, with the remainder being oxides of K, Mg, Ca, Ti and As (Corning Glass Works, Material Code 0315). A length of 9" was cut from the fiber, and the ends were filed flat. The glass fiber was cleaned by placing it in a solution of Nochromix (Godax Labs Inc.) in concentrated sulfuric acid for 6 hours, followed by washing thoroughly with distilled water, and finally drying for 45 minutes at 105°C in an oven.

A disposable hypodermic needle (18G) (Becton, Dickinson and Company) having a 1.5" long and 0.050" outer diameter stainless steel needle with an upper plastic part was used for holding the glass fiber. The sharp tip of the needle was cut flat, and ground round and smooth. The inner walls were

kept free from metal bits to ensure that the needle hole was not contaminated or blocked. The steel part of the needle was cleaned by placing it in a mixture of fuming HNO_3 and concentrated H_2SO_4 for 18 hours, followed by washing thoroughly with distilled water, and finally drying it for 45 minutes at 105°C in an oven.

Epoxy resin was composed of a mixture of epoxy, anhydride, and a cross linking accelerator. The epoxy was diglycidyl ether of bisphenol A (DGEBA) industrially known as EPON 828 (Shell). The anhydride was nadic methylanhydride (NMA)(Fisher). The accelerator was N,N-Benzyl dimethylamine (BDMA) (Eastman).

The cleaned needle was filled with an epoxy resin (1:1 EPON 828 : NMA + 1% by weight BDMA) by means of a syringe. About 2" of the cleaned fiber was first smeared with the resin and then placed in the needle, while keeping the capillary full by injecting the resin in the needle. The syringe was taken off, and the plastic end of the needle was sealed with silicon rubber. The sample was then placed in an oven, and heated for one hour at 150°C.

Three different amino silanes (Petrarch Systems Inc.) were used. They were 3-aminopropyltriethyloxysilane (APS); N-methylaminopropyltriethoxysilane (MAPS); N-2-aminoethyl-3-aminopropyltrimethoxysilane (AAPS). Solutions with 1% and 5% concentration were made by adding an amino silane to an aqueous solution having a pH of 5, and then retaining this pH by adding acetic acid.

The free end of the glass fiber, opposite to the hypodermic needle, was cleaned, washed and dried as before. This cleaned portion of fiber was dipped

into the silane solution for exactly 5 minutes, air dried for 3 hours, and finally oven dried for 15 minutes at 80°C. An epoxy resin comprizing 30% by weight NMA in EPON 828 plus 0.5 % of the total by weight BDMA was prepared, mixed thoroughly, and then degassed by means of vacuum until all the air bubbles were eliminated.

The mold was a glass vial having an internal diameter of 0.52" and an internal height of 1.74". An aluminum cylinder 0.518" in diameter and 0.65" in length, having a flange, just fitted in the vial. A concentric hole of 0.028" in diameter running vertically along the length of the cylinder kept the fiber concentrically in place in the vial.

The prepared epoxy resin (0.4gm) was placed in the glass vial by means of a 3cc syringe, making certain the inside wall of the vial was not smeared by the resin. The silane treated fiber was then placed in the resin in the vial through the hole of the aluminum cap. The fiber at this point was vertical and was in the center of the matrix in the vial. The thickness of the matrix, and hence the embedding length of the fiber in the resin was 2mm.

The specimen was de-aerated by means of vacuum in order to eliminate any air bubbles in the resin or at the interface, and then cured for $2\frac{1}{2}$ (or 8) hours at 105°C. The heating system was then switched off, letting the composite specimen to cool gradually to room temperature in the oven.

In the pullout test, the embed d length, ℓ, of the fiber is of prime importance (11-13, 16). It was found that with $\ell < 1\frac{1}{2}$mm, the matrix did not have enough physical strength to withstand any appreciable tensile force, and shattered. With $\ell > 2\frac{1}{2}$mm, no reproducible pullout was obtained. Hence, an embedded

length of 2mm, which was found to be satisfactory, was chosen for the specimen.
The interfacial bond strength of the composite sample was measured using an
Instron machine. The glass vial containing the composite was placed in the
sample holder, and the plastic part of the needle holding the fiber was gripped
by the nip of the two discs hanging from a chain as shown in Figure 1. The
entire set up, when subjected to a pulling force, was aligned to a vertical
position.

The Instron machine was adjusted with the following values:

cross-head speed,   0.05 cm./minute;

chart speed,   1 cm./minute;

load range,   1.25Kg(12.5Kg full-scale)

The fiber was sheared out of the matrix by means of a uniformly increasing
tensile force, and the mode of failure, as well as the interfacial debonding
force, obtained from the chart, were noted.

2.2 Modes of Failure

In this monofilament pullout method, when the specimen was subjected to
tension in an Instron tensile tester, three modes of failure were observed.

1. Fiber failed outside the matrix when its tensile strength was less than the
shear strength of the interface or the matrix. The fiber also failed at the point
of contact where the fiber entered the matrix. This was due to stress concen-
tration at that point as the result of misalignment of the fiber in the matrix.

In both cases the results were discarded, as there was no pullout.

2.   When the resin was properly cured to bear the load without any appreciable flow, and the matrix had enough thickness in order not to shatter under the applied stress, then, occasionally, the matrix failed when its strength was lower than that of the interface. The shear caused pullout failure of a part of the matrix, having a conical shape, round the fiber due to stress build-up. This showed that in such cases the overall interfacial strength was higher than that of the matrix. However, as such a result did not give a quantitative value for the interfacial strength, it was also discarded.

3.   Fiber pullout was obtained when the specimen was deliberately conditioned to give interfacial failure under a load, by choosing the proper embedded length and hence a limited interfacial contact between the glass and the interface. However, this did not limit the scope of the test for the actual and comparative determination of the interfacial strength of the composite under varying conditions.

2.3 The interfacial shear strength, τ, of the composite was calculated from the failure load, P, using the following equation:

$$\tau = \frac{P}{d\,\pi\,\ell}$$

where d is the diameter, and ℓ the embedded length of the fiber in the matrix.

The interfacial strength was taken as the total overall strength of the interface due to physical, mechanical and chemical bonding. The quantitative and

comparitive determination of the effects of different treatments on this overall property, giving a realistic practical result, was the prime purpose of this study.

3.0 Results and Discussion

3.1 Interfacial Strength

The effect of silane treatment on the interfacial strength of E - glass fiber-epoxy resin composites, using the three different amino silane coupling agents are summerized in Tables 1 and 2, and Figure 2.

Treatment with one percent solution of each of the three silanes improves the interfacial shear strength of the composite in comparison with that of the untreated sample. It was found that the extent of this interfacial bond strength improvement was about 17% for the primary amino silane APS, 15% for the secondary amino silane MAPS and over 46% for the diamino silane AAPS.

Increasing the concentration of the silane solutions, and hence depositing a thicker layer of silane on the fiber, not only does not result in any improvement, but on the contrary, decreases the interfacial bond strength of the composite. Table 2 and Figure 2 show that using 5% silane solutions for fiber treatment, decreases the interfacial bond strengths over the untreated sample by 36%, 20% and 14% for MAPS, APS and AAPS treatments respectively, with AAPS being still the best among the three.

The decrease in interfacial strength due to a thicker layer of silane between the glass and the epoxy matrix can be attributed to the following factors. Coupling agent acts as a link between the glass and the resin by forming co-valent chemical bonds with both the glass and the resin. According to Schrader et al. (17-19) there are three fractions of silane layers on silane treated glass: physisorbed and chemisorbed layers, and a last smooth layer having a thickness of about one monolayer on the surface of glass. Ishida and Koenig (21) have shown that there is order in the molecular organization, and a gradient in the structure of the coupling agent interphase. The silane layers farthest from the glass surface consist of small oligomers with almost no link-ages between them. In the next inner layers there are some bonds connecting the oligomers. In the last silane layer on the surface of glass fiber the inter-facial siloxane linkages to the glass, as well as those between the silanes them-selves develop a tight stable network.

Considering the silane-epoxy resin interface of the composite, it can be argued that, likewise, the copolymerized organic bonds between silane and epoxy form a tight stable network, and, similarly, there will be a gradient in the struc-ture of the coupling agent interphase. Hence, the aminosilane treated E - glass fiber-epoxy resin composite can be considered to consist of the following five regions:

1. E - glass fiber reinforcement
2. Glass-silane interface, with covalent chemical bonding
3. An interphase of amino silane oligomers having some siloxane linkages forming a structural network gradient with increasing crosslink density towards the glass-silane surface

4.   Silane-epoxy interface with   covalent copolymerized bonds

5.   Epoxy matrix network.

The mode of failure in this test showed that fiber treated with 5% silane solution resulted, not only, in failure at lower shear stress, but also a near perfect fiber pullout was obtained with practically no matrix adhering to the fiber. This shows that with thick layers of silane, there is mechanical failure at this weak interphase between the glass and the matrix. Further refinement of the test method is necessary for the attainment of greater degree of reproducibility in order to analyze the stresses attributed to each region with more reliable accuracy, but at this stage the following inference seems to be most probable. The maximum interfacial bond strength in E-glass fiber-epoxy resin composite would probably be obtained when a monolayer of the bifunctional amino silane coupling agent bonds covalently to both glass surface and epoxy matrix. However such monolayers are not available using current processing techniques. What is required is a continuous network of coupling agent bonds Si-O-Si between the fiber and the matrix with sufficient coupling agent matrix and coupling agent glass interfacial bonds to support the network. When unreacted amino silanes remain forming a soft oligomeric silane interphase, they act as weak regions in the composite interface and are detrimental to composite performance.

3.2 Hydrothermal Effect

Table 3 and figure 3 show the effect   of water at 95°C on the interfacial shear strength of E-glass fiber-epoxy resin composites, treated with 1%

AAPS solution.

Debonding occured and interfacial strength decreased steadily with increasing immersion time. The loss of interfacial strength was found to be nearly 50% after 3 hours and 65% after one week. Comparing untreated and AAPS treated specimens under the same hydrothermal conditions (Table 4 and figure 4) showed that the bond strengths in both cases were adversely affected, but the silane treated interface still retained its higher mechanical strength over the untreated one. Immersion in NaOH (pH12) at 90°C resulted in a more drastic shear strength loss (Table 4 and Figure 7) in AAPS treated composite showing that interfacial bonds are more vulnerable to NaOH, than water at the same temperature.

Water attacks the glass-coupling agent interface destroying the bond between them (5, 9, 22). Water also hydrolyzes the siloxane network in the interphase. Water penetrated the glass-resin interface by diffusion through the resin cracks, or by capillary migration along the fiber (23). As discussed before, silane coupling agents form three different fractions between the glass and the matrix. The soft oligomeric physisorbed layers are easily washed away with water. The second chemisorbed layers are more resistant to hydrothermal attack and are removed only by extraction with boiling water for several hours (17,20). The last highly crosslinked layers are more resistant to hydrothermal attack. The hydrolysis and reformation of SiOSi bonds are considered as reversible processes in this interfacial region (1, 20, 21).

The experimental results show that there is a sharp drop in interfacial strength (Figure 3) during the first three hours in hot water. This drop is

mainly due to the hydrolysis of the oligomeric silane layers thus eliminating the continuity of bonding between fiber and matrix. The bonding strength decreases less drastically after this initial stage since the remainder of the network has substantial crosslinking.

The debonding effect of moisture and heat on the interfacial bond strength of amino silane treated E-glass fiber-epoxy resin composites as the result of long term exposure, has been studied and will be reported at a later stage.

References

1. E.P. Plueddemann, J. Adhesion, 2, (July 1970) 184-201.

2. P.T.K. Shih and J.L. Koenig, Materials Sci. and Eng., 20 (1975) 145-154.

3. H. Ishida and J.L. Koenig, Polymer Eng. and Sci., 18, No. 2 (Mar.-Feb. 1978) 128-145.

4. J.L. Koenig and P.T.K. Shih, J. Colloid and Interface Sci., 36, No. 2 (June 1971) 247-253.

5. O.K. Johannson, et al., J. Composite Materials, 1, (1967) 278-292.

6. E.P. Plueddemann, Academic Press, Inc. (1978) 123-167.

7. H. Ishida and J.L. Koenig, J. of Polymer Sci., 18, 1980 (1931-1943).

8. H.W.C. Yip and J.B. Shortall, J. Adhesion, 8 (1976) 155-169, Part 2.

9. O.K. Johannson, et al., ASTM Technical Publication 452 (Interfaces in Composites), (June 1968) 168-191.

10. H.W.C. Yip and J.B. Shortall, J. Adhesion, 7, (1976) 311-332.

11. L.J. Broutman, Interfaces in Composites, ASTM STP, 452, (1969) 27,41.

12. A. Takaku and R.G.C. Arridge, J. Phys. D: Appl. Phys. 6, (1973) 2038-2047.

13. P. Lawrence, J. Mat. Sci. 7 (1972) 1-6.

14. K. Kendall, J. Mat. Sci., 10 (1975) 1011-1014.

15. R.W. Jech, ASTM STP 497 (1972) 516-524.

16. G.A. Cooper and A. Kelly, ASTM STP, 452 (1969) 90-106 , 195.

17. M.E. Schrader, I. Lerner and F.J. D'oria, Med. Plast., 45 (1967)

18. M.E. Schrader, J. Adhesion, 2 (1970), 202.

19. M.E. Schrader and A. Block, J. Polymer Sci., Part C, 34 (1971) 281.

20. H. Ishida and J.L. Koenig, J. Polymer Sci., 18, (1980) 233-237.

21. H. Ishida and J.L. Koenig, J. Polymer Sci, 17 (1979) 1807-13.

22. W.J. Eakins, Interfaces in Composites, ASTM STP 452, (1969) 137-148.

23. K.H.G. Ashbee and R.C. Wyatt, Proc. Roy. Soc. A. 312 (1969) 553-564.

FIGURE CAPTIONS

Figure 1: Pictures of Testing Device

Figure 2: Effect of Silane Concentration on Interfacial Strength of Glass Fiber-Epoxy Resin Composite

Figure 3: Hydrothermal Effect on Interfacial Strength of 1% AAPS Solution Treated E-Glass Fiber-Epoxy Resin Composite

Figure 4: Effects of Heat, Moisture, and NaOH on Interfacial Strength of Untreated and Silane-Treated E-Glass Fiber-Epoxy Resin Composites

LIST OF TABLES

Table 1: Effect of Silane Treatment on Interfacial Strength of E-Glass Fiber-Epoxy Resin Composite, Cure Time: 2.5 hours at 105°C

Table 2: Effect of Silane Concentration on Interfacial Strength of E-Glass Fiber-Epoxy Resin Composite, Cure Time: 8 hours at 105°C

Table 3: Hydrothermal Effect on Interfacial Strength of 1% AAPS Solution Treated E-Glass Fiber-Epoxy Resin Composite

Table 4: Effect of Heat, Moisture and NaOH on Interfacial Strength of Untreated and Silane Treated E-Glass Fiber-Epoxy Resin Composites
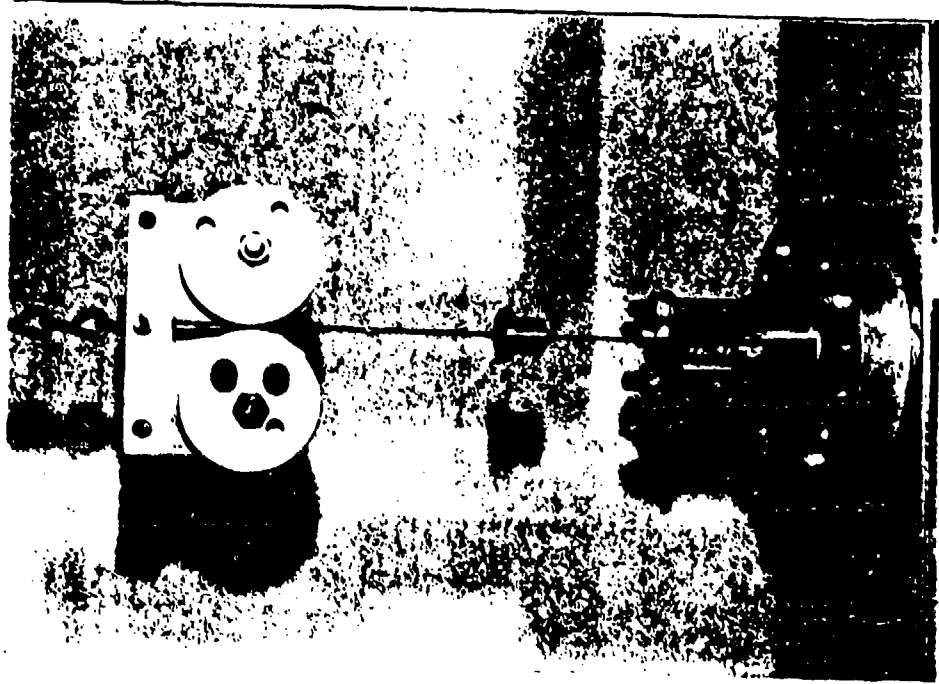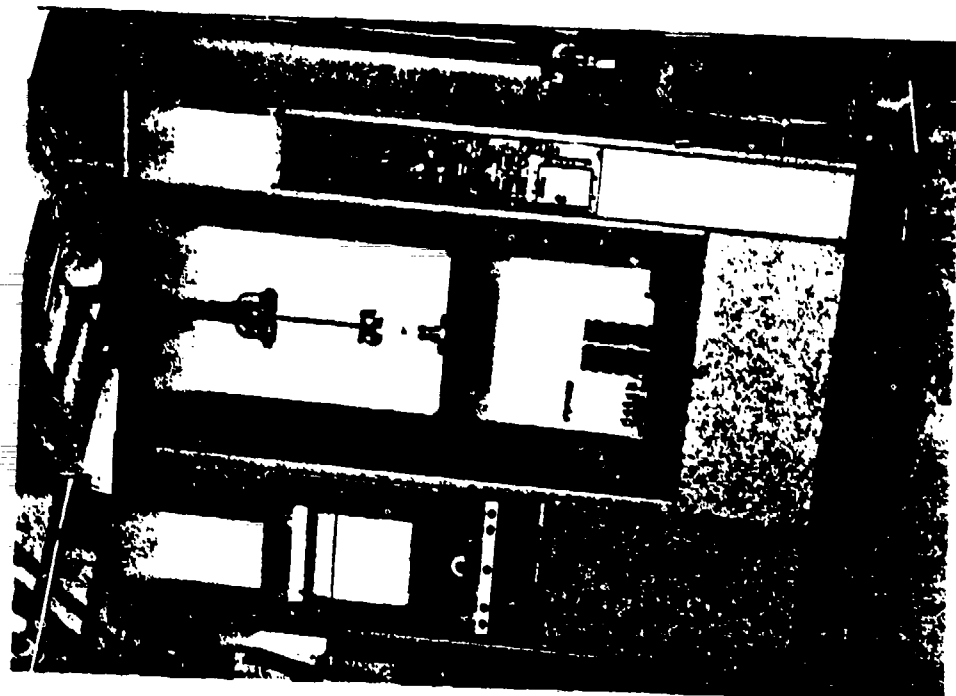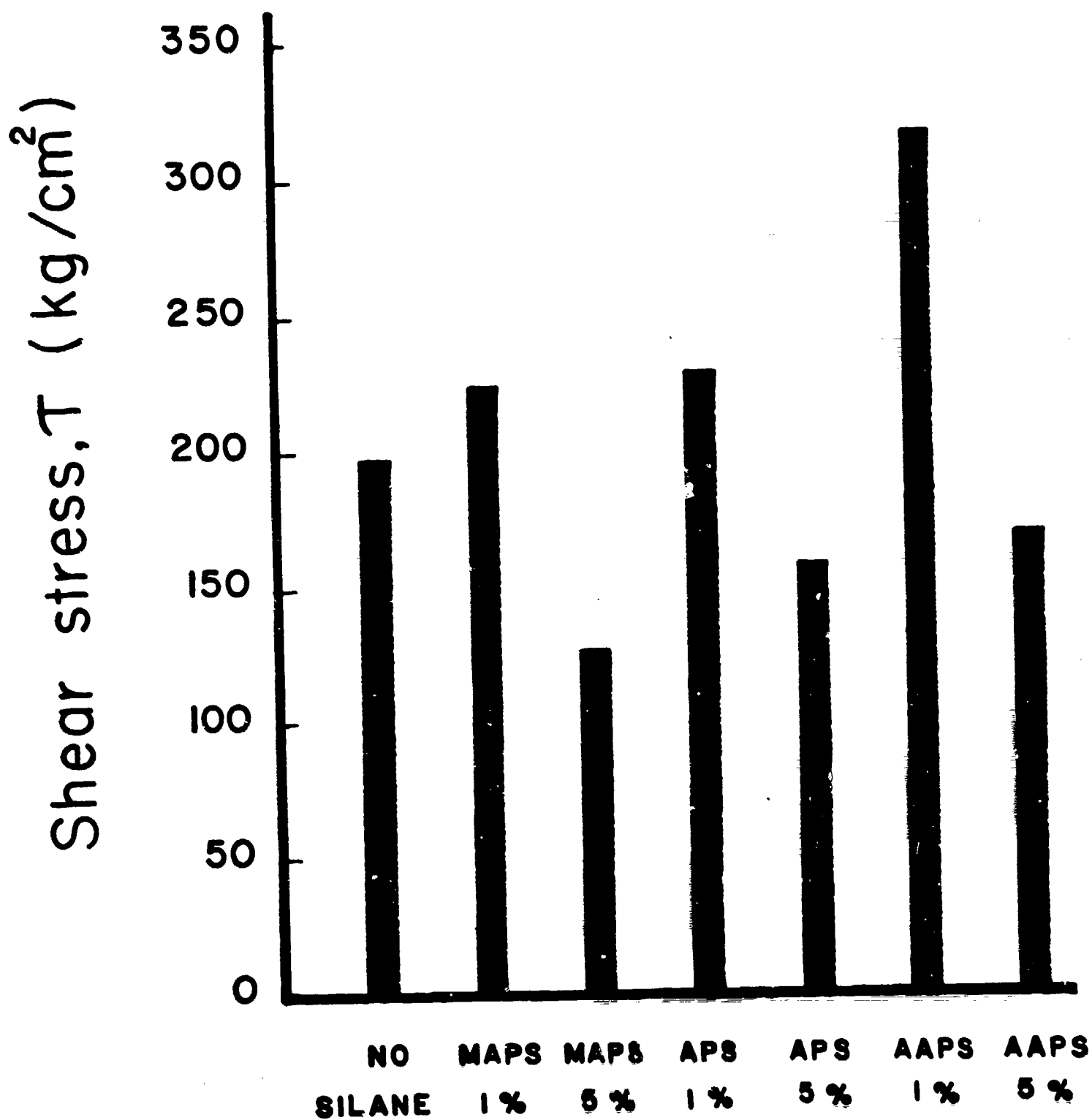
Figure 1

PICTURES OF TESTING DEVICE

FIGURE 2 - EFFECT OF SILANE CONCENTRATION ON INTERFACIAL STRENGTH OF GLASS FIBER-EPOXY RESIN COMPOSITE
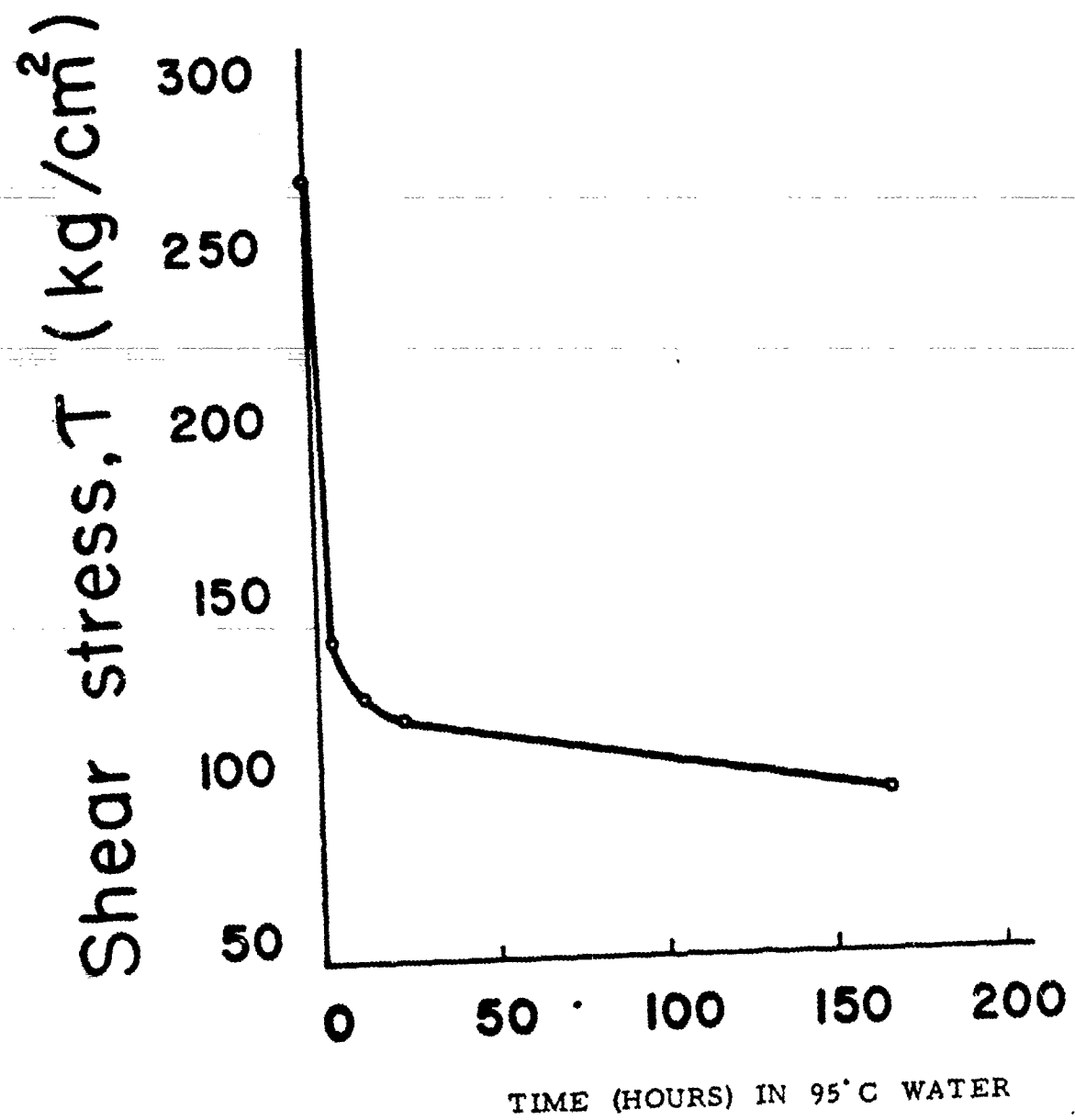
FIBER PULLOUT TEST

FIGURE 3 - HYDROTHERMAL EFFECT ON INTERFACIAL
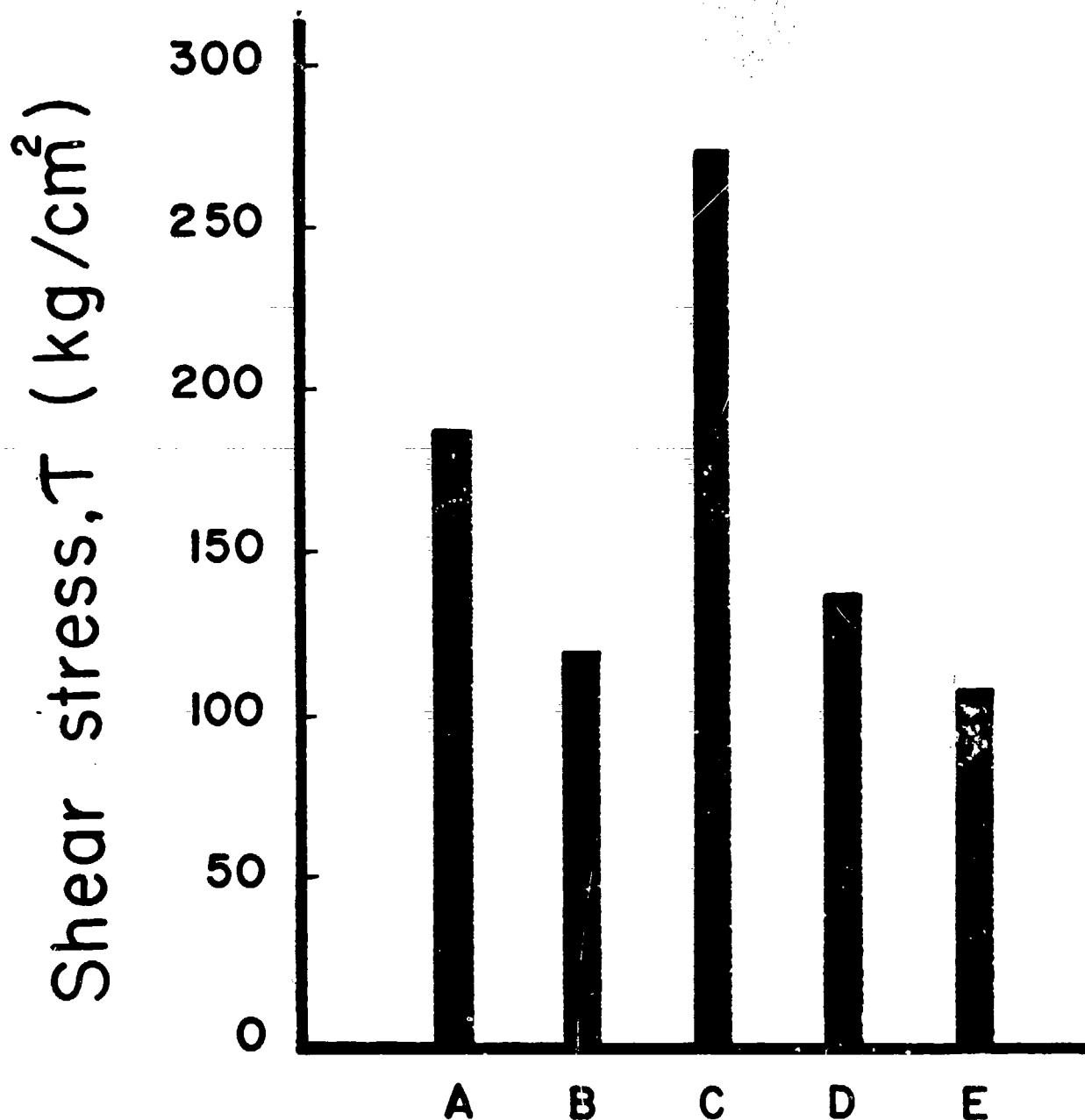STRENGTH OF 1% AAPS SOLUTION TREATED
E.GLASS FIBER-EPOXY RESIN COMPOSITE

FIGURE 4 - EFFECTS OF HEAT, MOISTURE, AND NaOH ON INTERFACIAL STRENGTH OF UNTREATED AND SILANE-TREATED E.GLASS FIBER-EPOXY RESIN COMPOSITES

A- UNTREATED, DRY
B- UNTREATED IN 90°C WATER FOR 6 HOURS
C- 1% AAPS SOLUTION TREATED, DRY
D- 1% AAPS SOLUTION TREATED IN 90°C WATER FOR 6 HOURS
E- 1% AAPS SOLUTION TREATED IN 90°C NaOH (pH=12) FOR 6 HOURS

TABLE 1

EFFECT OF SILANE TREATMENT ON INTERFACIAL STRENGTH

OF E-GLASS FIBER-EPOXY RESIN COMPOSITE

CURE TIME: 2.5 hours at 105°C

SILANE SOLUTION CONCENTRATION	SHEAR STRESS, Kg/Cm^2	% CHANGE IN SHEAR STRENGTH
UNTREATED	189	——
1% MAPS	217	+ 14.8
1% APS	221	+ 16.9
1% AAPS	277	+ 46.5

TABLE 2

EFFECT OF SILANE CONCENTRATION ON INTERFACIAL

STRENGTH OF E-GLASS FIBER-EPOXY RESIN COMPOSITE

CURE TIME: 8 hours at 105°C

UNTREATED	195	——
1% MAPS	223	+ 14.3
1% APS	228	+ 16.9
1% AAPS	316	+ 62.0
5% MAPS	125	— 35.9
5% APS	157	— 19.5
5% AAPS	168	— 13.8

TABLE 3

HYDROTHERMAL EFFECT ON INTERFACIAL STRENGTH OF 1%
AAPS SOLUTION TREATED E. GLASS FIBER - EPOXY RESIN COMPOSITE

CURE TIME: 2.5 hours at 105°C
WATER TEMPERATURE: 95°C

IMMERSION TIME (hours)	SHEAR STRESS Kg/Cm^2	% LOSS OF STRENGTH
0 (dry)	277	—
3	143	48.4
12	126	54.5
24	120	56.6
168	97	65.0

TABLE 4

EFFECT OF HEAT, MOISTURE AND NaOH ON INTERFACIAL
STRENGTH OF UNTREATED AND SILANE TREATED E.GLASS
FIBER-EPOXY RESIN COMPOSITES

CURE TIME: 2.5 hours at 105°C

SPECIMEN	SHEAR STRESS Kg/Cm^2	% LOSS OF STRENGTH
A	189	—
B	123	34.9
C	277	—
D	140	49.5
E	111	60.0

A- UNTREATED, DRY
B- UNTREATED IN 90°C WATER FOR 6 HOURS
C- 1% AAPS SOLUTION TREATED, DRY
D- 1% AAPS SOLUTION TREATED IN 90°C WATER FOR 6 HOURS
E- 1% AAPS SOLUTION TREATED IN 90°C NaOH (pH 12) FOR 6 HOURS

TABLE 4

EFFECT OF HEAT, MOISTURE AND NaOH ON INTERFACIAL
STRENGTH OF UNTREATED AND SILANE TREATED E.GLASS
FIBER-EPOXY RESIN COMPOSITES

CURE TIME: 2.5 hours at 105°C

SPECIMEN	SHEAR STRESS Kg/Cm^2	% LOSS OF STRENGTH
A	189	—
B	123	34.9
C	277	—
D	140	49.5
E	111	60.0

- -

A- UNTREATED, DRY

B- UNTREATED IN 90°C WATER FOR 6 HOURS

C- 1% AAPS SOLUTION TREATED, DRY

D- 1% AAPS SOLUTION TREATED IN 90°C WATER FOR 6 HOURS

E- 1% AAPS SOLUTION TREATED IN 90°C NaOH (pH 12) FOR 6 HOURS

COMPARISON OF PRIMARY AND SECONDARY AMINOSILANE COUPLING

AGENTS IN ANHYDRIDE-CURED EPOXY FIBERGLASS COMPOSITES

by

* Chwan-hwa Chiang and Jack L. Koenig

Department of Macromolecular Science

Case Western Reserve University
Cleveland, Ohio 44106

* Dr. Chiang's new address: Analytical Research, Sherwin Williams, 10909 South Cottage Grove Avenue, Chicago, Illinois 60628

COMPARISON OF PRIMARY AND SECONDARY AMINOSILANE COUPLING
AGENTS IN ANHYDRIDE-CURED EPOXY FIBERGLASS COMPOSITES

Abstract

by

* Chwan-hwa Chiang and Jack L. Koenig
Department of Macromolecular Science
Case Western Reserve University
Cleveland, Ohio 44106

Fourier transform infrared spectroscopy (FT-IR) has been utilized to
investigate the interfacial chemical bonding at the interfaces of the amino-
silanes and the nadic methyl anhydride cured epoxy matrix in fiber rein-
forced composites. It is found that the nadic methyl anhydride can react
with APS and MAPS. In comparing the relative reactivities of the two coup-
ling agents to the epoxy resin, the secondary aminosilane has a higher reac-
tivity than the primary aminosilane. An elevated temperature is required
for the copolymerization to take place between the silane and the epoxy
resin. The results indicate that covalent bonds form at the coupling agent-
matrix interfaces when the fiber is pre-treated with coupling agents. The
molecular structure of the interface in MAPS treated fiberglass reinforced
composites is different from that of the APS treated fiber composites. In
addition, an accelerated copolymerization initiated by the coupling agent
treated surface is also found in the resin interphase which may be important
in determining the mechanical properties of the composites.

* Dr. Chaing's new address: Analytical Research, Sherwin Williams Co.
   10909 South Cottage Grove Avenue, Chicago, Illinois 60628

INTRODUCTION

Application of chemical finishes to glass fibers in reinforced plastics improves the mechanical properties of these materials. These improvements have been most notable in the ability of the fiber composite to retain its strength under conditions of exposure to moisture. Although a large number of studies of the interface between polymers and mineral surfaces exists, there has been no generally accepted theory of adhesion of polymers to minerals or the function of adhesion-promoting coupling agents at the interface (1-4). A theory of chemical bonding has been used to interpret the improvement in adhesion. This theory states that the coupling agent forms a chemical bond with the surface of the glass fiber through a siloxane bond while the organic functional group on the silane molecule bonds to the polymer resin. Adhesion of the resin to the fiber is, therefore, strengthened through a bridge of chemical bonds (5-8). On this basis, the coupling agent should be capable of forming a hydrolytically stable chemical bond with the matrix and the glass. The exact chemical role of the silane coupling agents for fiber glass reinforced plastics still is not clear.

Nitrogen-substituted silane coupling agents have been established as one of the best available interfacial agents to improve the performance properties of composites (9-11). Gamma-aminopropyltriethoxysilane (APS) finished glass fiber yields the ultimate shear and tensile strengths and durability for an epoxy

composite (12). This shear strength is 75-100% over the conventional reinforcements. In our provious work we studied the molecular structure of APS on glass surfaces (13) and found that the primary aminosilane coupling agent forms a cyclic imide with the nadic methyl anhydride at the interface of anhydride-cured epoxy composites. The proposed molecular structure of the system is shown in Figure 1. The formation of the imide group inhibits the further copolymerization of the matrix so interfacial bonding does not occur. Therefore, the extent of adhesion between resin and fiber is decreased as the number of interfacial bonds decreases (14). Chemically, a secondary aminosilane can be used to replace the primary aminosilane thus avoiding the formation of imides.

The interfacial bonding of the polymer and the coupling agent in composites has been mainly studied by extraction methods, examining the residues of the glass powder after washing away the bulk polymer (15,16). This technique is complicated and also limited by the solubility of polymers.

Fourier transform infrared spectroscopy (FT-IR) has the capability of subtracting the absorbance of bulk resin and glass fiber allowing the spectra of the interfaces to be obtained, consequently, the difference spectrum allows the analysis of interface reactions. This technique is very useful when the matrix is a 3-dimensional network polymer which is not soluble in any solvent.

In this paper, we have utilized FT-IR spectroscopy to study the interfacial reactions between the polymeric matrix and with both primary and secondary aminosilane coupling agents. The reaction conditions are studied for producing interfacial bonds at the interfaces using these two aminosilanes in fiberglass reinforced composites.

EXPERIMENTAL

Methylbicycle(2,2,1)-heptene-2,3-dicarboxylic acid anhydride (nadic methyl anhydride, NMA) (Fisher), epichlorohydrin bisphenol A types of epoxy resin (EPON 828, Shell Cc.), and dimethylbenzyl-amine (BDMA, Eastman Kodak) are the major components of the polymer matrix. These mixtures were examined as a thin film between KBr salt plates using a DigLab FTS-14 Fourier transform infrared spectrometer (FT-IR) with 64 samples and reference beam scans for kinetic studies. The spectra utilized in kinetic studies were obtained at the various reaction temperatures. The samples were heated by a Perkin-Elmer heating jacket, monitored by chromel-alumel thermocouples providing temperature controls to $\pm 0.5^{\circ}C$.

The gamma-aminopropyltriethoxysilane (APS) and N-methyl-aminopropyltrimethoxysilane (MAPS) both were purchased from Petrarch Systems Inc. and used as received without any purification. The hydrolyzed polyaminosiloxanes were made by pouring APS or MAPS

onto a Teflon sheet and condensed by absorbing moisture from air at room temperature for three days. The solid siloxanes were ground into powder and dried in a vacuum at 50°C for several hours. The samples were ground into powder with KBr powder and pressed into a pellet. The spectra of siloxanes or the mixtures of siloxanes with epoxy resin were signal averaged with 200 coadded scans using Fourier transform infrared spectroscopy (DigLah FTS-14).

The E-glass fiber was kindly supplied by Cranes Co. (Cranglas, grade 50-01). The glass sheet was heat-cleaned at 500°C in air for one day. The silanes were dissolved in distilled water to form 1% by weight solutions. The cleaned fibers were immersed into silane aqueous solutions for 5 minutes and dried at room temperature. The composites were made by a hand lay-up method and cured at 150°C for 3 hours. Absorbance spectra of these composites were obtained from KBr pellets containing approximately 2 mg of finely-ground powder removed from the composites with a metal file.

RESULTS

Figure 2 compares the infrared spectra of hydrolyzed and unhydrolyzed N-methylaminopropyltrimethoxysilane (MAPS) after being at room temperature for one hour. All the absorbance bands from the methoxy group of MAPS, i.e. 2942, 2841, 1192, 1088, and 819 cm^{-1}, have disappeared or decreased in intensity after MAPS absorbed the moisture from the air and condensed. Two very strong

infrared bands at 1032 cm^{-1} and 1120 cm^{-1} are strongly influenced by the degree of crosslinking of the siloxanes (17). An active secondary amino group shows a weak absorbance band at 3290 cm^{-1} which is assigned to the N-H stretching mode in both hydrolyzed and unhydrolyzed silane coupling agents. All the infrared absorbance bands related to the secondary amino group in the fingerprint region are too weak to characterize the amino group of the silane. However, the characteristic band of the adduct of the MAPS and the anhydride or the epoxy may be used to determine the secondary amine.

The infrared spectrum of the solid cured MAPS powder after reaction with liquid nadic methyl anhydride (NMA) at 150°C for one hour is shown in Figure 3-A. The spectrum 3-B shows the absorbance of the pure and unreacted NMA, the difference spectrum of (A-B) shows the absorbance of the adduct of NMA and MAPS. The expected chemical addition of the anhydride and the secondary amine is shown in Equation 1. The strong band appearing about 1117 cm^{-1} is due to the siloxane group of this adduct. Two new bands appearing

$$-\overset{|}{\underset{|}{Si}}-CH_2CH_2CH_2NHCH_3 \;+\; \overset{O}{\underset{}{C}}\diagdown\overset{O}{\underset{}{}}\diagup\overset{O}{\underset{}{C}} \longrightarrow -\overset{|}{\underset{|}{Si}}-CH_2CH_2CH_2-N-\overset{O}{\underset{}{C}}\quad\overset{O}{\underset{}{C}}-OH \qquad (1)$$

at 1722 cm^{-1} and 1640 cm^{-1} can be assigned to the new functional groups of the acid and amide, respectively. The formation of the amide group indicates the addition of aminosilane to the anhydride. When the amide group is blocked by the methyl group, it cannot continue to react with the nearby acid group to form an imide group.

In order to understand the reactions of the epoxy resin and the aminosilane coupling agent, the hydrolyzed MAPS powder was mixed with the epoxy resin (EPON 828) and heated at 150°C for one hour without adding any catalyst. The infrared absorbance spectrum of the copolymer of the MAPS cured powder was mixed with the epoxy resin (EPON 828) and heated at 150°C for one hour without adding any catalyst. The infrared absorbance spectrum of the copolymer of the MAPS cured epoxy resin is shown in Figure 4-A. The spectra 4-B and 4-C are of the polymers of the cured MAPS and the epoxy resin, respectively. The doubly subtracted spectrum of (A minus B) minus C is due to the adducts of the interfacial reactions as shown in Figure 4-D. It is noted that the intensity of several bands decreases while only a few bands gain intensity. This result indicates that the copolymerization products have very weak infrared absorptions, but some changes have been observed. On the other hand, the intensity of the epoxy band at 915 cm^{-1} decreases and the sample becomes solidified when the mixture is heated to 150°C. These results suggest that MAPS does react with the epoxy resin, and copolymerize with the epoxide. The absorbance band at 1098 cm^{-1} may be assigned to the C-N stretching mode of the N-CH$_2$ group of the copolymerized adducts (18).

In order to understand the chemical reaction between the epoxy resin and the secondary amine, a model compound, methylbutylamine (MBA), is used. The spectrum of the product of the epoxy resin and the MBA is shown in Figure 5. Several positive bands appearing at 1327, 1098, and 1068 cm^{-1} are similar to the bands appearing in Figure 4-D which is the spectrum of the adduct of the MAPS and the epoxide. This result indicates that the secondary aminosilane does react with the epoxy resin.

The copolymerization of the primary and the secondary aminosilanes with the epoxy resin was studied under the same reaction conditions. The experiment was performed by using the APS and the MAPS powders mixed with the epoxy resins and heated between KBr salt plates at 150°C. The absorbance intensities at 915 cm^{-1} of the epoxy band for each sample are recorded every 6 minutes by the FT-IR. The reaction rates of these two samples are shown in Figure 6. The rate of reaction of the APS cured with the epoxy resin is slower than the rate of the MAPS cured with the epoxy resin. In the first ten minutes of the APS reaction, the epoxy resins react with moisture resulting in a slight decrease of the epoxy groups, after 10 minutes the concentration of the epoxy is unchanged. This result suggests that the APS did not react with the epoxy resin under this reaction condition, i.e. without adding the catalyst. Whereas, in the MAPS sample, the amount of the epoxide decreases as a function of heating time at 150°C. The results confirm that the secondary aminosilane, MAPS will react with the

epoxy resin, and a possible reaction is shown in Equation 2.

$$-\overset{|}{\underset{|}{Si}}-CH_2CH_2CH_2NHCH_3 \;+\; R-\overset{\displaystyle O}{\overset{\diagup\diagdown}{CH-CH_2}} \;\longrightarrow$$

$$\tag{2}$$

$$-\overset{|}{\underset{|}{Si}}-CH_2CH_2CH_2-\underset{\underset{CH_3}{|}}{N}-CH_2\underset{\underset{OH}{|}}{CH}-R$$

To determine whether the epoxide will react with the primary amine as well as the secondary amine, an experiment was carried out using a liquid aliphatic primary amine, n-propylamine. This primary amine was mixed with the epoxy resin and stored at room temperature for two weeks, then heated to $150^{\circ}C$ for one hour. The liquid mixture converts to a solid and the IR spectrum of the product is shown in Figure 7. Figure 7-B is the spectrum of the cured epoxy resin. The difference spectrum (Figure 7-C) shows several absorbance bands at 1462, 1252, and 1042 cm^{-1} which is due to the $NH-CH_2$ group in the product of copolymerization. The result suggests that the aliphatic primary amine can react with the epoxy resin.

The spectra of the APS and the epoxy resin mixtures heated at $200^{\circ}C$ and $300^{\circ}C$ for one hour are shown in Figure 8-A and Figure 8-B, respectively. It is observed that the epoxy band at 915 cm^{-1} is unchanged for the sample heated at $200^{\circ}C$, but the band disappeared for the sample heated at $300^{\circ}C$. The difference spectrum of these two samples shows that the peak intensities due to the epoxide

and the amine groups both become negative and the bands of the adduct group appearing at 1462 cm^{-1} and 1254 cm^{-1} become positive. Since the epoxy resin and the silane are thermally stable at a high temperature (19), the result suggests that the APS polymers react with the epoxy resin when they are heated at 300°C.

The tertiary amine, benzyldimethylamine (BDMA), is used as an accelerator in this study, at a level of 2% by weight. In the absence of the accelerator the anhydride group will not react with the epoxy resin. The infrared spectra of the mixture of the NMA and the epoxy resin are shown in Figure 9-C. The unreacted anhydride and the epoxy groups show several bands at 1860, 1780, 1229, 1040, and 915 cm^{-1}. These infrared absorbance bands disappear or decrease in intensity after being mixed with the hydrolyzed MAPS polymer with or without adding the catalyst when the samples are heated at 150°C for 1 hour (Figure 9-A and 9-B). The band at 1744 cm^{-1} indicates that an ester group is formed. The ester group is also obtained without adding the catalyst (Figure 9-B). Apparently MAPS reacts with the epoxy resin producing a hydroxyl group, and this hydroxyl group attacks the anhydride group to form an ester.

In order to understand the mechanism of the ester formation of the epoxy matrix, several experiments with different curing conditions were performed. Infrared spectra of the curing system with an initial ratio of equal weights of epoxy and anhydride is shown in Figure 10. The curing reaction carried out at 100°C took place between the salt plates and the spectra, are recorded at various times. The curing rates of the matrix at 90, 100, 120, and 150°C

with 2.0% BDMA are shown in Figure 11. The amount of the catalyst in the matrix is another important factor controlling the rate of curing.

The rates of curing of the matrix at $100^{o}C$ with 0.5%, 1.0%, and 2.0% BDMA are shown in Figure 12. It can be seen that the rate of esterification of the matrix is a function of the heating time, temperature, and the concentration of the accelerator. The concentrations of the ester groups were measured using the intensities of the ester band appearing at $1744 \, cm^{-1}$.

A fiber composite was made of the E-glass fiber treated with 1% MAPS aqueous solution and the epoxy-anhydride matrix with a 0.5% BDMA, then heated at $150^{o}C$ for 3 hours. The spectrum of the resulting fiber composite is shown in Figure 13-A. A control sample was made the same way but the fiber had no silane treatment. The spectrum of the control sample is shown in Figure 13-B. The difference spectrum of (A-B) is shown in Figure 13-C. Several positive bands appearing at 1744, 1640, 1215, 1183, and $1098 \, cm^{-1}$ are due to the reaction of the silane with the resin. The negative absorbances are caused by the consumption of the functional groups in the matrix and the coupling agent. The negative bands in the difference spectrum at $1780 \, cm^{-1}$ and $915 \, cm^{-1}$ reflect the consumption of the anhydride and the epoxide, respectively. The result confirms that copolymerization occurs at the interface of the coupling agent and the matrix in composites. Another interesting

result is the absorption of the ester groups at 1744 cm^{-1} remaining positive in the difference spectrum. This result suggests that the degree of curing in the matrix is higher than that in the control composites, when the fiber is treated with a silane coupling agent.

DISCUSSION

Under the same reaction conditions, the polymerized secondary aminosilane can copolymerize with the nadic methyl anhydride and the epoxy resin, but this is not the case for the primary amino- silane coupling agent. Thus the secondary aminosilane is more active than the primary aminosilane. The primary aminosilane, i.e. APS, is a very useful silane coupling agent used in many different polymer composites. However, it has been reported that the adhe- sion between the epoxy resin and the silane-treated fiber is not greatly improved by using APS in the composite (20). Our results indicate that the epoxy matrix will not react with the APS when the sample is heat-treated below 200°C or without adding the catalyst to the matrix. Therefore, no improvement in adhesion arises since the APS does not react with the matrix.

The processing temperature may influence the copolymerization of the aminosilanes and the epoxy resins. It was found that no

chemical reactions occur when the polymerized MAPS was heated with
the NMA below 80°C. When the sample was heated at 150°C for 1 hour,
the copolymerization took place and the bands, at 1860, 1780, 1227,
1084, and 915 cm^{-1}, representative of the anhydride group, showed
negative absorbance in the difference spectrum C of Figure 3. The
positive bands appearing at 1722 cm^{-1} and 1640 cm^{-1} correspond to
the acid and the amide groups of the adduct. The results indicate
that the MAPS polymer will copolymerize with the NMA when the
sample is processed at an elevated temperature. On the other hand,
when the polymerized MAPS was heated with the epoxy resin at 150°C
for 3 hours, the liquid epoxy resin became a solid sample. Several
epoxy bands of this product at 1250, 1040, and 915 cm^{-1} became
negative and several positive bands appeared at 1321, 1098, and
1068 cm^{-1} in the difference spectrum D of Figure 4. The spectrum
of the product using a secondary amine compound, methylbutylamine,
cured with the epoxy resin also shows a similar difference spectrum
(Figure 5). The result suggests that copolymerization takes place
between the coupling agent and the epoxy resin.

It is an interesting question whether or not the primary amine
can copolymerize with the epoxy resin. In fact, the primary amine,
n-propylamine, gives good curing at room temperature as shown in
Figure 7. The infrared bands appearing at 1462, 1252, and 1042
cm^{-1} in the difference spectrum in Figure 7-C are due to the adduct
of this amine and the epoxy resin. But there is no reaction when
the polymerized primary aminosilane is mixed with the epoxy resin

and heated to 200°C. After heating this mixture up to 300°C, from the infrared examination, both the amine and the epoxy bands decrease, and the infrared positive bands appear at 1254 cm^{-1} and 1045 cm^{-1} as shown in the difference spectrum in Figure 8. This result suggests that the copolymerization of the primary aminosilane and the epoxy resin only occurs at high temperatures. However, the polymeric matrix starts to degrade at the high curing temperatures which probably damage the structure of the matrix in composites (21). Since most epoxy resins cure below 200°C, it is apparent that few covalent bonds are formed between the epoxy resin and the APS layer in composites. Thus, physical absorption may also be important in determining the adhesion at the interfaces.

It has been shown that when aminosilanes are applied to glass surfaces from aqueous solution, the silane molecules on the glass may orient in such a manner that both the silanol and the amino ends of the molecule form a horeshoe-type structure (13). In order for the coupling agent to be effective, the amino group of the MAPS silane molecules in the outermost layer should be oriented away from the glass surface. In this manner it can be seen that the glass surface appears to be coated with an amine outer layer. After the epoxy resin is applied to the fibers and heated, a chemical reaction occurs between the anhydride cured epoxy resin and the aminosilane. The improved molecular structure model of this composite is shown in Figure 14. Since a secondary aminosilane

replaces the primary aminosilane in composites, the imide compound no lon-
ger can be formed in this system. In addition, the chemical reactivity of
MAPS is also higher than APS. The adhesion between the fiber and the matrix
may be improved by using MAPS, due to an increase in the number of inter-
facial bonds in the reinforced composites.

Besides the interfacial reactions at the matrix/coupling agent inter-
face, the curing mechanism of the matrix in the composite is quite different
from the bulk resin. Without adding the catalyst to the mixture of epoxy
resin and anhydride, the copolymerization is extremely slow. After adding
the MAPS to the mixture (since the silane coupling agent participates in the
curing of the epoxy resin), the copolymerization takes place very rapidly.
The strong ester band appearing at 1744 cm^{-1} (Figure 8) is evidence of this
reaction. The side products, hydroxyl and acid groups, are the major compon-
ents for curing the matrix as indicated in Equation 1.

The uncured epoxy resin serves two chemical purposes: A portion of the
epoxy resin reacts with the amino groups of the deposited silane to form a
tightly bonded coating which protects the fiber, and the other portion forms
a polymeric matrix. The cured epoxy resin will not react continuously with
the silane molecules. Therefore, the amount of uncured low moleuclar weight

epoxy resin will determine the amount of interfacial bonds at the interface. The curing of the resin causes the number of the reactive functional groups in the resin to decrease. Thus, it can be seen that if the curing rate of the epoxy resin goes too fast, then the number of interfacial bonding will decrease. The curing rate of the anhydride-epoxy resin at different reaction conditions is shown in Figures 10, 11, and 12. It is obvious to see, that the temperature, concentration of the accelerator, and the reaction time are important factors in controlling the curing of the resin and the composite.

In order to obtain a maximum number of interfacial bonds in the interface of the composite, the optimum process conditions must be found. Usually the chemical reaction is favorable at a higher temperature. However, a very high temperature will cause the polymer to degradate. Since the epoxy resin is cured very fast and at elevated temperatures, using the lowest amount of accelerators will decrease the rate of curing for the matrix. Therefore, higher curing temperatures and a lower amount of accelerators will increase the amount of interfacial bonding while fabricating the epoxy composites.

The improved E-glass fiber composite, treated with APS silane, was cured at $150^{o}C$ for 3 hours and only 0.5% benzyldimethylamine (BDMA) was employed. An amide band appearing at 1640 cm^{-1} due to the adduct of the copolymerization of the silane coupling agent and the matrix, is shown in the difference spectrum in Figure 13. This

band is evidence that a covalent bond is formed at the interface of the matrix and the silane coupling agent. Furthermore, the positive ester bands appearing at 1744 cm^{-1} and 1183 cm^{-1} are additional evidence proving that the secondary aminosilane induced curing of the epoxy resin in this composite. These extra amounts of esterification of the matrix, may contribute improvements in the mechanical properties of the fiber reinforced composites.

ACKNOWLEDGEMENT

REFERENCES

1. H. Ishida and J.L. Koenig, Polym. Eng. & Sci., 36, 128 (1978).

2. E.P. Plueddemann, Interfaces in Polymer Matrix Composites, Academic Press, 1974, Chapter 1.

3. R.L. Schwartz and H.S. Schwartz, Fundamental Aspects of Fiber Reinforced Plastic Composites. Wiley Sons, N.Y., 1968, p163.

4. R.L. McCullough, Concepts of Fiber-Resin Composites, Marcel Dekker, N.Y., 1971, p61.

5. P.T.K. Shih and J.L. Koenig, J. Colloid & Interface Sci., 36, 247 (1971).

6. D.L. Chamberlain, M.W. Christensen, and M. Bertoluci, Proc. 24th Ann. Tech. Conf., Reinforced Plastics Div., SPI, 19-C, (1969).

7. E.P. Plueddemann, Additives for Plastics, 2, 123 (1978).

8. J.A. Laird and W.F. Nelson, Proc. 19th Ann. Tech. Conf., Reinforced Plastics Div., SPI, 11-C (1964).

9. J.G. Marsden, Proc. 27th Ann. Tech. Conf., Reinforced Plastics Div., SPI, 21-A (1972).

10. S. Sterman and H.B. Bradley, Proc. 16th Ann. Tech. Conf., Reinforced Plastics Div., SPI, 8-D (1960).

11. S.E. Berger, P.J. Orenski, and M.W. Ranney, Fillers and Rein-forcements for Plastics, ACS Advan. Chem. Ser. No. 176, 73 (1974).

12. R. Wang, Mechanism of Coupling by Silanes of Epoxies to Glass Fibers, in Fundamental Aspects of Fiber Reinforced Plastic Composites, Wiley & Sons, N.Y., 1974, p237.

13. C.H. Chiang, H. Ishida, and J.L. Koenig, Proc. 35th Ann. Tech. Conf., Reinforced Plastics Div., SPI, 23-D (1980).

14. C.H. Chiang, H. Ishida, and J.L. Koenig, J. Colloid & Interface Sci., 14 (2), 396 (1980).

15. O.K. Johannson, F.O. Stark, G.E. Vogel, and R.M. Fleischmann, J. Composite Materials, 1, 278 (1967).

16. H. Ishida and J.L. Koenig, J. Polym. Sci., Physics, 17, 615 (1979).

17. H. Ishida and J.L. Koenig, Appl. Spectrosc., 32, 462 (1978).

18. L.J. Bellamy, The Infra-Red Spectra of Complex Molecules, Wiley, N.Y., 1975.

19. H. Lee and K. Neville, Handbook of Epoxy Resin, McGraw-Hill, New York, 1967, Chapter 5.

20. E. Bagda, Kunststoffe (Ger.), 65(7), 417 (1975).

21. S.C. Lin, B.J. Bulkin, and E. M. Pearce, J. Polym. Sci., Part 1, 3121 (1980).

FIGURE CAPTIONS

Figure 1:   The molecular structure of interfaces between the nadic methyl anhydride cured epoxy resin and APS treated fiberglass in composite.

Figure 2:   The infrared spectra of A: Poly-N-methylaminopropylsiloxane polymer; B: N-methylaminopropyltrimethoxysilane.

Figure 3:   The infrared absorbance spectra of the adduct of nadic methyl anhydride and MAPS. A: the adduct of NMA and MAPS; B: nadic methyl anhydride; C: difference spectrum of A-B.

Figure 4:   The infrared absorbance spectra of the adduct of epoxy resin and MAPS. A: epoxy resin was heated with hydrolyzed MAPS at 150°C for 3 hours; B: hydrolyzed MAPS; C: uncured epoxy resin; and D: difference of A-B-C.

Figure 5:   The infrared absorbance spectra of the adduct of epoxy resin and N-methylbutylamine (MBA). A: the adduct of MBA and epoxy resin; B: epoxy resin; C:N-methylbutylamine; and D: difference of A-B-C.

Figure 6:   When APS and MAPS are reacted with epoxy resin with a tertiary amine (BDMA), the epoxy resin preferentially reacts with MAPS at an elevated temperature.
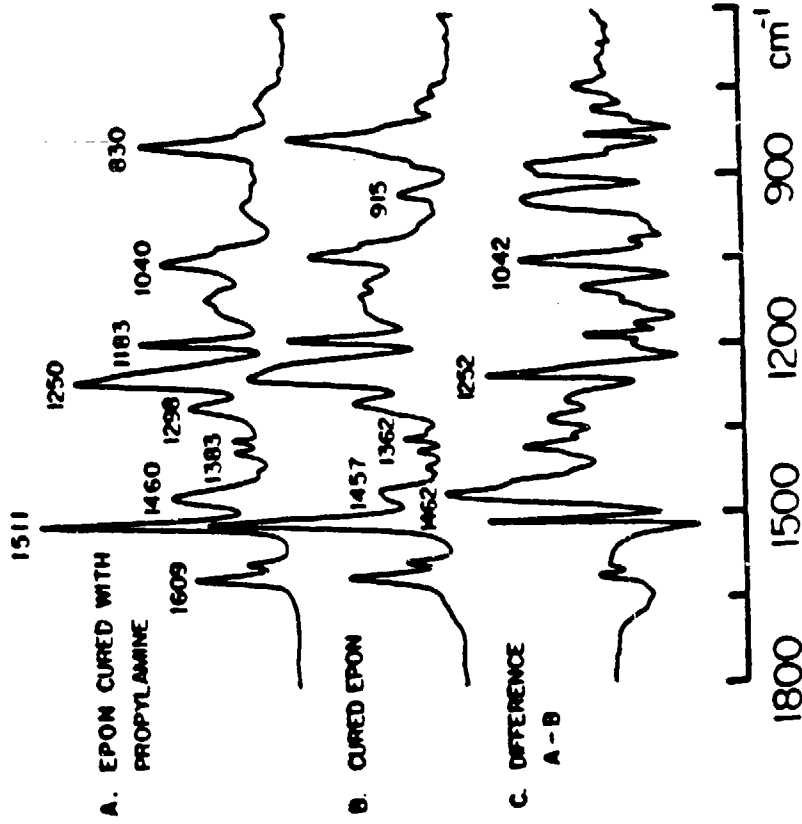
Figure 7:   The infrared absorbance spectra of the copolymerization of epoxy resin and n-propylamine. A: the product of n-propylamine cured epoxy resin; B: BDMA cured epoxy resin; C: difference spectrum of A-B.
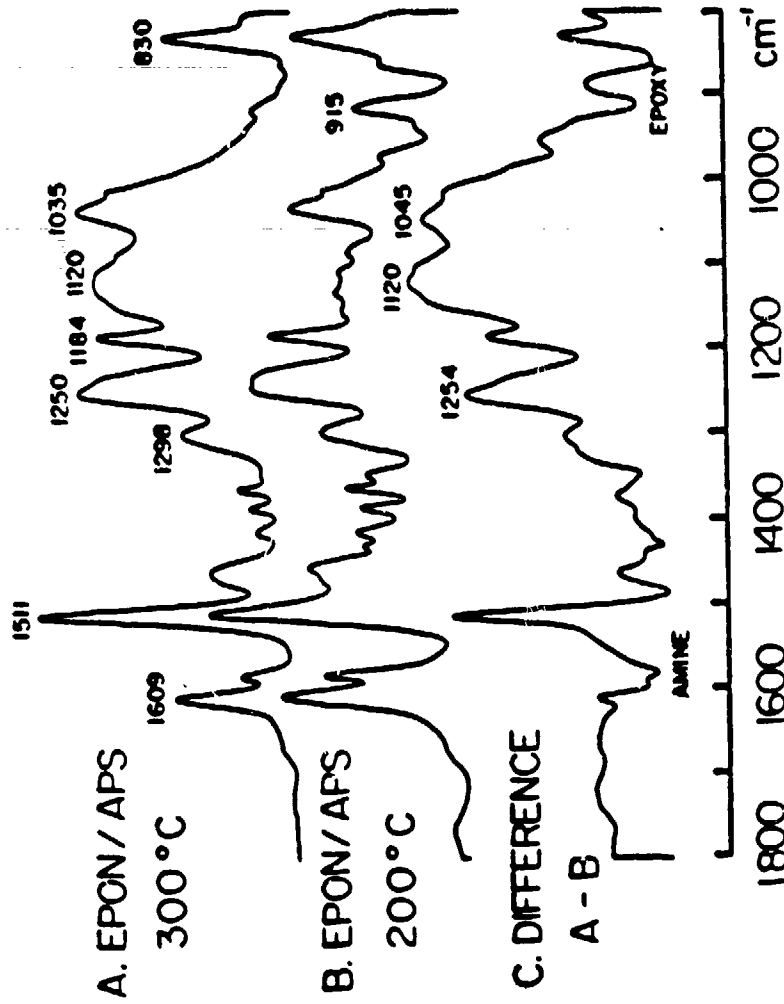
117

Figure captions continued...

Figure 8:   The infrared absorbance spectra of the products of APS cured epoxy
resin at different temperatures. A: sample was heated at 300°C for one hour;
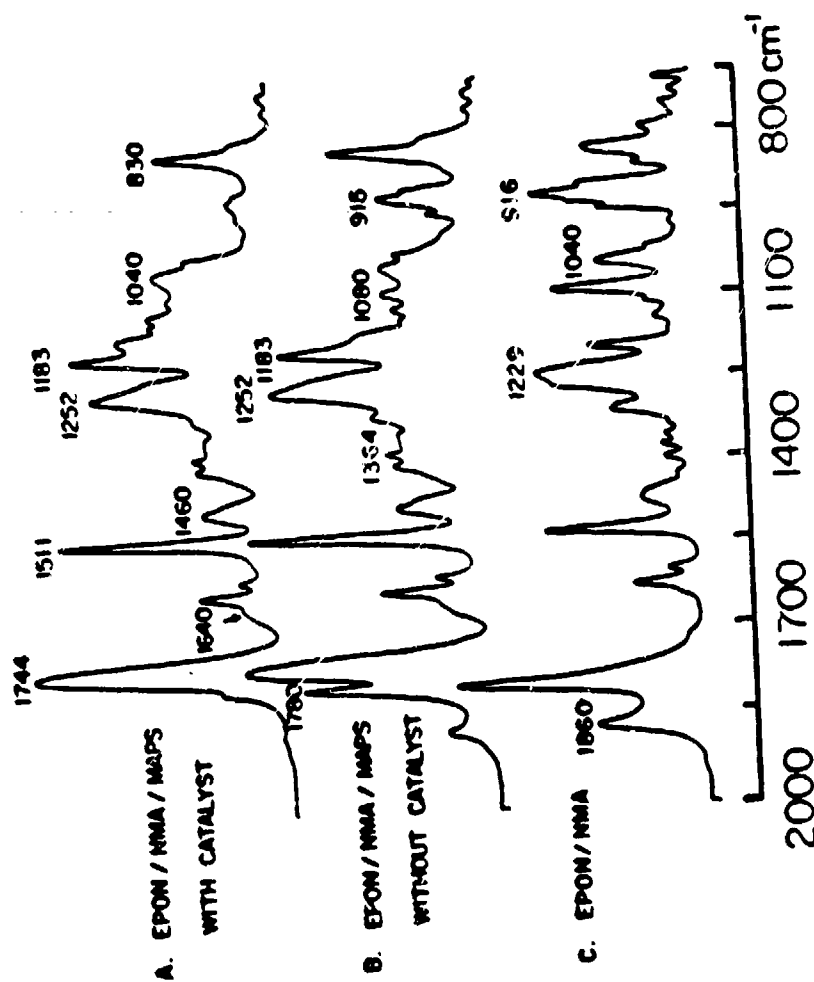B: sample was heated at 200°C for 1 hour; C: difference spectrum A-B.

Figure 9:   The infrared absorbance spectra of the products of epoxy resin and
hydrolyzed MAPS with and without accelerator BDMA. A: with BDMA; 3: without
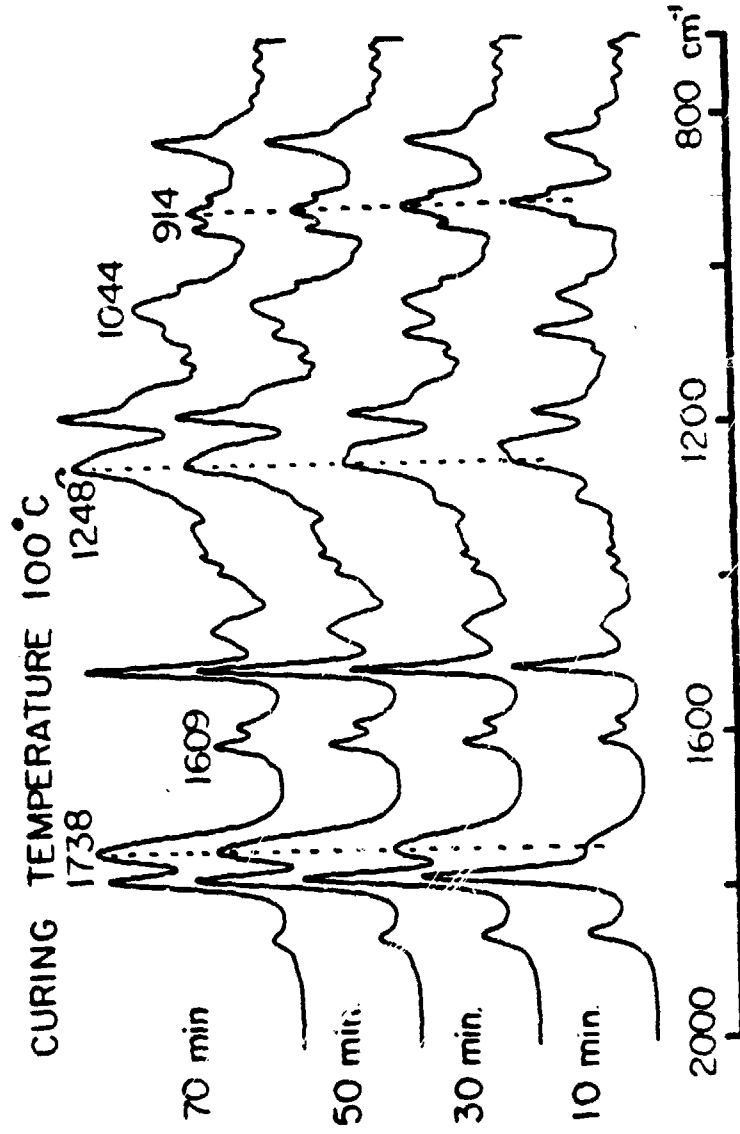BDMA; and C: without BDMA and MAPS.

Figure 10: The infrared absorbance spectra of epoxy resin during cure with
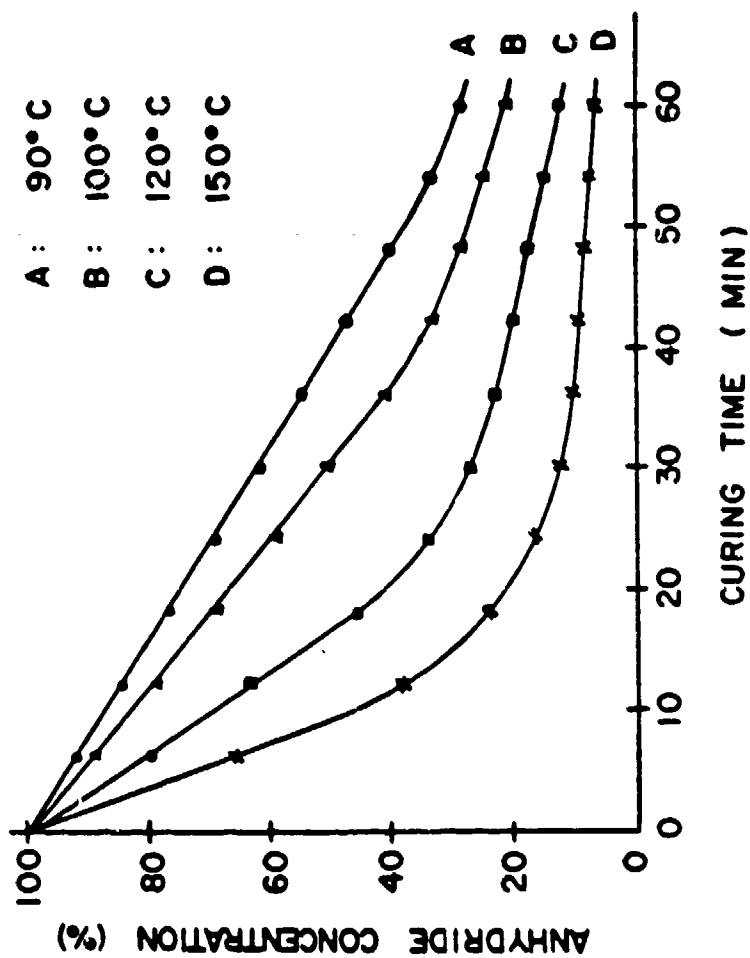anhydride at 100°C at various times.
Figure 11: The rates of curing reaction between epoxy resin and nadic methyl
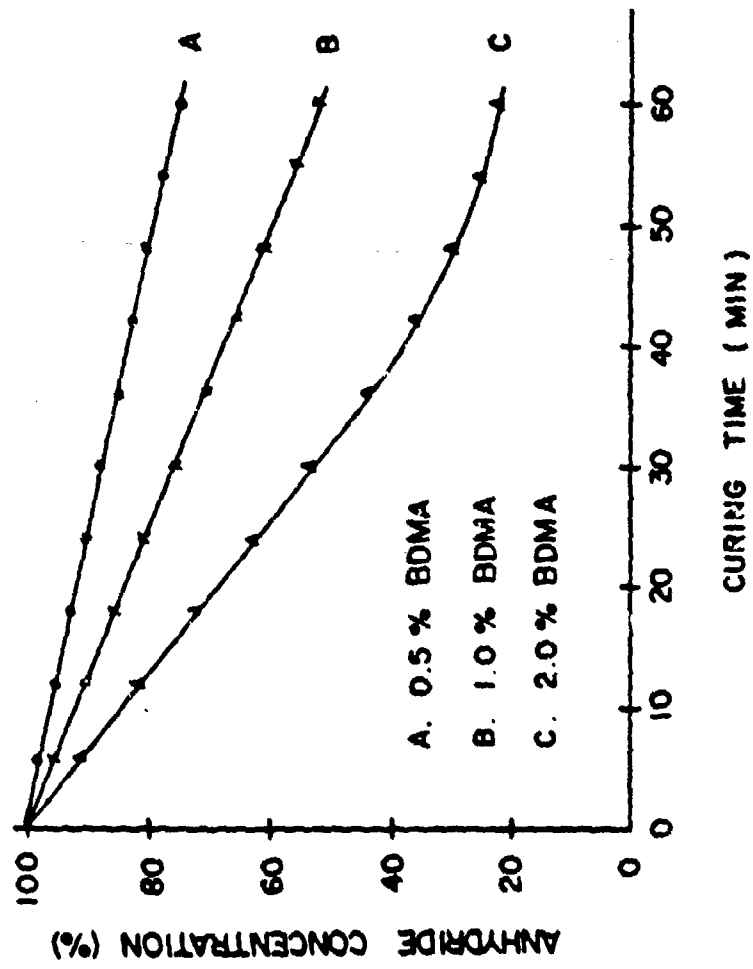anhydride are accelerated by 2% BDMA at various temperatures.

Figure 12: The rate of curing reactions of epoxy resin and nadic methyl
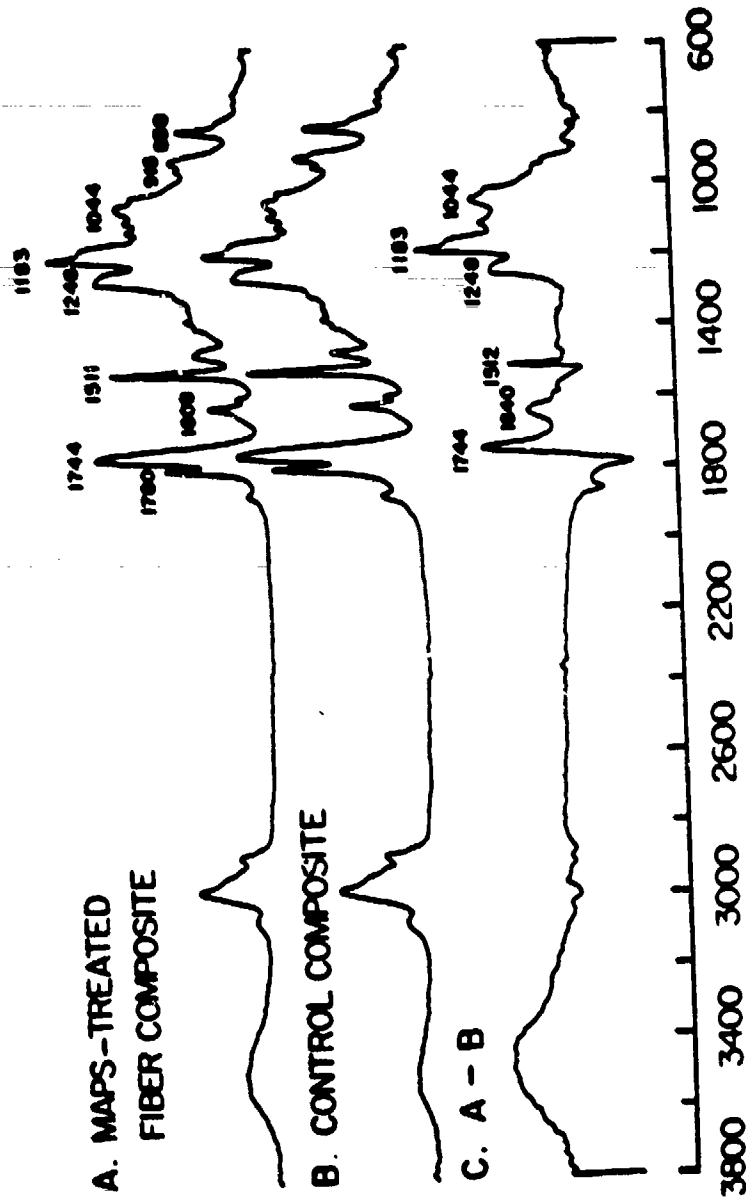anhydride are accelerated by various amounts of BDMA at 100°C.

Figure 13: The infrared absorbance spectra of E-glass fiber reinforced compos-
ites. A: the glass fiber was treated with 1% of MAPS; B: the fiber was non-
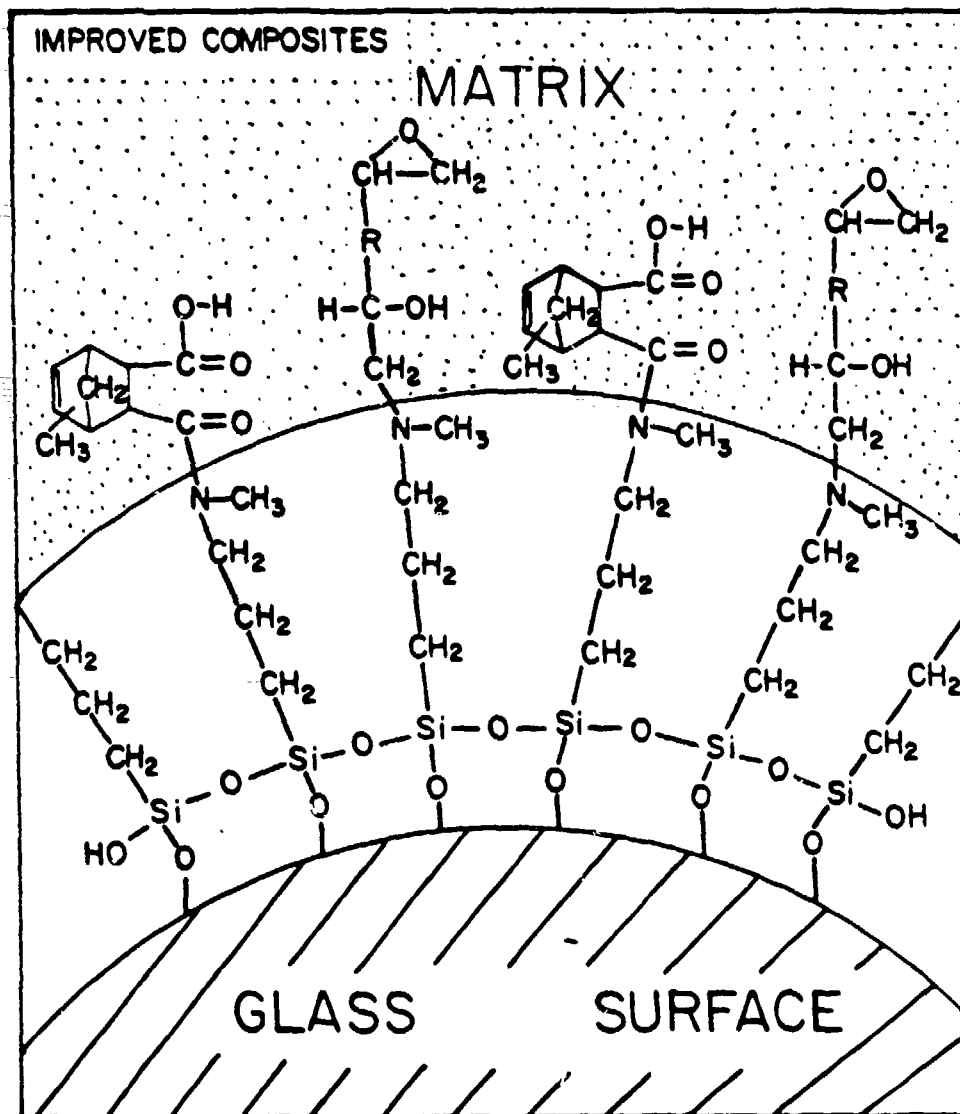treated; and C: the difference spectrum of A-B.

Figure 14: The model of molecular structure of a MAPS-treated fiberglass rein-
forced composites.

Figure 1: The molecular structure of interfaces between the nadic methyl anhydride cured epoxy resin and APS treated fiberglass in composite.

Figure 2: The infrared spectra of A: Poly-N-methylaminopropylsiloxane polymer;
B: N-methylaminopropyltrimethoxysilane.
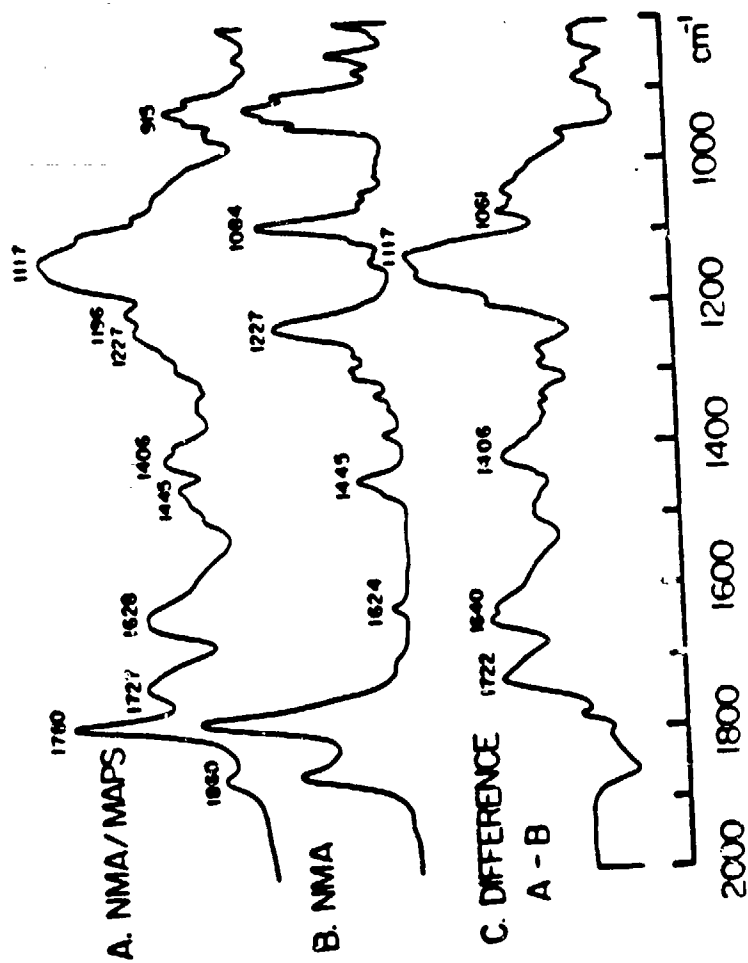
Figure 3: The infrared absorbance spectra of the adduct of nadic methyl anhydride and MAPS. A: the adduct of NMA and MAPS; B: nadic methyl anhydride; C: difference spectrum of A-B.

Figure 4: The infrared absorbance spectra of the adduct of epoxy resin and MAPS.
A: epoxy resin was heated with hydrolyzed MAPS at 150°C for 3 hrs;
B: hydrolyzed MAPS; C: uncured epoxy resin; and D: difference of A-B-C.

Figure 5: The infrared absorbance spectra of the adduct of epoxy resin and N-methylbutylamine (MBA). A: the adduct of MBA and epoxy resin; B: epoxy resin; C N-methylbutylamine; and D: difference of A-B-C.

Figure 6: When APS and MAPS are reacted with epoxy resin with a tertiary amine (BDMA), the epoxy resin preferentially reacts with MAPS at an elevated temperature.

Figure 7: The infrared absorbance spectra of the copolymerization of epoxy resin and n-propylamine. A: the product of n-propylamine cured epoxy resin; B: BDMA cured epoxy resin.; C: difference spectrum of A-B.

125

Figure 8: The infrared absorbance spectra of the products of APS cured epoxy resin at different temperatures. A: sample was heated at 300°C for one hour; B: sample was heated at 200°C for 1 hour; C: difference spectrum A-B.

Figure 9: The infrared absorbance spectra of the products of epoxy resin and hydrolyzed MAPS with and without accelerator BDMA. A: with BDMA; B: Without BDMA; and C: without BDMA and MAPS.

Figure 10: The infrared absorbance spectra of epoxy resin during cure with anhydride at 100°C at various times.

Figure 11: The rates of curing reaction between epoxy resin and nadic methyl anhydride are accelerated by 2% BDMA at various temperatures.

Figure 12: The rate of curing reactions of epoxy resin and nadic methyl anhydride are accelerated by various amounts of BDMA at 100°C.

Figure 13: The infrared absorbance spectra of E-glass fiber reinforced composites.
A: the glass fiber was treated with 1% of MAPS; B: the fiber was
non-treated; and C: the difference spectrum of A-B.

131

Figure 14:   The model of molecular structure of a MAPS-treated
            fiberglass reinforced composites.

CHEMICAL REACTIONS OCCURRING AT THE INTERFACE OF

EPOXY MATRIX AND AMINOSILANE COUPLING AGENTS

IN FIBER-REINFORCED COMPOSITES

by

Chwan Hwa Chiang and Jack L. Koenig

Department of Macromolecular Sci .ce

Case Western Reserve University

Cleveland, Ohio 44106

CHEMICAL REACTIONS OCCURRING AT THE INTERFACE OF

EPOXY MATRIX AND AMINOSILANE COUPLING AGENTS

IN FIBER-REINFORCED COMPOSITES

by

Chwan Hwa Chiang and Jack L. Koenig
Department of Macromolecular Science
Case Western Reserve University
Cleveland, Ohio 44106

Abstract

The chemical reactions at the interface between an anhydride-cured epoxy resin and an aminosilane treated fiber have been investigated using FT-IR. The results indicate that chemical bonds are formed in the interfacial region between the matrix and the coupling agents. The amount of interfacial bonding depends on the composition and the processing conditions.

Introduction

It has been found that the application of silane coupling agents to glass fibers in reinforced plastics results in improved laminate properties (1-3). These improvements have been most notable in the ability of the laminates to retain strength under conditions of exposure to moisture. While no completely satisfactory explanation has been offered for this phenomenon, the theory of chemical bonding appears useful. This theory proposes that the coupling agent forms a chemical bond with the surface of the glass fiber through a silanol group while the organic functional group chemically bonds with the resin. Adhesion of the resin to the fiber is therefore, strengthened through a chain of chemical bonds (4-6).

The chemical bonding between the matrix and the coupling agent has been studied in a variety of ways. Sterman and Marsden (7) determined the extractability of polystyrene and polyethylene from composites with E-glass and E-glass finished with 3-methacryloxypropyltrimethoxysilane as the coupling agent. Residual carbon analysis indicated that a thin layer of polymer was retained on the surface through long periods of extraction with the coupling agent. Johannson (8) et al. utilized ^{14}C-labeled poly-(methylmethacrylate-co-styrene) to determine the extractibility of the resin from its composite with E-glass in the presence and absence of coupling agent. They found that the presence of coupling agents results in retention of a sizable residue of resin after the extraction procedure. Gent and Hsu (9) have demonstrated existance of chemical bonding between model silane compounds and finely divided silica particles by near infrared measurements.

Fourier transform infrared (FT-IR) spectrometers (10,11) can produce spectra which are useful for the study of the structure and reactions of silane coupling agents on glass surfaces. Some studies of this type have been reported from our laboratory (12-16). One of the most effective coupling agents is an aminosilane and we have reported the molecular structure of the amino silane coupling agent adsorbed on glass surfaces (16). In this paper we report the copolymerization of the anhydride-cured epoxide matrix with the aminosilane coupling agents at the interface of fiber-glass reinforced composites.

Experimental

Sample Preparation

Diglycidyl ethers of bisphenol (EPON 828 epoxy resin, shell) cured with methylbicyclo(2,2,1)hept-5-ene-2,3-dicarboxylic anhydride (Fisher) have been studied. The curing accelerator was benzyldimethyl-amine (BDMA) (Fisher). The coupling agent, γ-aminopropyltriethoxysilane (A-1100) was purchased from Petrarch Chemicals Inc. Two kinds of glass substances were used in this experiment; a high surface-area silica powder (Cab-O-Sil, grade EH-5, Cabot Corp.), and E-glass fibers kindly supplied by Crane & Co. Inc. (Crane-50-01). The glass sheet was heat cleaned at $500^{o}C$ for one day in air then stored in a descicator. After completion of the hydrolysis reaction of a silane coupling agent, the glass sheet was immersed into the 1% by weight aqueous solution of the silane for 5 min and dried at room temperature. The silica powder was treated by the usual methods (16).

Infrared Spectroscopy

The infrared spectra were obtained on a Digilab Model FTS-14 Fourier Transform Spectrophotomer. Each spectrum was recorded in double precision at a resolution of 2 or 4 cm^{-1} with a total of 200 scans. The frequency scale is calibrated internally with a reference helium-neon laser to an accuracy of 0.01 cm^{-1}. The precision in this reported frequencies is 1 cm^{-1}. The spectra were stored in the tape for further data manipulation.

Results and Discussion

In this study we have concentrated on the interaction between an anhydride-cured epoxy resin and an aminosilane treated fiber. Anhydride-cured epoxy resins generally exhibit improved high-temperature stability over the amine-cured resins and have better physical and electrical properties above their deflection temperature (17). The chemical structure and infrared absorbance spectra of epoxy resin (EPON 828) and nadic methyl anhydride (NMA) are shown in Figure 1. A tertiary amine, benzyldimethylamine (BDMA) is used as an accelerator, at a level of 1% by weight. In the absence of accelerator the anhydride group will not react directly with the epoxy group. If hydroxyl groups are present on the resin, the anhydride will react to produce carboxylic acids, which may then react with epoxy groups to generate additional hydroxyls capable of reacting with additional anhydride groups. Several experiments with different curing conditions have been tested, such as changes in temperature, amount of accelerator, and the relative stoichiometric amounts of NMA and epoxy resin, in order to under-stand the curing processes. Infrared spectra of the curing system which

proceeds at room temperature with a ratio of epoxy and anhydride of 1:1 by weight are shown in Figure 2. The curing reaction took place between the salt plates, and spectra are recorded at various times. The esterification of this system is shown in Equation 1.

$$\text{(structure)} \quad (1)$$
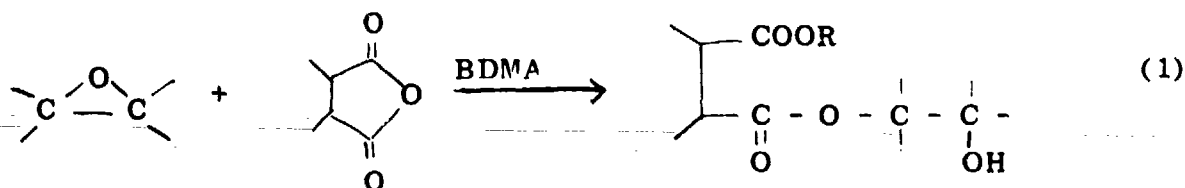
The infrared bands of the anhydride groups disappeared steadily at 1858, 1780, 1227, 1082, and 916 cm^{-1}. The bands due to the epoxy groups at 916 and 864 cm^{-1}, overlap with those of the anhydride groups, also disappeared as the reaction proceeds. The band intensities of the ester groups at 1738 cm^{-1} and ether groups at 1248 cm^{-1} increase as the curing progress. Obviously, the reaction mechanism is quite complex, and several mechanisms have been proposed (17-20). The curing rates are governed by reaction temperature and amount of accelerator.

The aminosilane coupling agent was one of the first organo-functional silanes to find wide acceptance as a coupling agent in reinforced plastics. The high reactivity and versatility of the aminofunctionality has led to an increasing number of diverse applications. Our previous study (16) indicated that hydrolyzed γ-aminopropyltriethoxysilane exists in two different forms; one a chelate ring and the other a non-ring extended structure. The APS coupling agent exists as a multilayer on the E-glass fiber surfaces and forms a polyaminosiloxane. However, the aminosilane adsorbs onto the high-surface-area silica as a monolayer and the amino groups interact with the silica surface (16).

In order to understand the reactions of the interface between the coupling agents and matrix, we first studied the reactions between each individual matrix component and the polyaminosiloxane. First, epoxy resin was heated with 30% by weight polyaminosiloxane at $160^{\circ}C$ for 2 hours with and without benzyldimethylamine, the infrared absorbance spectra are shown in Figure 3. Sample A (without BDMA) was a viscous liquid and the intensity of the band at 916 cm^{-1} due to the epoxy group decreased about 17%. A very groad band appeared at about 3300–3500 cm^{-1}, probably due to hydroxyl groups and secondary N–H groups. These results indicated that the primary amine of APS attacks the epoxy resin through the chemical reaction shown below.

$$RNH_2 \;+\; \text{\Large >C}\!\!-\!\!\overset{O}{\triangle}\!\!-\!\!\text{\Large C<} \;\longrightarrow\; R - \underset{\underset{H}{|}}{N} - \overset{|}{\underset{|}{C}} - \overset{\overset{OH}{|}}{\underset{|}{C}} - \qquad (2)$$
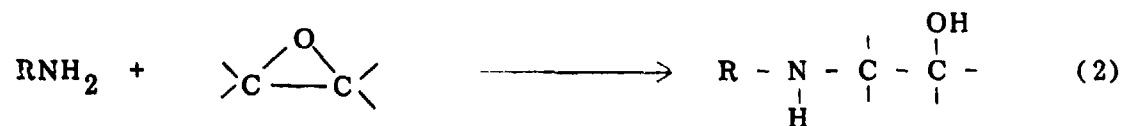
Sample B (without BDMA) became a yellow solid and the band due to epoxy group almost completely disappeared. The intensity of the infrared band at 3300 cm^{-1} due to the secondary amine decreased. At least 35% of the epoxy groups reacted with the secondary amine to form a tertiary amine. The reaction is shown as Equation 3.

$$R - \underset{\underset{H}{|}}{N} - \overset{|}{\underset{|}{C}} - \overset{\overset{OH}{|}}{\underset{|}{C}} - \;+\; \text{\Large >C}\!\!-\!\!\overset{O}{\triangle}\!\!-\!\!\text{\Large C<} \;\longrightarrow\; R - N \Big\langle \begin{array}{c} \overset{|}{C} - \overset{\overset{OH}{|}}{\underset{|}{C}} - \\[2pt] \overset{\underset{OH}{|}}{C} - \overset{|}{\underset{|}{C}} - \end{array} \qquad (3)$$
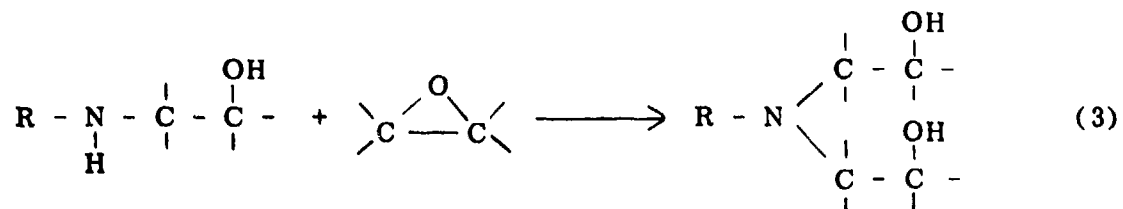
Methylbicyclo(2,2,1)hept-5-ene-2,3-dicarboxylic anhydride (NMA) and 30% by weight polyaminopropylsiloxane was heated at $160^{\circ}C$ for one hour with and without BMA. The resulting spectra are shown in Figure 4. Sample A (without BDMA) was an elastomeric-like yellow solid. The spectrum of sample A showed new bands at 1700 cm^{-1} and 1399 cm^{-1}. The expected

product was an amide and the chemical reaction expected is below:
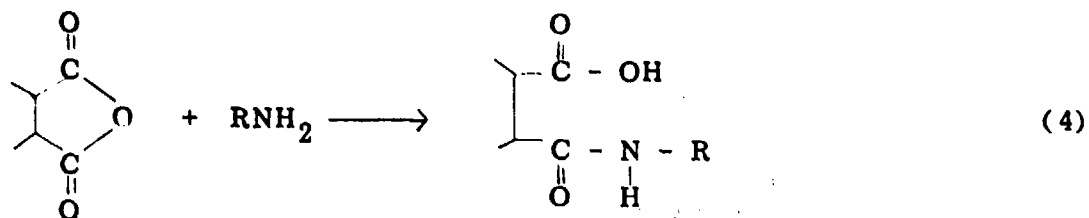
Typically, amide groups show two strong IR bands at about 1650 and 1550 cm^{-1}. The spectrum of sample A shows only a single band at 1700 cm^{-1}, which makes it unlikely that the reaction indicated by Equation 4 occurred with NMA.

The sample B (with BDMA) is a yellow liquid and the spectrum shows that NMA does not react appreciably with the amine. Apparently, BDMA inhibits the amine reaction, i.e. the Lewis base reacts preferentially with an anhydride to generate a complex. The chemical reaction is shown in Equation 5.
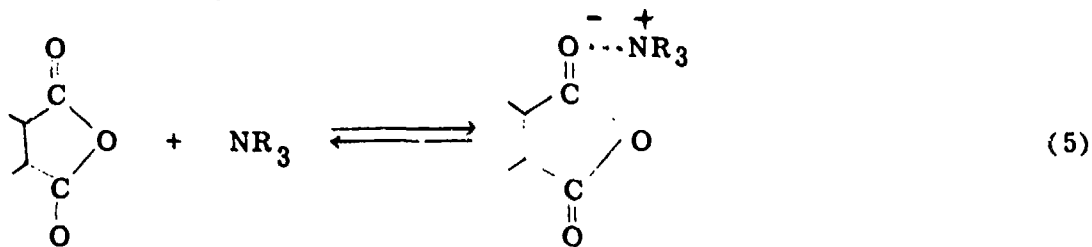
These results indicate that BDMA plays a role in retarding the reaction of NMA with APS amine.

In other words, the anhydride group might react with the amine to form the amide (like Eq. 4) without added tertiary amine. Possibly the reaction then proceeds and forms an imide as shown in Equation 6 (21).

$$\begin{matrix} \text{O} \\ \parallel \\ \diagdown \text{C} - \text{OH} \\ \\ \diagup \text{C} - \text{NHR} \\ \parallel \\ \text{O} \end{matrix} \quad \longrightarrow \quad \begin{matrix} \text{O} \\ \parallel \\ \text{C} \\ \diagup \quad \diagdown \\ \quad\quad \text{N} - \text{R} \\ \diagdown \quad \diagup \\ \text{C} \\ \parallel \\ \text{O} \end{matrix} \qquad (6)$$
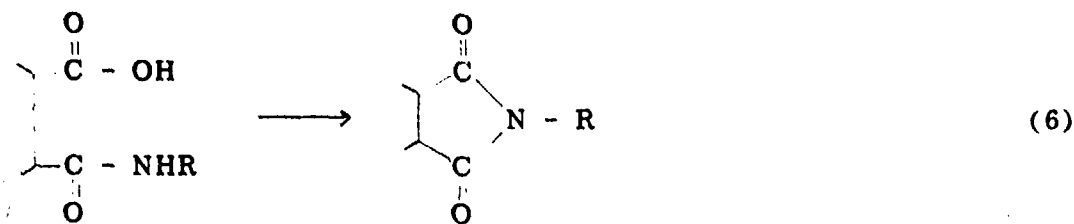
If the reaction to the imide occurs, the amide is an intermediate and may not be observed. Two model compounds have been made in order to test this reaction and band assignment. The anhydride NMA was mixed with n-propylamine at room temperature, and infrared spectrum is shown in Figure 5-a. As we can see, two very strong bands appear at 1650 and 1553 cm^{-1} which are assigned to the amide group (2). When this sample is heated at 150$^{\text{o}}$C for one hour, the sample becomes a yellow liquid. The spectrum is shown in Figure 5-b. Two strong bands appear at 1700 and 1397 cm^{-1}, in a fashion similar to the bands in spectrum 4-a. These results indicate the formation of imides. The infrared band at 1700 cm^{-1} can be assigned as the out-of-phase stretching mode of the C=O groups, and the band at 1397 cm^{-1} is C-N stretching mode of the imide compound (22).

Before studying the fiber composite, two matrix samples of 1:1 by weight epoxy and anhydride were prepared, one with 30% of polyamino-siloxane, and one without. Both samples were heated to 160$^{\text{o}}$C for two hours. The spectra of these two samples are shown in Figure 6. Using the band at 1511 cm^{-1} as an internal standard, the difference spectrum was obtained and is shown in Figure 6-c. It was found that several negative bands appeared at 1858, 1780, 914, and 866 cm^{-1}. These bands are due to the anhydride and epoxy groups. Thus the aminosiloxane reacted with both the anhydride and epoxy and increasing the degree of

crosslinking in this sample. Several new bands appeared at 3300, 1700, 1663, 1567, and 1399 cm^{-1}. As we mentioned before, a broad band appears at about 3300 cm^{-1}, which is due to the N-H stretching mode of secondary amines and OH groups. This is additional evidence for the interaction of amine and epoxy groups. Two bands at 1663 and 1567 cm^{-1}, which are assigned to the amide group, indicate that the APS amine has reacted with the anhydride, i.e. only one carbonyl group reacted with the amine and the other reacted with the epoxy in matrix. This is another type of chemical bond between the matrix and the coupling agent layer. The bands at 1700 and 1399 cm^{-1} due to the imide compound form as the adduct of APS amine and anhydride NMA. This side reaction terminates the polymerization so no further crosslinking will occur. This imide product yields no interfacial coupling between the coupling agent and the matrix.

A composite was made using E-glass fibers treated with 1% APS and a matrix with stoichiometric amounts of epoxy and anhydride which was heated to 160°C for three hours between two teflon alumina foils. The absorbance spectra of the composite, E-glass fibers, and the cured matrix are shown in Figure 7. After double subtraction of the spectra of the fiber and cured matrix from the composite spectrum, the resulting difference spectrum is shown in Figure 7-d. The aminosiloxane is shown to react with the matrix as bands appear at 1663 and 1567 cm^{-1}. These results indicate that an amide forms in the interfacial region. The imide also forms as bands appear at 1700 and 1399 cm^{-1}. A band appears at 3300 cm^{-1} due to N - H groups which means the coupling agent reacted with the epoxy group. These results indicate there is chemical bond formation between the amine and the epoxy resin. The primary amine of APS effectively acts as an

epoxy curing agent. These chemical bonds probably play a role in determining the mechanical properties of reinforced composites. The imide compound of the interface limits the amount of interfacial bonding.

In order to study the influence of the glass surface on the reactivity between the coupling agent and the matrix, 30% by weight of treated Cab-O-Sil was added to 1:1 epoxy/anhydride matrix, and heated to $160^{\circ}C$ for two hours. The difference spectrum of epoxy laminate and cured matrix is shown in Figure 8-c. The two positive bands at 1700 and 1399 cm^{-1} indicate that the imide is present at the interface. But no amide bands are detected. These results indicate that either the acidity of the silica surface or the moisture on the silica surface favor imide formation. Thus the interaction of the APS amine with the epoxy portion of the resin is the only interfacial reaction occurring at the interface. Therefore the amount of epoxy in the matrix governs the extent of chemical bonding in the interfacial region of APS-treated fiber reinforced composites.

Conclusion

The chemical reactions at the interfacial region of anhydride-cured epoxy resin and polyaminosiloxane in fiber reinforced composites has been studied by Fourier transform infrared spectroscopy. Several conclusions about the interface reactions are deduced from these experiments:

1. The epoxy resin reacts with polyaminosiloxane forming chemical bonds at the interface. The primary amine of APS works as a curing agent for the epoxy resin.

2. The curing accelerator, BDMA, increases the reaction rate of the epoxy resin and polyaminosiloxane.

3. Nadic methyl anhydride reacts with the polyaminosiloxane forming an imide which does not chemically bond across the surface.

4. The curing accelerator, BDMA, decreases the rate of the reaction between NMA and polyaminosiloxane.

5. Several competing reactions take place at the interface, producing esters, amides, imides, secondary amines, and tertiary amines.

6. The major chemical bonding between the matrix and the amine coupling agent occurs between the epoxy and amine groups. A small amount of amide bonding also have been found.

Many different chemical species are produced in the interfacial region of glass reinforced anhydride-cured epoxide resins. Each chemical species will respond differently to environmental effects, especially with respect to moisture attack.

Acknowledgment

References

1. E.P. Plueddemann, "Interfaces in Polymer Matrix Composites", Academic Press (1974).

2. P.W. Erickson, A.A. Volpe, and E.R. Cooper, Proc. SPI Conf. Reinforced Plast. Div., 19th Sect. 21-a (1964).

3. E. Lotz, D. Wood, and R. Barnes, Proc. SPI Conf. Reinforced Plast. Div. 26th Sect. 14-D (1971).

4. P.T.K. Shih and J.L. Koenig, J. Colloid Interface Sci. 36, 247 (1971).

5. H. Ishida and J.L. Koenig, Polymer Eng. & Sci. 18, 128 (1978).

6. D.L. Chamberlain, M.V. Christensen, and M. Bertolucci, Proc. SPI Conf. Reinforced Plast. Div., 24th, 19-C (1969).

7. S. Sterman and J.G. Marsden, Proc. SPI Conf. Reinforced Plas. Div. 21 (1966).

8. O.K. Johannson, F.O. Stark, G.E. Vogel, and R.M. Fleischman, J. Compos. Mater., 1, 278 (1967).

9. A.N. Gent and E.C. Hsu, Macromolecule, 7, 933 (1974).

10. P. Griffiths, Fourier Transform Infrared Spectroscopy, Wiley, New York (1975).

11. R.J. Bell, Introductory Fourier Transform Spectroscopy, Academic Press, New York (1972).

12. H. Ishida and J.L. Koenig, J. Colloid Interface Sci., 64, 555 (1978).

13. H. Ishida and J.L. Koenig, J. Appl. Spectr., 32, 462 (1978).

14. H. Ishida and J.L Koenig, J. Appl. Spectr., 32, 469 (1978).

15. D.L. Tabb and J.L. Koenig, Macromolecules 8, 929 (1975).

16. C.H. Chiang, H. Ishida and J.L. Koenig, J. of Colloid Interface Sci. (accepted).

17. H. Lee and K. Neville, Handbook of Epoxy Resins, McGraw Hill,
     New York (1967).

18. G.H. Fleming, Naval Ordnance Laboratory Technical Report, 65-101
     (1965).

19. H.C. Anderson, J. Appl. Polymer Sci., 6, 484 (1962).

20. J.P. Bell, J. of Polymer Sci., 6, 417 (1970).

21. M. Fieser and L.F. Fieser, Reagents for Organic Synthesis, Harvard
     University (1971).

22. L.J. Bellamy, The Infrared Spectra of Complex Molecules, Wiley & Sons,
     N.Y. (1975).

· `146`

Figure Captions

Figure 1: The chemical structure and infrared absorbance spectra of
A. epoxy resin (EPON 828); B. Nadic methyl anhydride.

Figure 2: Infrared absorbance spectra of epoxy resin during cure with
anhydride NMA at room temperature.

Figure 3: The infrared spectra of products of epoxy resin and poly-
aminosiloxane at $160^{o}C$, 2 hours.

Figure 4: The infrared absorbance spectra of nadic methyl anhydride (NMA)
reacted with polyaminosiloxane at $160^{o}C$ and one hour with and
without BDMA.

Figure 5: The infrared absorbance spectra of products of A. NMA mixed
with propylamine and B. sample A heated at $150^{o}C$ and one hour.

Figure 6: The infrared absorbance of A. the product of aminosiloxane/epoxy/
anhydride heated at $160^{o}C$ and 2 hours, B. the same condition
except without aminosiloxane, C. difference of A and B.

Figure 7: The infrared absorbance spectra of A. composite, B. pure E-glass
fiber, C. cured matrix, D. difference after subtracted spectra
B and C.

Figure 8: The infrared absorbance spectra of A. matrix with 30%
aminosilane treated silica powder, B. heat cured matrix, C.
difference spectrum of A and B.
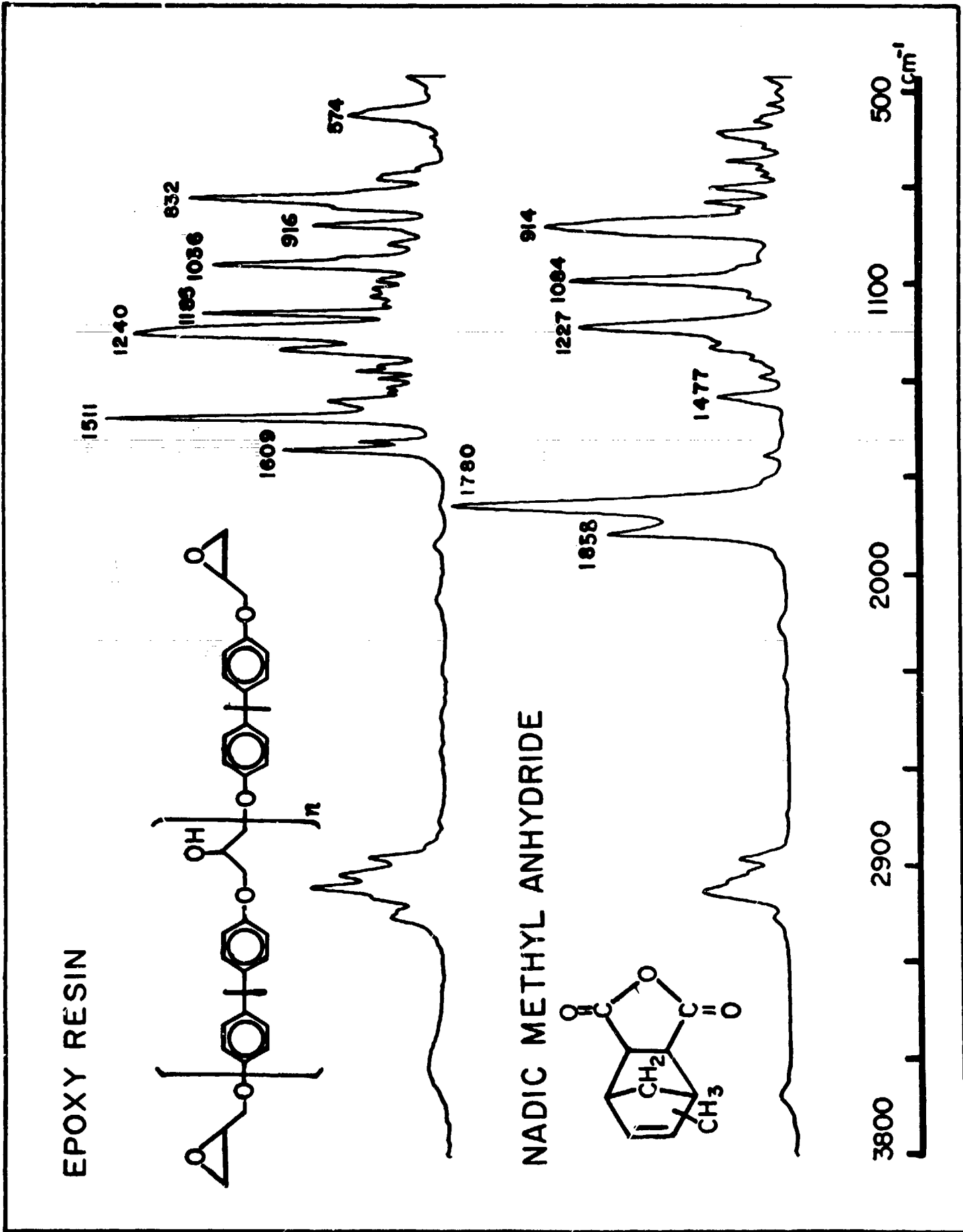
Figure 1.

Figure 2.

A. WITHOUT BDMA

2967 — 1609 1511 1246 1298 1036 1457 832 961 575

B. WITH BDMA

3400 2931 — 1609 1511 1511 1250 1123 1038 828 558

3800 3200 2600 2000 1400 800 cm^{-1}

Figure 3.

A. WITHOUT BDMA

2977

1780
1700

1858

1443
1399

1107 914

B. WITH BDMA

2977

1780

1858

1227
1082 914

3800 3200 2600 2000 1400 800 cm⁻¹
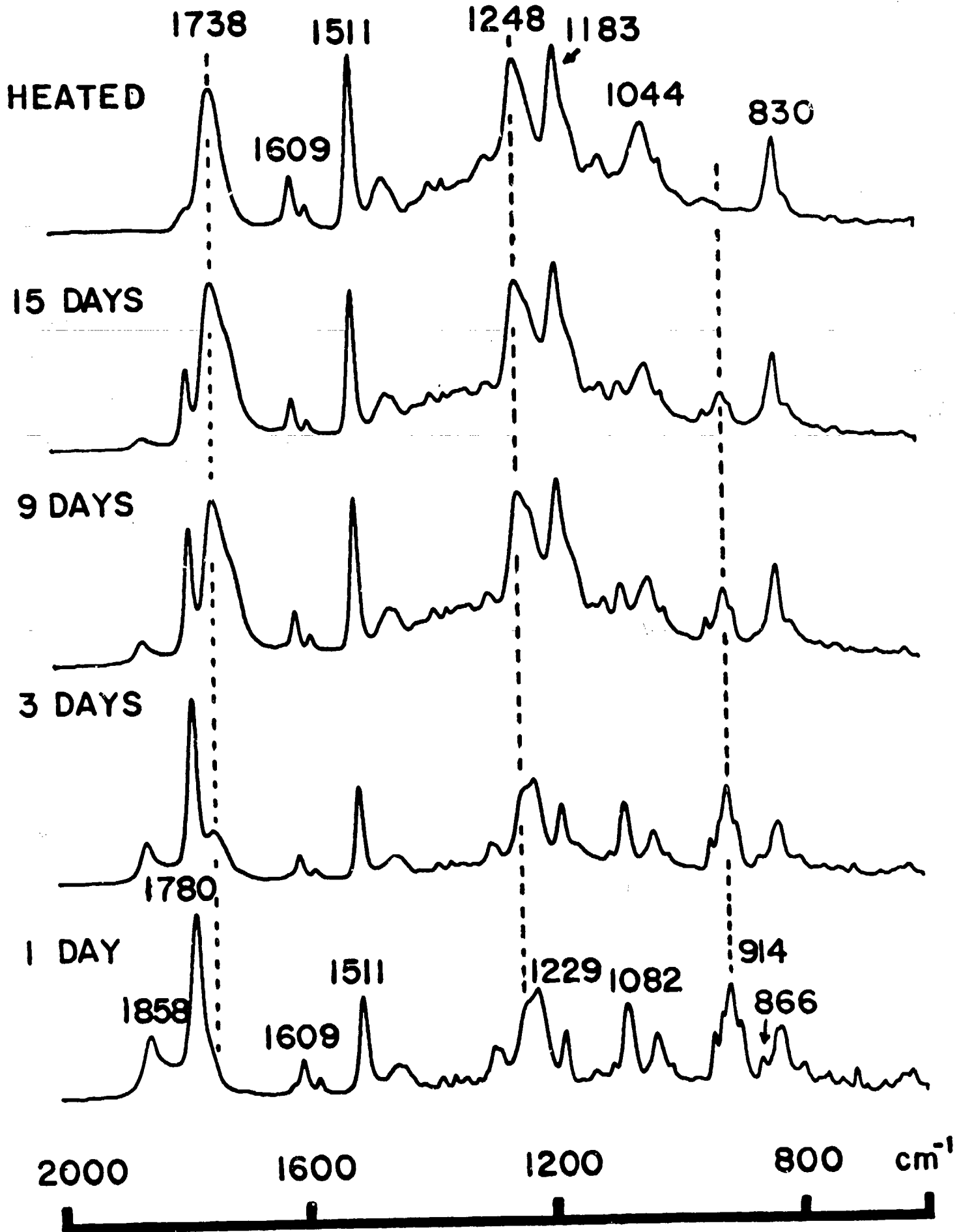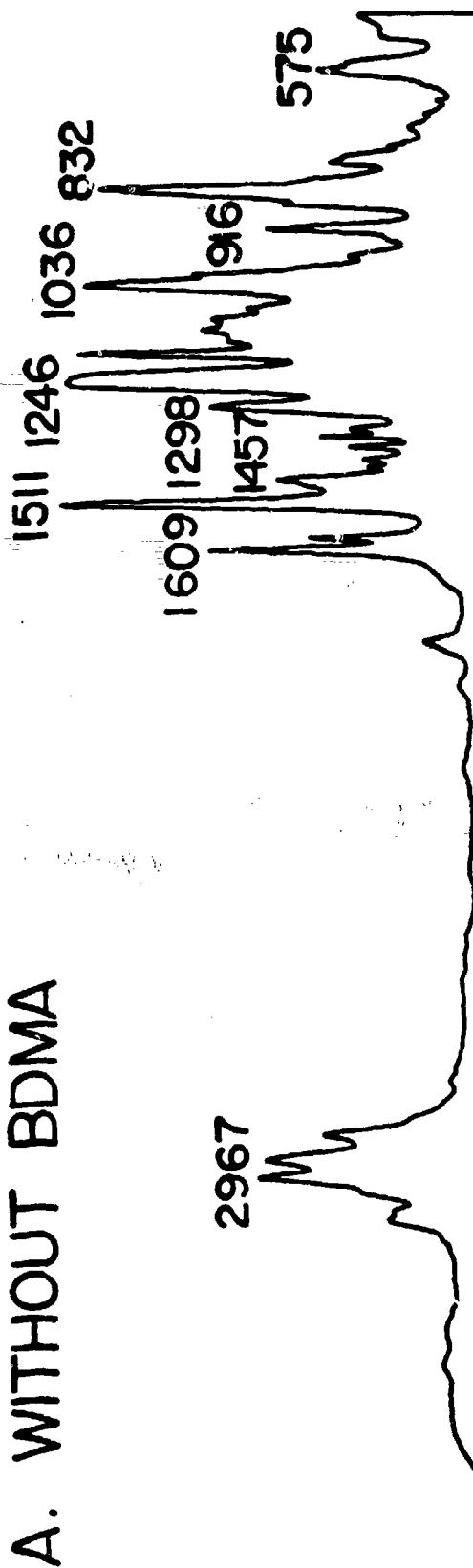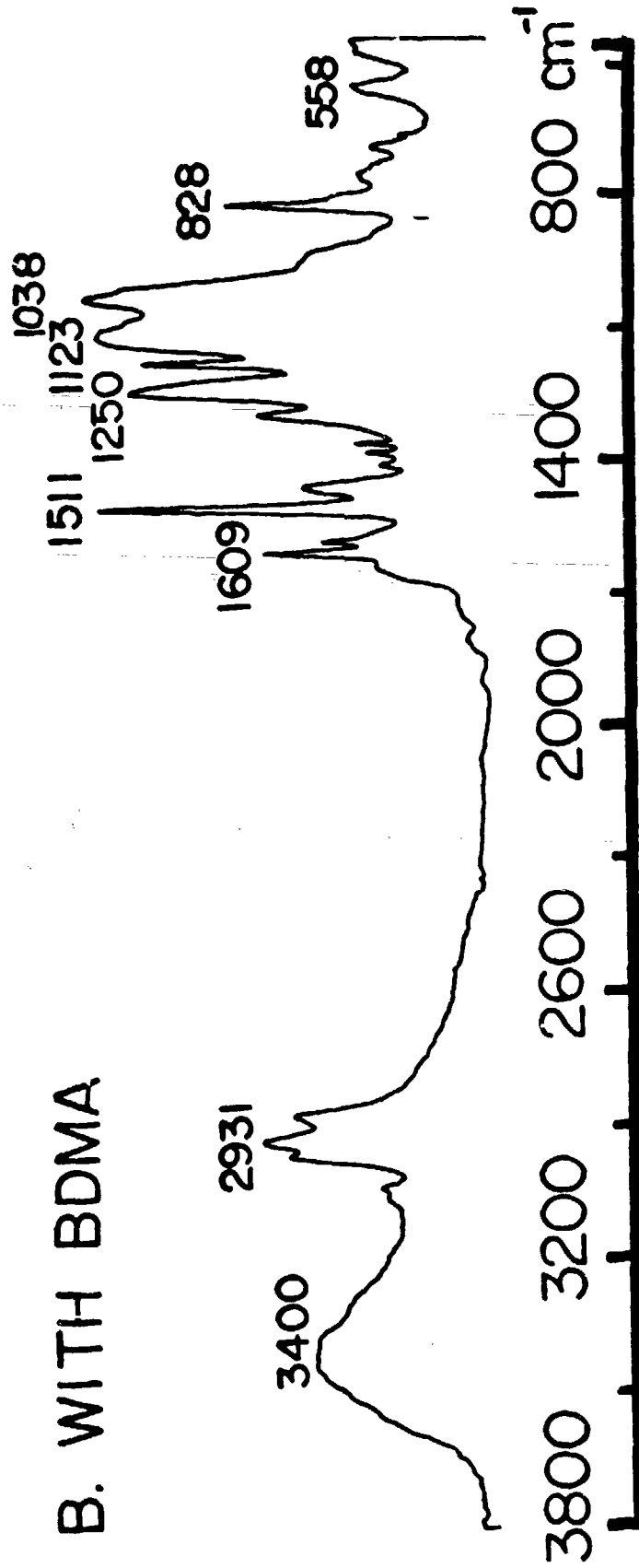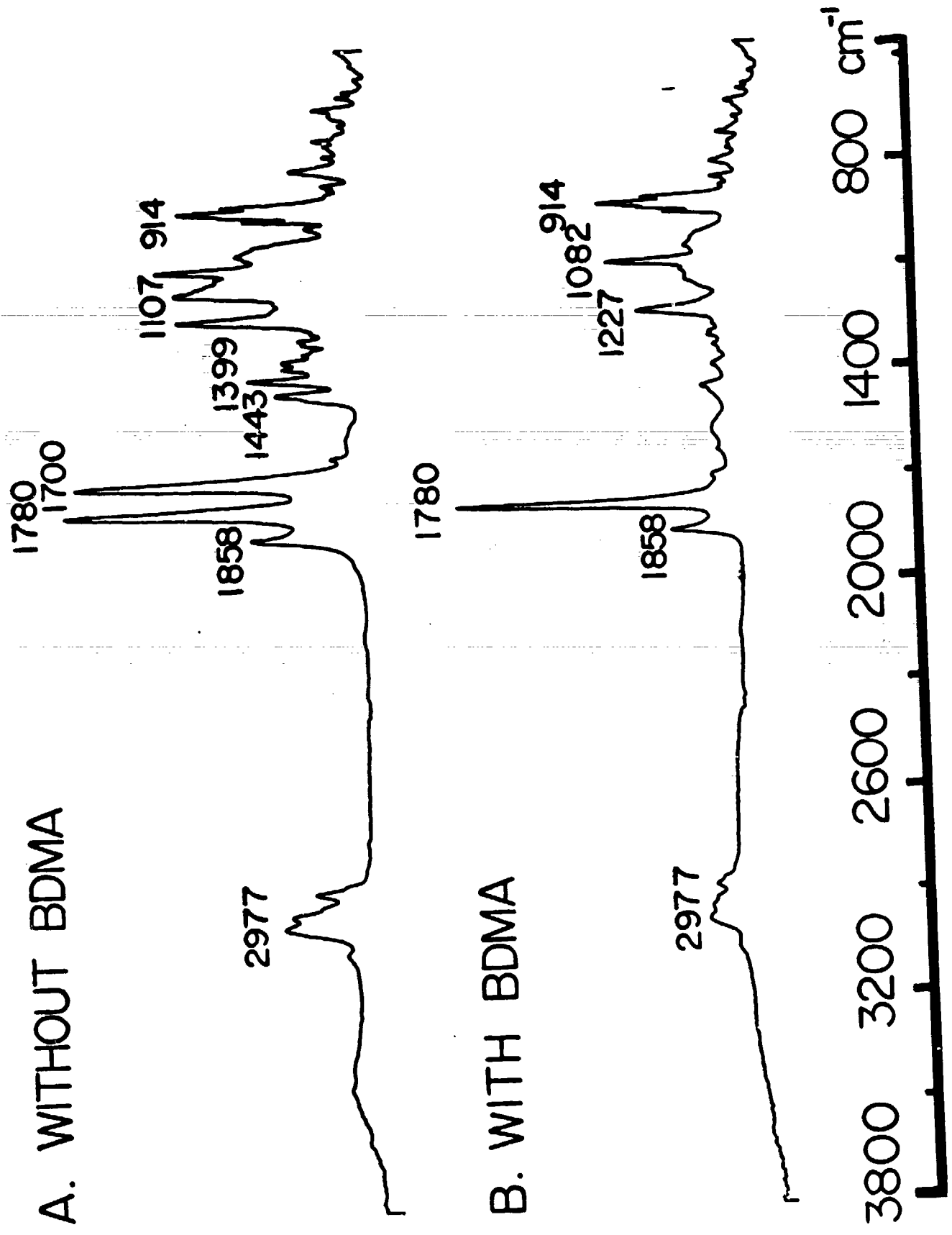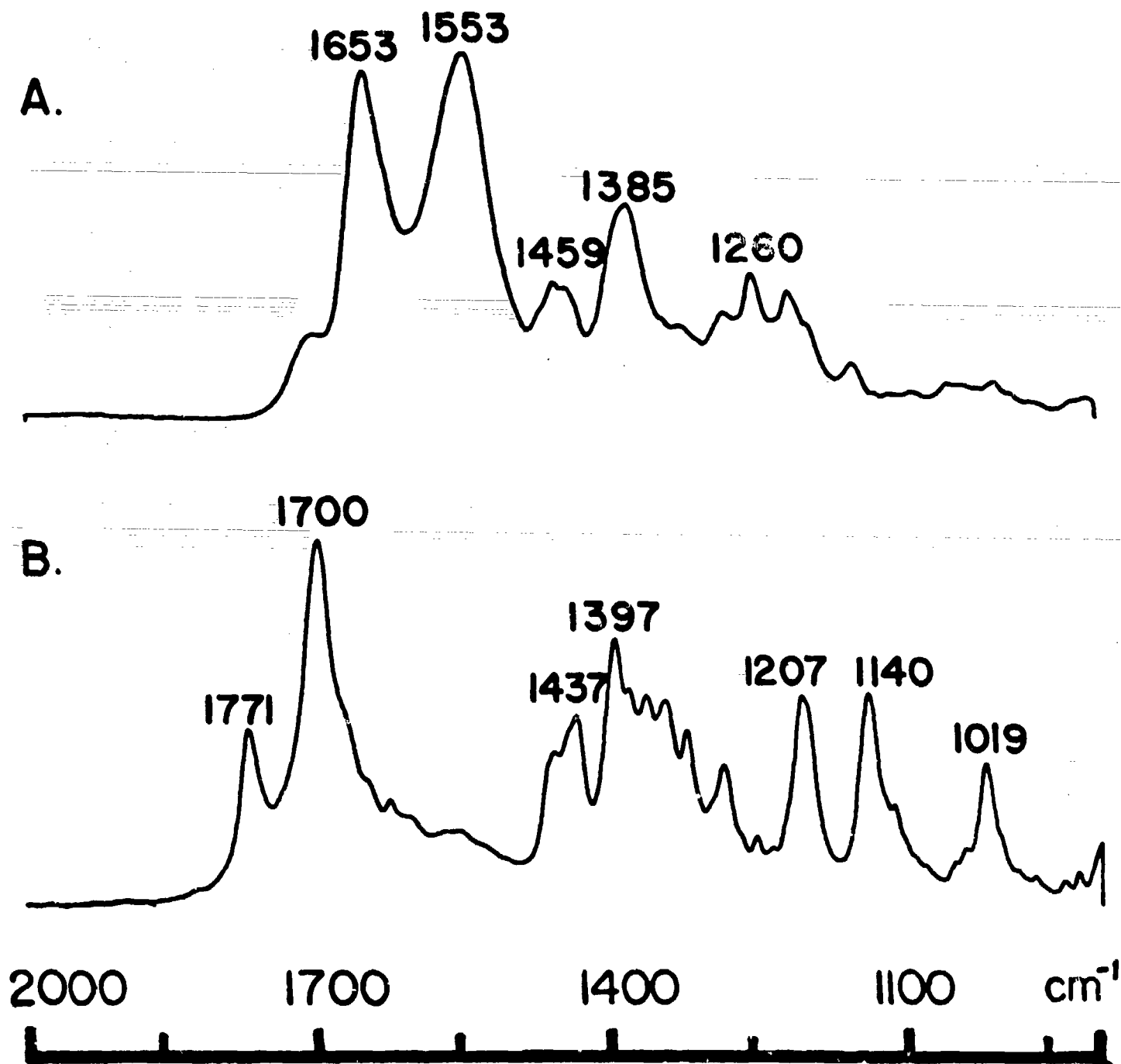
Figure 4.

Figure 5.

REACTION BETWEEN AMINOSILOXANE / EPOXY / ANHYDRIDE
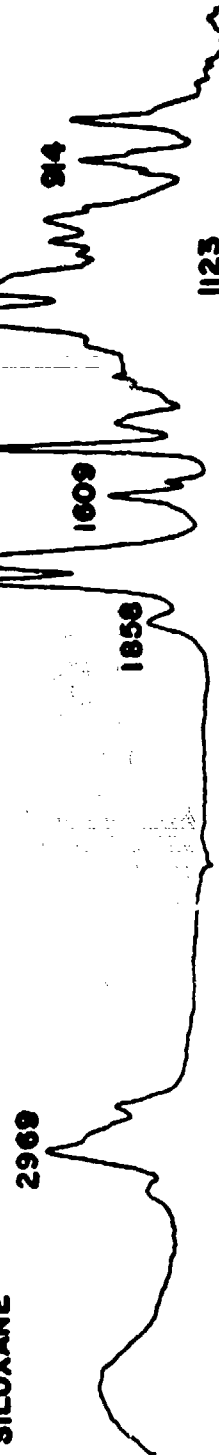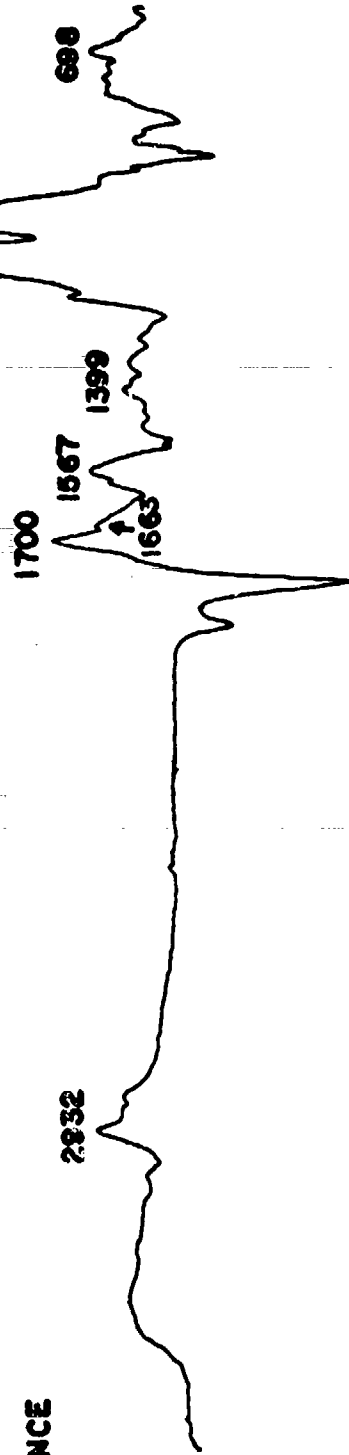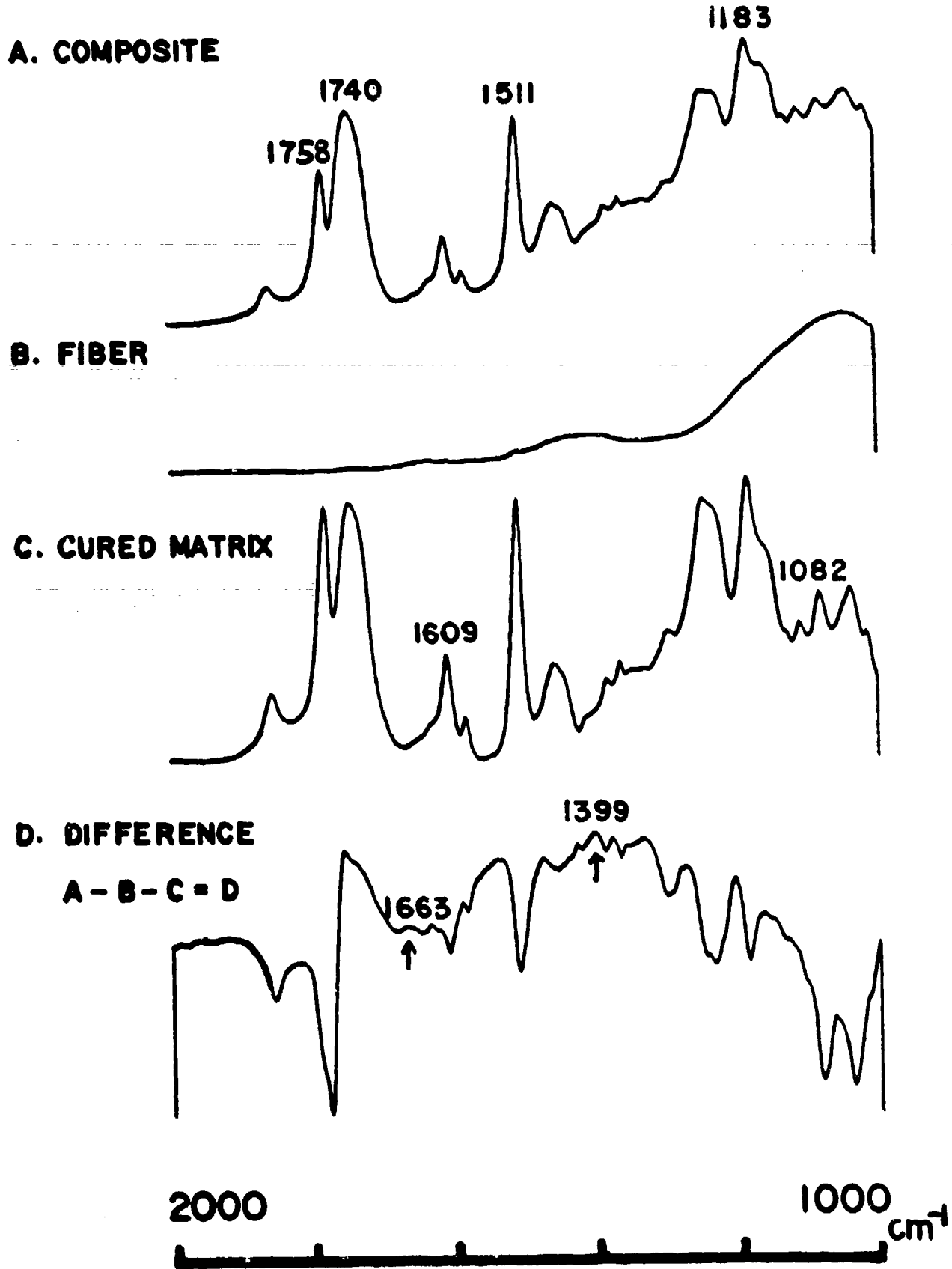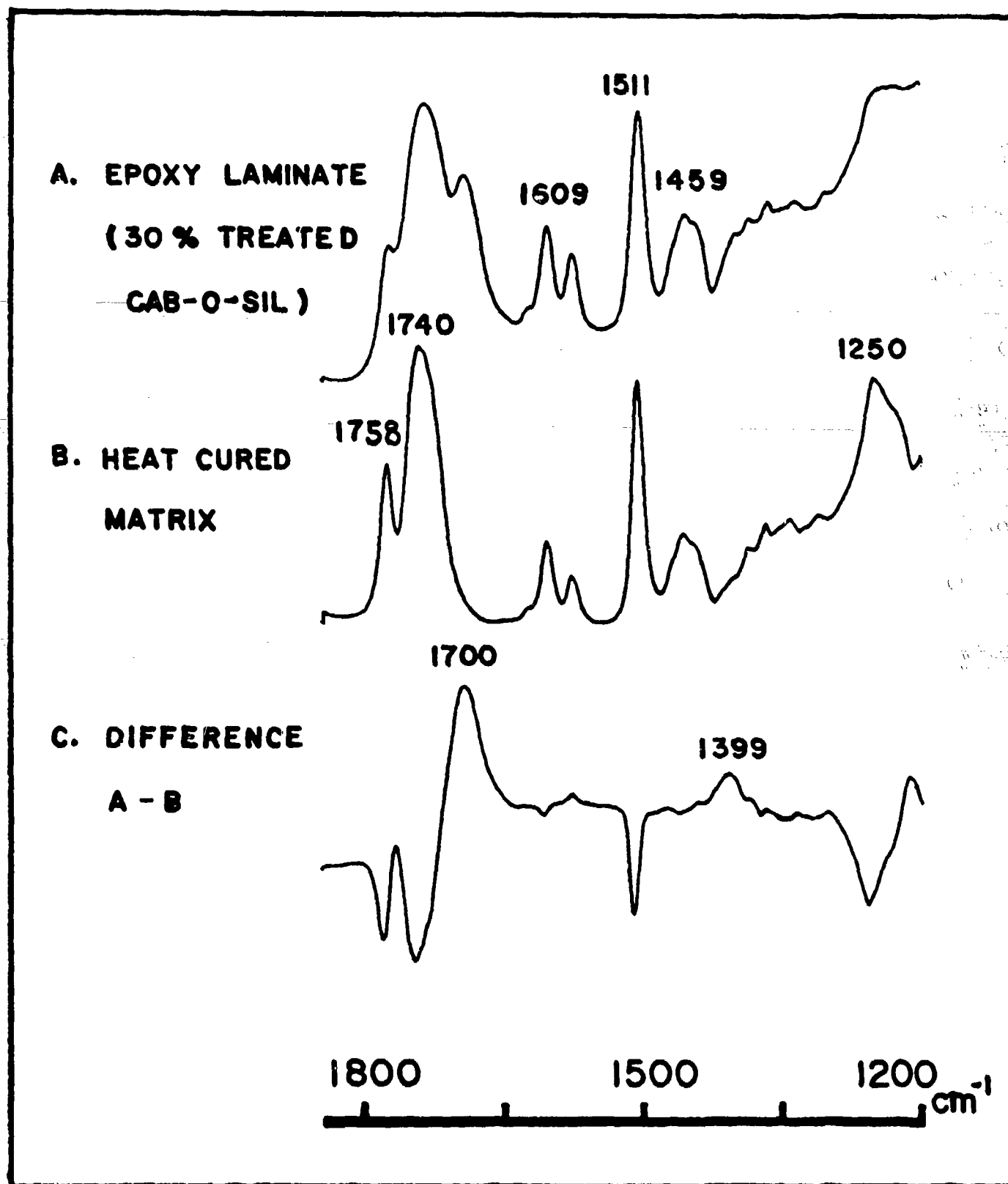
Figure 6.

Figure 7.

Figure 8.

MAGIC-ANGLE CROSS-POLARIZATION CARBON-13 NMR STUDY OF

AMINOSILANE COUPLING AGENTS ON SILICA SURFACES

by

Chwan-hwa Chiang, Nan-I Liu, and Jack L. Koenig

Department of Macromolecular Science

Case Western Reserve University

Cleveland, Ohio 44106

ABSTRACT

The high resolution solid state carbon-13 nuclear magnetic resonance spectra of γ-aminopropyltriethoxysilane (APS) and N-2-aminoethyl-3-aminopropyltrimethoxysilane (AAPS) condensed as bulk polymers and adsorbed on glass surfaces have been investigated. It is shown that the ^{13}C NMR resonance peaks of the low-cured and high-cured polyaminopropylsiloxanes are chemically shifted from one to another. The hydrogen-bonded APS propyl chain produces an upfield shoulder on the central methylene carbon resonance peak in a cross-polarization with magic angle sample spinning (CPMASS) experiment. Measurements of the chemical shifts of non-heat-treated and heat-treated APS/glass samples were also made and the chemical shift trends are discussed in terms of oriented and extended conformational effects of propyl units. Three molecular structure models of APS are proposed involving a hydrogen bonding interaction by the amine and SiOH groups. The chemical shifts induced by electric field effects on the β-carbon nucleus for different APS isomers have been calculated and the results agree with the observed resonances.

INTRODUCTION

Coupling agents are used for improving the bonding between fibers and a matrix resin (1,3). Silane coupling agents have received a great deal of attention over the past couple of years (4). Yet little is known about the molecular structure of these coupling agents on the silica surface. It is expected that elucidation of the structure of coupling agents on the surface will be helpful in understanding the fundamental nature of adhesion of organic polymers to inorganic surfaces.

Several techniques have been used to investigate the nature of the interface between the filler and aminosilane coupling agents. Schrader et al. (5) utilized ^{14}C-labeled silane coupling agents and studied the desorption characteristics of γ-aminopropyltriethoxy-silane (APS) on a glass surface as a function of time in boiling water. DiBenedetto and Scola (6) used ion scattering spectroscopy (ISS) and secondary ion mass spectroscopy (SIMS) to study the depth profile of the structure of aminosilane on the surface of S-glass fibers. Boerio and Greivenkamp (7) studied adsorption of aminosilane onto some bulk metals by employing infrared external reflection spectroscopy with polarized light. In our laboratory, we have employer Fourier transform infrared spectroscopy (FT-IR) for the study of the nature of the interface between APS and E-glass fiber surfaces by using Cab-O-Sil as model glass surface (8,9). Since glass absorbs infrared strongly, IR studies are generally complicated.

Carbon-13 nuclear magnetic resonance spectroscopy has seldom

been used in surface studies, probably due to the poor resolution and low sensitivity (10). But using NMR techniques to study silane coupling agents on glass provides an experimental advantage because no interference from bulk glass occurs. The last decade has witnessed the development of high resolution carbon-13 techniques for study of solids, and consequently, the opening of several new avenues of scientific research (11-13). The combined techniques of proton decoupling, cross polarization, and magic angle sample spinning offer the promise that solid state ^{13}C NMR spectra can approach liquid spectra in resolution and sensitivity.

The utility of ^{13}C chemical shift measurements in conformational analysis has been amply demonstrated in many systems (14-15). It is expected that electric field effects will contribute significantly to ^{13}C shielding in aminosilane solid samples since these compounds contain both dipolar and point charge sources. The theory of electric field induced shifts in molecules was treated by Buckingham et al (16-18). Furthermore, since electric field shifts have orientational dependence they may be useful in the determination of molecular structure. In this paper, we report results of magic angle sample spinning experiments performed on aminosilanes as bulk polymers and on the silica surfaces. The topic to be discussed include conformationally dependent chemical shifts, electric field effect of isomers, the mobility of molecular chains, and the molecular structures of APS on glass surfaces.

EXPERIMENTAL

A. Sample Preparation

The γ-aminopropyltriethoxysilane (APS) and N-2-aminoethyl-3-aminopropyltrimethoxysilane (AAPS) were purchased from Petrarch Systems, Inc. Both silane coupling agents were used as received without further purification. The polymers of these two silane compounds were made by puring pure APS and AAPS on Teflon coated aluminum dishes and condensing in air at room temperature. The condensed solid polymers were ground to powder and heated in a vacuum at $130^{o}C$ for one day.

Fumed silica (Cab-O-Sil, grade EH-5) was obtained from Cobat Corp., which is a fine glass powder having a high specific surface 390 $\pm$ 40 m^2/g). The silica was heated under vacuum to $110^{o}C$ for one day before use. For the adsorption of the coupling agents on silica surfaces, a sample of heat-cleaned silica was added to the aqueous solution of the coupling agent. Enough solution was used to ensure that the concentration of the solution remained constant. After five minutes of contact, the solution was centrifuged and decanted. The coupling agent adsorbed on silica was dried either at room temperature for three days in vacuum or dried in vacuum at $130^{o}C$ for one day.

B. Instrumental

The ^{13}C solid state NMR spectra was obtained at room temperature on a Nicolet NT-150 spectrometer operating at 37.7 MHz. Magic

angle sample spinning, proton decoupling, and cross polarization were used to achieve high resolution and sensitivity for the study of solid samples. The instrumental conditions were set as follows: 90^{0} pulse width for C-13 and proton, 3 u sec; spectra width 10 KHz; aquisition time, 0.05 sec; proton decoupling power 20 Gauss; sample spinning speed 2.1 KHz; contact time, 1 msec; time delay between scans, 3 sec.

The weighed powder samples and polyoxymethylene reference were packed into an Andrews type rotor made of Kel-F (12). The dimensions of the rotor are 15 mm long and 5.5 mm in diameter. The double turned coil is 15 mm in height and 10 mm in diameter. The coil support and entire magic angle spinning device are made of Kel-F and non-magnetic metals. Two purposes were served by mixing Delrin with the sample; first as an internal reference for scaling the chemical shifts, second as a reference to measure the amount of couplin   ent on the glass surface. For APS polymer and APS adsorbed on glass, the total number of scans were 2,000 and 10,000 times, respectively.

The liquid spectra were obtained at room temperature with a standard probe provided by Nicolet. Twently ml. sample tubes were used for all of the liquid samples. All chemical shifts shown in this chapter are related to TMS.

RESULTS and DISCUSSION

The CPMASS spectra of polyaminopropylsiloxanes at room tempe-
rature are displayed in Figure 1. These spectra are normalized to
the same total intensity and are plotted at two amplicication levels.
Figure 1-A spectrum is for the solid γ-aminopropyltriethoxysilane
(APS) which was hydrolyzed at room temperature without any subsequent
heat treatment. Figure 1-B spectrum is for the sample which was
hydrolyzed at room temperaute and heated at $130^{\circ}C$ in a vacuum for
one day. Both spectra show three peaks. These three peaks are
associated with the aminopropyl chain of silane and are associated
with the carbons where the following carbon designations are used.

$$APS : \quad (C_2H_5O)_3 - Si - \underset{1}{CH_2} - \underset{2}{CH_2} - \underset{3}{CH_2} - NH_2$$
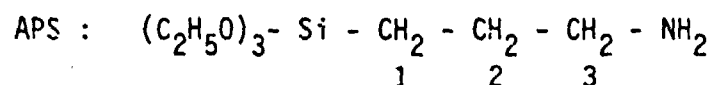
The absence of ethoxy group peaks confirms that the APS is completely
hydrolyzed. The broader peak widths of spectrum 1-A are probably
associated with the presence of short cyclic APS oligomers, while
the heat-treated APS is highly cured with a high degree of polymeri-
zation. It is interesting that the C_2 of spectrum 1-A shows a
shoulder which is about 4.1 ppm upfield from the initial peak at
27.3 ppm. We have also observed that after heating, the resonance
of APS for C_1 shifts up about 0.4 ppm, C_2 shifts down about 1.1 ppm,
and C_3 shifts down about 0.5 ppm. The shoulder peak of C_2 almost
completely disappeared after heat treatment. These results suggest
that the chemical shift change for each carbon in the organic portion of

the silane is related to differences in the molecular structure of APS. Silane molecules condense very rapidly and form a high cured polymer at elevated temperatures.

It has been proposed that the hydrolyzed APS exists in two structural forms; a chelate ring form and nonring extended form (8). The six-membered chelate ring form is formed by the intramolecular hydrogen bonding of amino groups and unreacted silanols. Heat treatment causes the condensation of the silanols to siloxanes and the destruction of the hydrogen bonding so acyclic chain-structured aminopropylsiloxanes are formed. If strong hydrogen bonding occurs in the hydrolyzed APS, then an electric field effect should be observed (16). The protonation of the amino group will cause a large upfield shifts of the C_2 carbon. The strong shoulder appearing near the C_2 resonance of spectrum 1 is probably due to this effect. The source of protons is the uncured silanols of the APS molecules, since the acidity of the silanol is sufficient to donate protons to the amino groups.

It is shown that the width of a resonance line is determined by molecular motion (12). A narrow and sharp resonance reflects high flexibility or freedom of the molecular unit. Before the heat treatment, the amino group of propyl chain was restricted by the hydrogen bonding, so the flexibility of propyl chain is very low. The resonances of carbon peaks are broad and weak (Figure 1-A). The silanols of APS are condensed by heat treatment and form silo-xane bonds so the hydrogen bonding is destroyed. As the amount

of silanol groups decreases and the restriction by the hydrogen bonding is decreased, the propyl chain of silane increases in flexibility. Therefore, the peak width of each carbon of the propyl group of silanes narrow and also shift after heat treatment as shown in Figure 1-B. The possible chemical reaction from low-cured siloxane to high-cured siloxane is shown in the following equation.
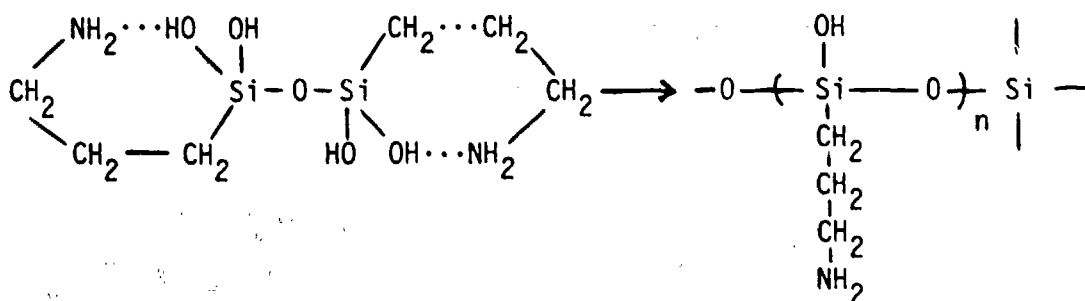
Comparing the broadness of each carbon in the high-cured siloxane, the linewidth of C_1 is higher than C_2 and C_3 as shown in Figure 1-B. The results suggest that the mobility of C_2 and C_3 are higher than C_1, which is expected since C_1 is adjacent to the silicon atom.

The carbon-13 NMR of pure liquid γ-aminopropyltriethoxysilane is shown in Figure 2-B and a 5% aqueous solution of APS in Figure 2-A. Upon solution, the following reaction occurs:

$$(C_2H_5O)_3SiCH_2CH_2CH_2NH_2 \xrightarrow{H_2O} (OH)_3SiCH_2CH_2CH_2NH_2 + 3 C_2H_5OH$$
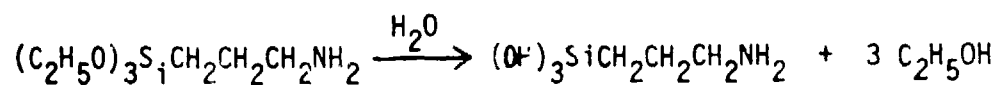
The slight chemical shift of the two lines from 18.6 ppm to 17.4 ppm and 58.4 ppm to 57.5 ppm associated with the ethyl carbons reflects the occurrence of this hydrolysis reaction. The other three lines

are associated with the propyl portion of the silane. The slight chemical shifts and increased broadness of the resonances arise from the slow condensation of the silane triols to APS oligomers. The carbon C_1 shifts slightly to a lower field and the C_2 and C_3 resonances shift to a higher field as shown in Table 1. The width of the resonances for the hydrolyzed system arise from the coagulation associated with the polymerization as well as the variable chemical shifts associated with the presence of several oligomeric states. These results are consistent with the work of Tanaka et al (19) who studied APS suspended in deuterium oxide with silica and observed that the C_1 carbon adjacent to silicon shifted to lower field and exhibited a reduction in T_1.

The carbon-13 NMR spectrum of a Cab-O-Sil sample which was treated with an aqueous solution containing 1% by weight APS is shown in Figure 3. Spectrum 3-A is the APS deposited on Cab-O-Sil without any heat treatment. Spectrum 3-B is form the sample heated at $130^{\circ}C$ in a vacuum for one day. All peaks of both spectra 3-A and 3-B shift to higher fields by about 2 ppm compared to the bulk APS polymer in Figure 2. These additional chemical shifts are probably due to the presence of the glass. The same phenomenon has also been observed for several simple molecules on the surface of adsorbents (26). Based on the bulk APS polymer study these results indicate that the peak at 20.7 ppm arises due to protonation of amino groups inducing an electric field effect. We may consider that the APS molecule adsorbs on the surface of glass and the

amino group is oriented towards the surface due to the strong hydrogen bonding between the amino and silanol groups of the glass surfaces. The shifted resonance of C_2 appears at 20.7 ppm as compared to 25.9 ppm in aqueous solution which suggests that the orientation effect does occur when APS absorbs on the Cab-O-Sil surfaces. Spectrum 3-B shows the silica sample after heat treatment, the C_2 peak height decreases and a new peak is generated at 25.0 ppm. The linewidths of all the overlapped resonances in Figure 3-B are broader than in Figure 3-A. This broadening probably arises from decreased mobility associated with chemical bonding to the glass surface. These results suggest that two different APS molecular structures exist on the Cab-O-Sil surface. We may consider that during the heat treatment, two things happen; first the hydrogen bonding between the amino and the silanol groups is destroyed and the aminopropyl group becomes a free extended side chain due to the reaction shown above; secondly, the uncured silanol groups of APS on the silica surface either condense with other silanol molecules or form a covalent bond with the silica. The more covalent bonds which form on the silica surface, the less hydrogen bonds remain. The decreased intensity of the resonance at 20.7 ppm of the heat-treated silica sample suggests that heat treatment destroys about 60% of the hydrogen bonding. The generated line at 25.0 ppm is associated with the chain extended form at APS on the silica surface.

The carbon-13 NMR spectra of N-2-aminoethyl-3-aminopropyl-trimethoxysilane (AAPS) are shown in Figure 4. The spectrum 4-C is of the neat AAPS liquid sample. The spectra A and B are the AAPS adsorbed on the silica surface and AAPS bulk polymer, respectively. The chemical shifts of AAPS are tabulated in Table 1. The line appears at 50.4 ppm which is assigned to the methoxy carbon resonance as shown in Figure 4-C. The carbon numbers are designated from the silicon atom of the AAPS molecule.

$$AAPS : (CH_3O)_3Si-CH_2-CH_2-NH-CH_2-CH_2-CH_2-NH_2$$
$$12345$$
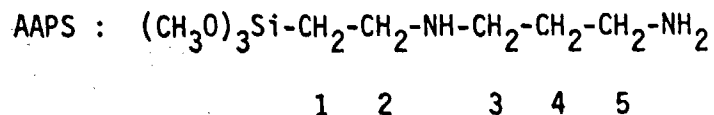
It is easy to see that all of the lines C_2, C_4, and C_5 of AAPS adsorbed on the glass surface have very broad shoulders on the upfield side compared to the spectrum of bulk polymer as shown in Figure 4-A and 4-B. Since AAPS has two amino groups, both of the amino groups can attach to the silica surface (25). Therefore, the β-effect of protonation shifts the resonance of C_2, C_4, and C_5 of the adsorbed AAPS on the silica surface. These results are similar to APS adsorbed on the surface of glass. It confirms that AAPS like other aminosilanes will adsorb on the surface of silica, and the amino groups are chemisorbed to the silica surface.

The carbon-13 NMR shifts induced by changing the molecular structure of γ-aminopropylsiloxane (APS) are shown in Table 1. It has been shown that an electric field effect due to the protonation of the amino group will cause an upfield shift of the C_1, C_2, and C_3 carbons (16). The largest shift will occur for the C_2 carbon at 27.9 ppm and is about 2-6 ppm. The shoulder at 23.2 ppm on the C_2 line of spectrum 2-A is probably due to this effect. The shoulder of the C_2 carbon line of spectrum 1-A may arise from the intramolecular chelate ring structure. The ring form of APS may exist in bulk polymer before heat treatment. After heat treatment of APS, most of the silanol groups are condensed and the amino groups cannot interact with them through hydrogen bonding. Under these circumstances, the aminopropyl chain becomes free and flexible, so the resonance lines become narrow and sharp as shown in Figure 1-B.

In order to determine the chemical shifts of each of the APS molecular isomers, a tentative calculation using the electric field theory was made. The equation for the electric field shift is (18, 19, 20)

$$\Delta\delta = A\Delta E_z + B\Delta(B^2) - D\Delta(FG), \tag{1}$$

where A, B, and D are parameters, E is the electric field at the proton nucleus due to the nearby charge, and E_z is the component

of that field acting along the C-H bond. The term $-D\Delta(FG)$ signifies a shift due to a field gradient term which is derived as (18).

$$\Delta(FG) = \Sigma e(3\cos^2\theta - 1)/r^3 \qquad (2)$$

Batchelor (21) and Jaques (18) both have applied this theory to ^{13}C shifts of symmetric and assymmetric carbon molecules and their results indicate that an electric field theory can successfully predict the chemical shifts arising from protonation. The schematic models of APS for the three isomers are shown in Figure 5. Model A is the extended chain form of APS, the C_1 and NH_2 groups are located on different sides of the C_1-C_2 bond. Model B is the ring closed form of APS, where the NH_2 group is strongly hydrogen bonded with the Si-OH, and C_1 and NH_2 groups are on the same side of the C_2-C_3 bond. Model C is the APS chemically adsorbed on glass surface and the amino group is oriented toward the glass surface.

The angles and distances of each model computed from Cartesian coordinates as shown in Table 2. It is necessary to assume the thermal parameters are zero, since we suppose the samples have fixed bond angles and bond distances. The positive charge (P) was assume to be concentrated at 1 $\AA$ from the N atom along the C_3-N bond direction. The bond distance of the $O\cdots H\cdots N$ group was 2 $\AA$ (24). The resulting structural information is given in Table 3. We have used the following values given by Batchelor (21): $A_{C-C} = 2.4 \times 10^{-11}$ and $A_{C-H} = 4.5 \times 10^{-11}$ esu, where the B value is 4.9×10^{-18} esu, $l_{C-C} = 1.53$ $\AA$ and $l_{C-H} = 1.1$ $\AA$ are given by Jaques. The value of B is

4.9×10^{-18} esu for methyl carbon, and he suggested the value of B depends on the nature of the substituted groups. In this calculation we used a value of $B = 6.5 \times 10^{-18}$ esu and the calculated $\Delta\delta$ are shown in the final column of Table 3.

The calculated chemical shifts for C_2 of the isomers A, B, and C are 4.28, 4.29, and 4.39 ppm, respectively. The observed chemical shifts of B and C isomers are 4.1 and 4.3 ppm. Since alkoxy groups of APS are sensitive to moisture, practically, we cannot obtain a protonated APS without hydrolyzed alkoxy groups for the model A. The observed chemical shifts are similiar to the calculated chemical shifts for the B and C models. The chemical shifts induced by variation of environments correlate with the molecular structure of APS on the glass surfaces. The differences between the magnitudes of the shifts in the B and C isomers must be attributed to interactions with the silanols, but these differences cannot be distinguished in this experiment. The experimental results agree with theoretical predictions within experimental error. Further refinements in the calculations or improvements in theory are needed.

CONCLUSIONS

The experimental results obtained in this study indicate that the high resolution solid state carbon-13 nuclear magnetic resonance spectroscopy provides extremely useful information for the study of organofunctional silane coupling agents adsorbed on the glass surfaces. The electric-field induced chemical shifts of the hydrogen-bonded and non-bonded aminopropyl chains of the solid poly-γ-aminopropylsiloxanes can be identified. This technique is capable of detecting less than a monolayer equivalent of coupling agent on the surface of glass. Application of this spectroscopy makes examination of the adsorbed polymers more attractive and should help to probe other fertile areas.

ACKNOWLEDGEMENT

REFERENCES

1. E.P. Plueddemann, Interface in Polymer Matrix Composites, Academic, N.Y., 1974.

2. T.K. Kwei, J. Polym. Sci., 3-A, 3229 (1965).

3. E.P. Pluedemann, J. Adhesion, 2, 184 (1970).

4. European Rubber J., 3, 37 (1974).

5. M.E. Schrader and A. Block, J. Polym. Sci., C, 34, 281 (1971).

6. A.T. DiBenedetto and D.T. Scola, J. Colloid & Interface Sci., 64, 480 (1978).

7. F.J. Boerio, L.H. Schenlein, and J.E. Grievenkamp, A ppl. Spect., 22, 203 (1978).

8. C.H. Chiang, H. Ishida, and J.L. Koenig, J. Colloid & Interface Sci.,74, 396 (1980).

9. H. Ishida and J.L. Koenig, Polym. Eng. & Sci., 18, 128 (1978).

10. J.J. Chang, A. Pines, J.J. Fripiat, and H.A. Resing, Surface Sci., 47, 661 (1975).

11. J. Schaefer, E.O.Stejskal, and R. Buchdahl, Macromolecules, 10, 384 (1977).

12. F.W. Wehrli and T. Wirthlin, Interpretation of C-13 NMR Spectra, Heyden, 1978.

13. R.G. Griffin, Anal. Chem., 49, 951 (1977).

14. D.M. Grant, B.V. Cheng, J. Amer. Chem. Soc., 89, 5315 (1967).

15. D.K. Dalling and D.H. Grant, J. Amer. Chem. Soc., 94, 5318 (1972).

16. A.D. Buckingham Can. J. Chem., 38, 300 (1960).

17. J.W. Jaques, J.B. Macaskill, and W. Weltner, J. Phy. Chem., 83, 1412 (1979).

18. J.G. Batchelor, R.J. Cushley, and J.H. Prestegard, J. Org. Chem., 39, 1698 (1974).

19. K. Tanaka, S. Shinoda, and Y. Ssito, Chem. Letter, 179 (1979).

20. J.G. Batchelor, J. Freeney, and G.C.K. Roberts, J. Mag. Res., 20, 19 (1975).

21. J.G. Batchelor, J. Amer. Chem. Soc., 97, 3410 (1975).

22. B.E. Douglas and D.H. McDaniel, Concepts and Models of Inorganic Chemistry, Oxford, 1965, chapter 3.

23. M.E. Schrader, J. Adhesion, 2, 202 (1970.

24. G.C. Pimentel and A.L. McClellan, The Hydrogen Bond, Freeman, N.Y., 1960.

25. B. Arkles, Chemtech, 7, 766 (1977).

26. D. Denney, V.M. Mastikhin, S. Namba, and J. Turkevich, J. Phys. Chem., 82, 1752 (1978).

LIST OF TABLES

Table 1: Carbon-13 NMR chemical shifts of the γ-aminopropyltriethoxysilane and N-2-aminoethyl-3-aminopropylsiloxane in different states.

Table 2: Angles and distances used in calculation of ^{13}C shifts at C-2 of APS in different states.

Table 3: Calculated contributions and observed induced ^{13}C shifts of γ-aminopropylsiloxanes (APS) at different states.[a]

FIGURE CAPTIONS:

Figure 1: Carbon-13 NMR spectra of hydrolyzed γ-aminopropylsiloxane. A: APS initially dried polymer at room temperature.
B: APS condensed polymer which was heat-treated at 130°C.

Figure 2: Carbon-13 NMR spectra of the γ-aminopropyltriethoxysilane (APS). A: 5% APS aqueous solution;
B: APS as neat liquid.

Figure 3: Carbon-13 spectra of hydrolyzed γ-aminopropylsilixane on the surface of silica.
A. APS absorbed on the high-surface-area silica and dried at room temperature;
B: APS absorbed on the silica and heat-treated at 130°C in vacuum for one day.

Figure captions continued...

Figure 4:   Carbon-13 NMR spectra of N-2-aminoethyl-3-aminopropy-
ltrimethoxysilane (AAPS).

A: Hydrolyzed AAPS absorbed on high-surface-area silica;

B: hydrolyzed AAPS bulk polymer; and

C: AAPS as neat liquid.

Figure 5:   Schematic models of APS on the surface of silica.

A: An extended open chain APS;

B: a ring closed APS; and

C: NH_2 absorbed on the surface of silica.

TABLE 1 : Carbon-13 NMR chemical shifts of the γ-aminopropyltriethoxysilane and N-2-aminoethyl-3-aminopropylsiloxane in different states.

Samples	Chemical Shifts (ppm)					Proposed Isomers
	C_1	C_2	C_3	C_4	C_5	
	$-Si-CH_2-$	CH_2-	CH_2-NH_2 (APS)			
APS bulk polymer						
neat liquid	3.1	27.9	45.5			A
5% aqueous solution	10.8	25.9	43.7			A & B
initial dried	12.1	27.3 (23.2)	45.5			A & B
heat treated	11.7	28.4	46.0			A
APS adsorbed on Cab-O-Sil						
initial dried	8.8	20.7 (25.0)	42.5			A, B, & C
heat treated	8.7	25.0 (20.7)	43.0			A & C
	$-Si-CH_2-$	CH_2-	$CH_2-NH-CH_2-$		CH_2-NH_2	
neat liquid	7.2	23.8	53.1	53.2	42.4	
condensed polymer	12.2	24.2	52.7	52.7	41.9	
adsorbed on silica	9.8	22.3	50.2	50.2	40.4	

* The parentheses is the value of chemical shift at shoulder.

TABLE 2 : Angles and distances used in calculation of ^{13}C shifts at C-2 of APS in different states.

Bond Type	P			N		
	θ, deg.	r_{BC}, $\overset{o}{A}$	r_C, $\overset{o}{A}$	θ, deg.	r_{BC}, $\overset{o}{A}$	r_C, $\overset{o}{A}$
open chain APS (model A)						
C_2-C_1	152.3	4.76	3.72	157.5	5.66	4.67
C_2-H_3	84.4	3.85		77.3	4.67	
C_2-H_4	84.4	3.85		77.3	4.67	
C_2-C_3	40.2	3.10		45.0	4.14	
Ring closed APS (model B)						
C_2-C_1	82.3	3.85	3.77	56.3	3.72	4.14
C_2-H_3	156.0	4.34		163.5	4.80	
C_2-H_4	95.3	3.90		83.5	4.26	
C_2-C_3	39.7	3.19		70.5	4.01	
APS adsorbed on silica (model C)						
C_2-C_1	83.0	3.85		79.1	4.55	4.68
C_2-H_3	162.0	4.34		157.5	5.25	
C_2-H_4	95.3	3.85		79.5	4.71	
C_2-C_3	39.8	3.18		45.0	4.14	

* Calculation base on the cartesian coordinates for the different molecular structure models. θ = N-C-X or P-C-X angle, r_{BC} = distance from N or P to center of C-X bond, r_C = N-C or P-C distance.

TABLE 3 : Calculated contributions and observed induced ^{13}C shifts of γ-aminopropylsiloxanes (APS) at different states.[a]

Models	P			N			Total			$\Delta\delta$(ppm) (Obsd)	$\Delta\delta$(ppm) (Calcd)
	$A\Delta E_z$	ΔE^2	$D\Delta(FC)$	$-A\Delta E_z$	ΔE^2	$-D\acute{a}(FC)$	$A\Delta E_z$	ΔE^2	$D\Delta(FC)$		
A	7.498	0.504	-1.772	-5.796	0.197	0.424	1.702	0.701	-1.348	-	4.280
B	-1.856	0.491	1.786	0.632	0.322	-0.824	-1.224	0.813	0.962	4.1	4.290
C	-2.555	0.500	2.780	1.053	0.209	-0.856	-1.50	0.709	1.924	4.3	4.394

a. Terms are those in eq. 1 . $A\Delta E_z = 48\,A\cos\theta / r_{BC}^2$, $\Delta E^2 = (4.8)^2 / r^4$. $D\Delta(FC) = 48\,A\,l_{C-X}\,(3\cos^2\theta - 1)/ r^3$.
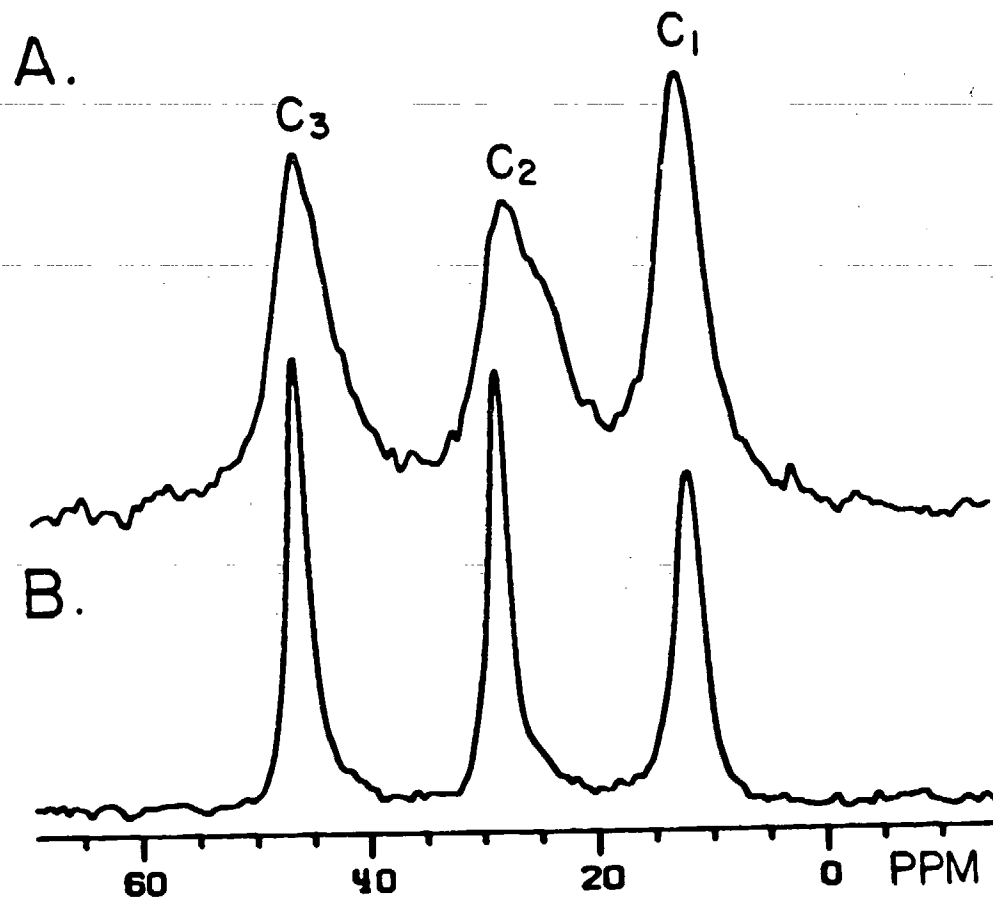
178

Figure 1: Carbon-13 NMR spectra of hydrolyzed γ-aminopropylsiloxane.
A: APS initially dried polymer at room temperature.
B: APS condensed polymer which was heat-treated at $130^{o}C$.
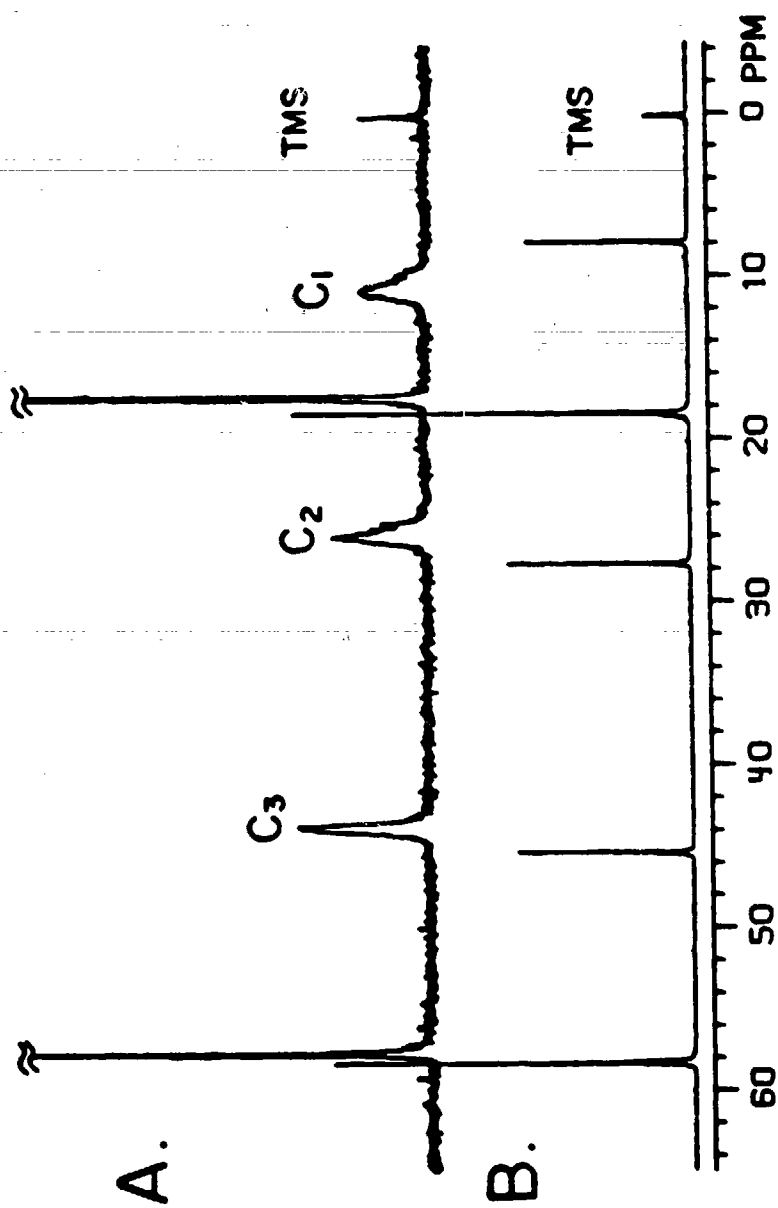
Figure 2: Carbon-13 NMR spectra of the γ-aminopropyltriethoxysilane (APS).
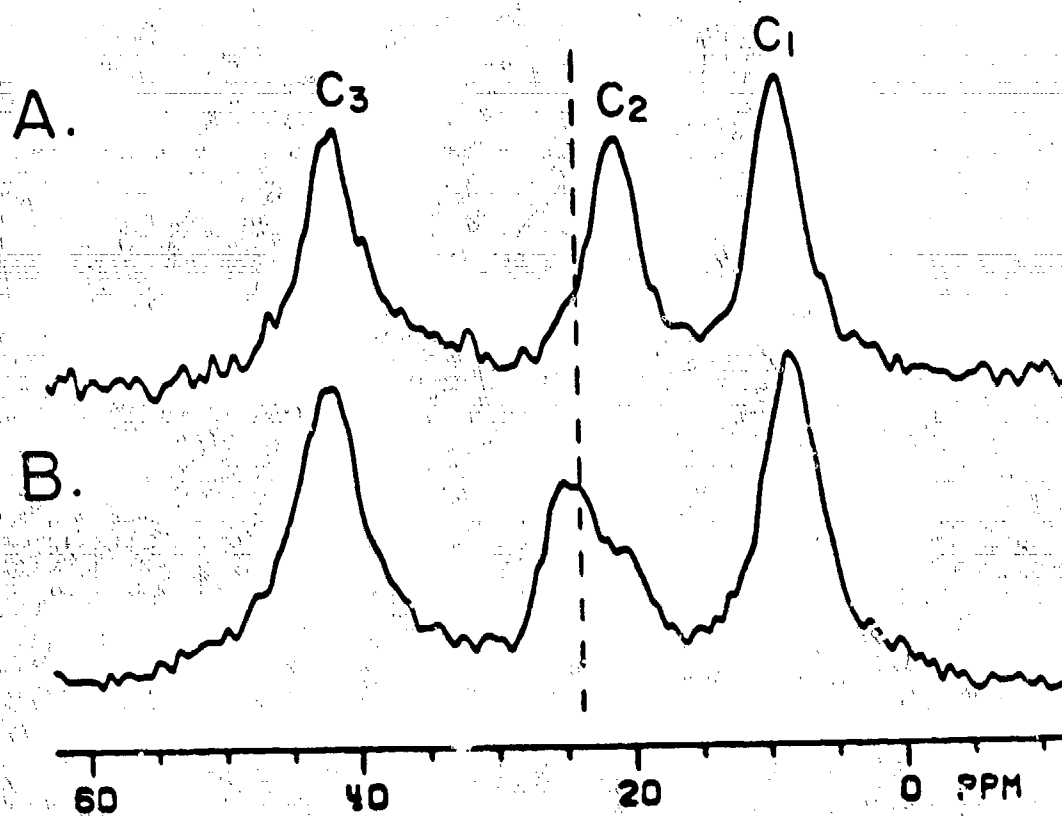A: 5% APS aqueous solution; B: APS as neat liquid.

Figure 3: Carbon-13 spectra of hydrolyzed γ-aminopropylsilixane on the surface of silica. A: APS adsorbed on the high-surface-area silica and dried at room temperature; B: APS adsorbed on the the silica and heat-treated at 130^{C}C in vacuum for one day.
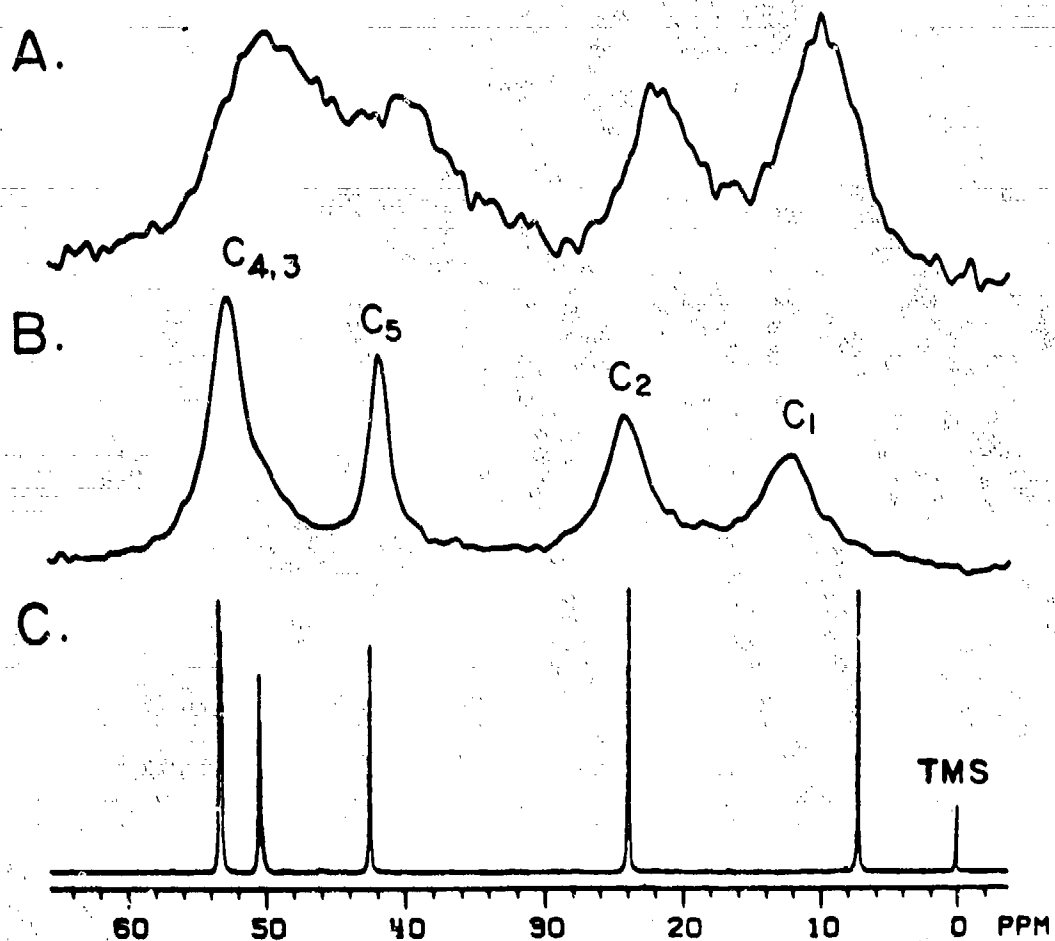
Figure 4: Carbon-13 NMR spectra of N-2-aminoethyl-3-aminopropyltri-
methoxysilane (AAPS). A: Hydrolyzed AAPS adsorbed on high-
surface-area silica; B: hydrolyzed AAPS bulk polymer; and
C: AAPS as neat liquid.